

Easily processable ultra high molecular weight polyethylene with narrow molecular weight distribution

Citation for published version (APA):

Garkhail Sharma, K. (2005). *Easily processable ultra high molecular weight polyethylene with narrow molecular weight distribution*. [Phd Thesis 1 (Research TU/e / Graduation TU/e), Chemical Engineering and Chemistry]. Technische Universiteit Eindhoven. <https://doi.org/10.6100/IR583519>

DOI:

[10.6100/IR583519](https://doi.org/10.6100/IR583519)

Document status and date:

Published: 01/01/2005

Document Version:

Publisher's PDF, also known as Version of Record (includes final page, issue and volume numbers)

Please check the document version of this publication:

- A submitted manuscript is the version of the article upon submission and before peer-review. There can be important differences between the submitted version and the official published version of record. People interested in the research are advised to contact the author for the final version of the publication, or visit the DOI to the publisher's website.
- The final author version and the galley proof are versions of the publication after peer review.
- The final published version features the final layout of the paper including the volume, issue and page numbers.

[Link to publication](#)

General rights

Copyright and moral rights for the publications made accessible in the public portal are retained by the authors and/or other copyright owners and it is a condition of accessing publications that users recognise and abide by the legal requirements associated with these rights.

- Users may download and print one copy of any publication from the public portal for the purpose of private study or research.
- You may not further distribute the material or use it for any profit-making activity or commercial gain
- You may freely distribute the URL identifying the publication in the public portal.

If the publication is distributed under the terms of Article 25fa of the Dutch Copyright Act, indicated by the "Taverne" license above, please follow below link for the End User Agreement:

www.tue.nl/taverne

Take down policy

If you believe that this document breaches copyright please contact us at:

openaccess@tue.nl

providing details and we will investigate your claim.

**Easily Processable Ultra High Molecular Weight Polyethylene
with Narrow Molecular Weight Distribution.**

PROEFSCHRIFT

ter verkrijging van de graad van doctor aan de
Technische Universiteit Eindhoven, op gezag van de
Rector Magnificus, prof.dr. R.A. van Santen, voor een
commissie aangewezen door het College voor
Promoties in het openbaar te verdedigen
op donderdag 20 januari 2005 om 16.00 uur

door

Kirti Garkhail Sharma

geboren te New Delhi, India

Dit proefschrift is goedgekeurd door de promotoren:

prof.dr. G.J.M. Gruter
en
prof.dr. P.J. Lemstra

Copromotor:
dr. R. Duchateau

**Easily Processable Ultra High Molecular Weight Polyethylene
with Narrow Molecular Weight Distribution.**

Kirti Garkhail Sharma

CIP-DATA LIBRARY TECHNISCHE UNIVERSITEIT EINDHOVEN

Garkhail Sharma, Kirti

Easily processable ultra high molecular weight polyethylene with narrow molecular weight distribution / by Kirti Garkhail Sharma. – Eindhoven: Technische Universiteit Eindhoven, 2005.

Proefschrift. – ISBN 90-386-2836-6

NUR 913

Trefwoorden: polymeren ; morfologie / polymerisatiekatalysatoren / kunststofverwerking ; gieten / polyetheen ; UHMWPE / molmassaverdeling / biomedische materialen ; kunstgewrichten / röntgendiffractie ; WAXD / röntgenverstrooiing ; SAXS

Subject headings: polymer morphology / polymerization catalysts / polymer processing ; molding / polyethylene ; UHMWPE / molecular weight distribution / prosthetic materials ; artificial joints / X-ray diffraction ; WAXD / X-ray scattering ; SAXS

© 2005, Kirti Garkhail Sharma

Printed by the Eindhoven University Press, Eindhoven, The Netherlands.

This research was financially supported by Dutch Polymer Institute (DPI)

Dedicated to my Grand Parents

and

Prakriti

Contents

Chapter 1 General Introduction.

1.1 Introduction	1
1.2 Historical Development	3
1.3 Crystallization of Polymers	7
1.4 Processing of Polyolefins	10
1.5 Scope of the Thesis	14
1.6 References	15

Chapter 2 Synthesis of UHMWPE using a single site catalyst: bis[(pentamethyl)cyclopentadienyl] samarium (II) bis(tetrahydrofuran).

2.1 Introduction	20
2.2 Experimental Section	23
2.2.1 General Comments	23
2.2.2 Catalyst Synthesis	23
2.2.3 Polymerizations	24
2.3 Results and Discussions	25
2.3.1 Mass transfer of ethylene: preliminary polymerization experiments	25
2.3.2 Effect of Dilution during Polymerization	28
2.3.3 Effect of Polymerization Temperature	30
2.4 Conclusions	32
2.5 References	32

Chapter 3 Nascent UHMWPE obtained using homogeneous catalysts: *exploring the versatility of the catalysts to generate UHMWPE with unique morphology.*

3.1 Introduction	36
3.2 Experimental Section	38
3.2.1 General Comments	38
3.2.2 Polymerization with $[3-t\text{-Bu-2-O-C}_6\text{H}_3\text{CH=N(C}_6\text{F}_5)_2\text{TiCl}_2$	38
3.2.3 Polymerization with $[\text{PhC(N-2,6-i-Pr}_2\text{C}_6\text{H}_3)_2\text{Y(CH}_2\text{SiMe}_3)_2\text{(THF)}$	39
3.3 Results and Discussions	39
3.3.1 Polymerization with $[3-t\text{-Bu-2-O-C}_6\text{H}_3\text{CH=N(C}_6\text{F}_5)_2\text{TiCl}_2$	39
3.3.2 Polymerization with $[\text{PhC(N-2,6-i-Pr}_2\text{C}_6\text{H}_3)_2\text{Y(CH}_2\text{SiMe}_3)_2\text{(THF)}$	48
3.4 Conclusions	49
3.5 References	50

Chapter 4 Characterization of Nascent UHMWPE as synthesized via Single Site Catalysts: *estimation of Entanglements in Nascent Powders.*

4.1 Introduction	54
4.2 Results and Discussions	55
4.2.1 Mechanical Deformation of Polymers	55
4.2.2 Compression Molding	59
4.2.3 Differential Scanning Calorimetry	60
4.2.4 Temperature Modulated DSC	65
4.2.5 Determination of Entanglements by Rheology	71
4.3 Conclusions	84
4.4 References	86

Chapter 5 Structure determination of nascent morphology: *a SAXS/WAXS study.*

5.1 Introduction	90
5.2 Experimental Section	91
5.3 Results and Discussions	91
5.3.1 Time resolved SAXS during heating and cooling at atmospheric pressure on commercial grade UHMWPE (GHR1080)	91
5.3.2 Time resolved SAXS during heating and cooling at atmospheric pressure on BW grade UHMWPE	95
5.3.3 Time resolved SAXS during heating and cooling at atmospheric pressure on bis(phenoxy-imine)titanium grade UHMWPE	97
5.3.4 Time resolved SAXS during heating and cooling at atmospheric pressure on samarocene grade UHMWPE	99
5.4 Conclusions	103
5.5 References	104

Technology Assessment	105
------------------------------	-----

Summary	107
----------------	-----

Samenvatting	113
---------------------	-----

Acknowledgements	119
-------------------------	-----

Curriculum Vitae	121
-------------------------	-----

Chapter 1

General Introduction.

1.1 Introduction.

Synthetic polymers have become a part of our daily life. We see so many things around us ranging from our basic necessities such as tooth brushes, clothing, storage bottles and carry bags to special applications like gas pipelines, bullet proof jackets, aerospace application and biomedical implants that are made of plastics. The extensive and still increasing usage of polymeric materials stems from their unique properties and economical advantages and in many applications their performance is better than conventional materials such as metals, wood and natural fibers.

What are polymers? Polymers are macromolecules containing simple repeating units called *monomers*. A wide range of material properties can be achieved depending on the type of monomer(s) (homo- or co-polymer), their architecture (linear, branched, star shape) and microstructure (tacticity, amount and distribution of regio- and/or stereo errors). Polymers can be amorphous or semi-crystalline depending on the amorphous content. Highly crystalline materials with a glass transition temperature above room temperature are brittle, whereas semi-crystalline materials with a glass transition temperature below room

temperature and amorphous material like for example elastomers are tough. By mixing polymers with certain fillers, their properties such as toughness and flame retardance can be modified.

The study of structure property relationships in polymers has become an exciting and demanding field of research in recent decades. This study is, however, complicated since polymer performance not only depends on the polymer microstructure but also on the molecular weight, the molecular weight distribution, the processing technique and influence of additives.

Polyethylene (PE) is one of the most widely used commodity plastics with a global demand (high density, linear low density, and low density polyethylenes) of 50 million metric tons and has the simplest chemical structure of all the commercial polymers.

Polyolefins are prepared either via free radical polymerization or via coordination polymerization using a catalyst. Free radical polymerization is used commercially to synthesize polymers at high pressure such as polyethylene, polymethylmetacrylate, polyvinyl acetate, polystyrene and copolymers of ethylene with vinyl acetate, maleic anhydride and ethyl acrylate.

Coordination polymerization has also attracted serious attention in the last few decades and has been used to homopolymerize a wide range of monomers (ethylene, propylene, 1-hexene, 4-methyl-1-pentene etc) and to afford copolymers involving ethylene and α -olefins (propylene, 1-butene, 1-pentene, 1-hexene, 1-octene, 1, 5-hexadiene, norbornene, styrene etc.), terpolymers of ethylene, propylene with styrene or ethylidene norbornene (EPDM), terpolymers of ethylene, 1-pentene and 1-butene, 1-hexene or 1-octene, cyclic olefins, vinyl aromatic olefins. The type of polymerization, reaction conditions such as temperature, pressure, type of catalyst, cocatalyst, scavenger and comonomer can considerably influence the composition, molecular weight and degree of branching in the polymer and hence the final architecture. Based on the polymer architecture and the resulting density of packing, polyethylenes are classified into high density polyethylene (HDPE; few short or no branches), linear low density polyethylene (LLDPE; many equal short branches) and low density polyethylene (LDPE; various branches on branches) (Figure 1.1). A special class of HDPE is ultra high molecular weight PE, UHMWPE, with a molar mass of over 1×10^6 g/mol whereas HDPE typically has a molar mass between 50,000-300,000 g/mol.

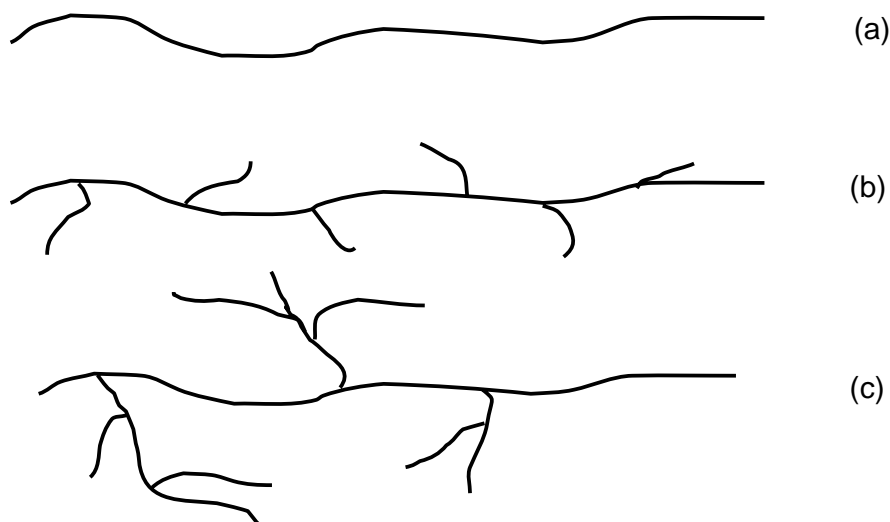


Figure 1.1 Chemical structures of various kinds of polyethylene (a) HDPE (linear) (b) LLDPE (many equal short branches) (c) LDPE (various branches on branches).

1.2 Historical Development.

Polyethylene was first synthesized by chance in 1898 as a waxy solid by Hans von Pechmann while heating diazomethane.¹ The first industrial synthesis of PE also took place accidentally in 1933, when Eric Fawcett and Reginald Gibson from ICI chemicals subjected a mixture of benzaldehyde and ethylene to high pressure (1400 bar and 170°C), thereby producing a waxy solid.¹ The PE thus produced had a branched structure and a low density and hence was denoted as LDPE. Attempts to synthesize PE at lower temp and pressure led to the discovery of the Phillips catalyst (chromium trioxide on silica) in 1951 by Robert Banks and John Hogan.² Later in 1953, Karl Ziegler discovered heterogeneous catalysts based on titanium halides ($\text{TiCl}_3 \cdot 1/3 \text{ AlCl}_3$) that produced HDPE upon activation with organoaluminum cocatalysts such as $\text{Al}(\text{C}_2\text{H}_5)_2\text{Cl}$ by coordination polymerization at low temperature and pressure.³ Later, Natta independently discovered stereoregular polymers such as propylene, butene-1 and styrene.³ The subsequent discovery of MgCl_2 supported TiCl_4 catalyst system resulted in a two fold increase in the activity.³ The basic mechanism of ethylene polymerization by coordination polymerization is shown in Figure 1.2.⁴

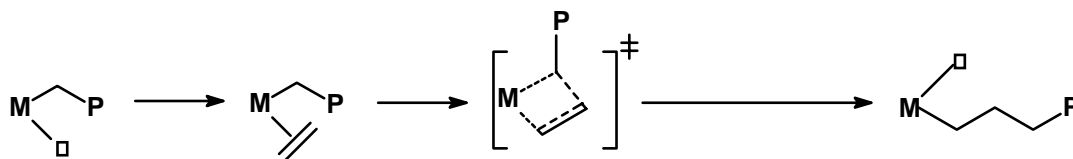


Figure 1.2 *Cossee-Arlman mechanism for the polymerization of olefins (heterogeneous and homogeneous catalysts).*

As shown in Figure 1.2, the olefin insertion takes place by coordination of the monomer at the vacant active metal center followed by cis-opening of the double bond. Once the monomer is inserted, chain migration takes place generating a vacant site once again where another monomer can insert for the chain to grow. The catalysts used in the coordination polymerization can be classified into two groups: heterogeneous and homogeneous. In the case of homogeneous systems, the catalyst is soluble in the polymerization medium, while for heterogeneous systems the catalyst is supported on various supports such as silica or magnesium dichloride which makes it insoluble in the polymerization medium. Most of the heterogeneous catalysts are based on TiCl_4 , $\text{Ti}(\text{O}i\text{Bu})_4$ supported on TiCl_3 , SiO_2 and MgCl_2 or CrO_3 supported on SiO_2 and usually yields polymers with controlled particle morphology, high bulk density and no reactor fouling. Although the heterogeneous Ziegler-Natta catalysts are used extensively, one of the drawbacks of a heterogeneous catalyst system is the presence of many different active sites on the catalyst surface. These different active sites display different activities and selectivities towards monomer insertion and hence exercise poor control over polymer architecture, resulting in polymers having broad molecular weight distributions and non-uniform comonomer distributions, thereby influencing the product morphology, processability and properties.

With respect to controllability of the polymer architecture, homogeneous catalysts offer advantages over heterogeneous catalysts. Due to the single site character of these catalysts, the active sites exhibit uniform behavior. The discovery of methylalumoxane (MAO) as an efficient cocatalyst for homogeneous single site catalysts (metallocenes) in 1976 by Walter Kaminsky and Hansjörg Sinn,⁵ started a new era in the polyolefin industry. The discovery and use of MAO as a cocatalyst led to extremely active homogeneous ethylene polymerization catalysts. Tailor-made monodisperse polymers with well-defined architectures, microstructures and properties could be produced due to the advantages of being able to tune the ligands of the catalyst.

Metallocenes have been mainly used to synthesize HDPE, PP (isotactic and syndiotactic), and copolymers of ethylene with α -olefins (LLDPE).⁶ Typically a metallocene catalyst is a sandwich complex with a transition metal coordinated to two cyclopentadienyl derivatives (Figure 1.3). Unbridged catalysts such as $(C_5Me_5)_2ZrCl_2$ (**1**), $(Indenyl)_2ZrCl_2$ (**2**) and bridged metallocenes such as $[Me_2Si(Indenyl)_2]ZrCl_2$ (**3**), $[Me_2Si(2,4,7-Me_3-Indenyl)_2]ZrCl_2$ (**4**), $[C_2H_4(Indenyl)_2]ZrCl_2$ (**5**) are some of the systems which are highly active for α -olefin polymerization.⁶ Depending on the symmetry of the catalyst and the substituents on the cyclopentadienyl ring polypropylene with different tacticity can be produced.

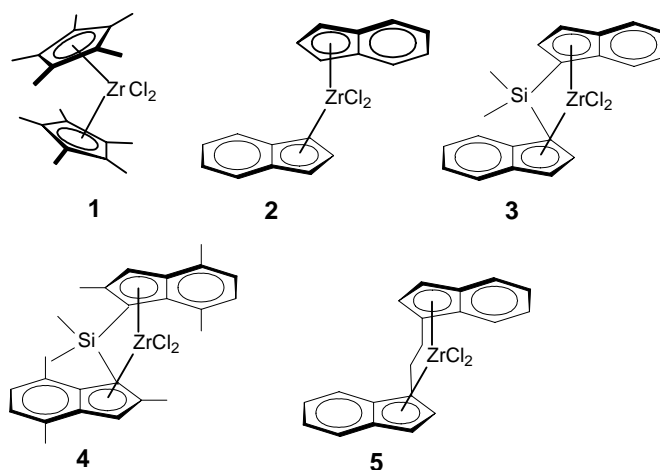


Figure 1.3 Highly active metallocene catalysts for the polymerization of α -olefins.

Highly isotactic PP is obtained with C_2 -symmetric ansa-metallocene complexes such as $[Me_2Si(2-Me-4-naphthylindenyl)_2]ZrCl_2$ ⁷ and $[Me_2Si(2-Me-4-phenylindenyl)_2]ZrCl_2$ ⁷ or $[Me_2Si(2,3,5-Me_3-Cp)_2]HfCl_2$.⁸ The C_1 -symmetric complex $Me_2C(3-MeCp)(Flu)ZrCl_2$ produces hemiisotactic PP.^{9a} However, if the methyl group at the 3-position of the cyclopentadienyl ring is replaced by a *tert*-butyl group, *i*-PP is formed. Interestingly, the use of oscillating metallocenes $(2-phenylindenyl)_2ZrCl_2$ has been reported to produce atactic and isotactic PP block copolymers and the C_s -symmetric $[Me_2C(Flu)(Cp)]ZrCl_2$ produces syndiotactic PP.^{6,9b} After the success of metallocenes, additional catalyst families have been developed based on mono-cyclopentadienyl or non-cyclopentadienyl ligands using transition metals from group 3 to 10 of the periodic table. With these post-metallocene catalysts a wide range of polyolefins can be produced. The constrained geometry catalyst $[Me_2Si(C_5Me_4)(N-*t*-Bu)]TiCl_2$ ^{6,10} enables polymerization of ethene with 1-octene resulting in C_6 -branched PE. These catalysts have a very high comonomer affinity resulting in re-incorporation of polymer

chains having an unsaturated chain end (long chain branching). In addition, with complexes of the type $[\text{Me}_2\text{Si}(\text{Flu})(\text{N}-t\text{-Bu})]\text{TiMe}_2$ syndiotactic PP can be obtained.¹¹ Recently, Fujita *et al.*¹² discovered post metallocene catalysts based on phenoxy-imine chelate ligands (FI) with group 4 transition metals. When activated by a cocatalyst under mild conditions these catalysts proved to be at least as active as metallocenes for the polymerization of ethylene at moderate temperatures. By simply varying the ligand structure of this class of catalyst or the nature of the cocatalyst, polyethylene with a wide range of molecular weights can be synthesized with narrow molecular weight distribution. The titanium catalyst $[3-t\text{-Bu-2-O-C}_6\text{H}_3\text{CH}=\text{N}(\text{C}_6\text{F}_5)]_2\text{TiCl}_2$ is the first example of a polymerization catalyst that promotes living polymerization of ethylene even at 50°C.

Iron based catalysts with bis(imino) pyridine ligands yield HDPE.¹³ With the catalysts based on late transition metals like nickel and palladium, it is possible to either synthesize HDPE or highly branched amorphous polyethylene (Figure 1.4) from ethylene alone. Cationic palladium α -diimine complexes afford LLDPE-like polymers at low pressure whereas the nickel based polyethylene is linear. Therefore, depending on the catalyst used and on the process conditions applied a diverse range of polymers, from highly branched amorphous polyethylene as viscous oils (at low pressure) via less branched thermoplastic elastomers (at higher pressure) to linear PE (with specific catalyst variations), can be produced. Therefore a rubbery material, equivalent to an ethylene-propylene rubber (EPR), could be produced from only ethylene monomer using a cationic α -diimine based palladium catalyst.

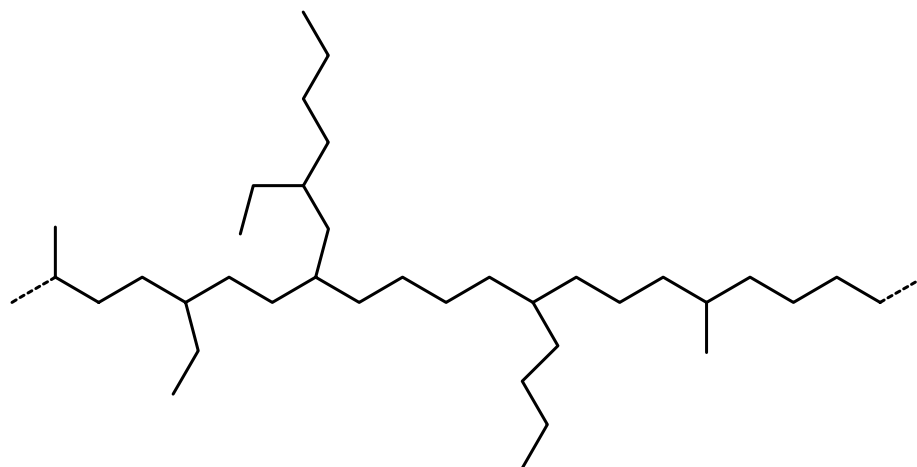


Figure 1.4 The structure of rubbery polymers formed with a homogeneous cationic α -diimine based palladium catalyst.

A detailed examination of these rubbery polymers showed not only the presence of methyl branches but also of longer alkyl branches such as *sec*-butyl ended branched and larger branches on branches (Figure 1.4). As shown above with these new homogeneous catalysts new polymer microstructures have been reported that were not accessible with traditional heterogeneous Ziegler-Natta catalysts. For slurry and gas phase processes, however, a heterogeneous catalyst is required. Most of the commercial production of polyolefins today takes place using heterogeneous catalyst technology. As many other factors influence the economics of olefin polymerization processes, only a few grades of polyethylene, mainly LLDPE (a copolymer of ethylene and an α -olefin such as butene, hexene or octene) and a small fraction of polypropylene are commercially synthesized using homogeneous catalysts in solution processes.

1.3 Crystallization of Polymers.

Crystallizable polymers are different from normal crystalline solids in that they possess amorphous segments and therefore are generally semi-crystalline. The crystallinity of polymers is governed by the extent of branching (number and type) (Figure 1.1), type and composition of comonomers and by tacticity (isotactic, syndiotactic, atactic) (Figure 1.5). For example, polymers with long chain branching or atactic polymers are usually non-crystalline. On the other hand isotactic and syndiotactic polymers or copolymer of ethylene with small amount of propylene have the ability to crystallize. The degree of crystallinity as well as the T_g determines the brittleness or toughness of the polymer. In addition, the size and the spatial arrangement of the crystallites profoundly influence the physical and mechanical properties of the polymer.

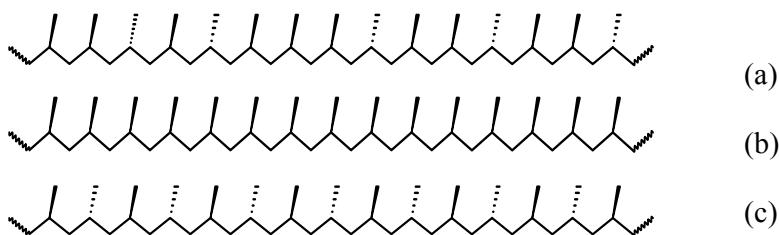


Figure 1.5 Polypropylene with different tacticity (a) completely amorphous atactic PP (b) semi-crystalline isotactic PP (c) semi-crystalline syndiotactic PP.

The drive towards crystallization in polymers can be understood from the thermodynamics of the process.¹⁴ In the molten state the polymer chains are in the random coil configuration and are entangled which is an entropy driven process. However, when the melt is cooled slowly, the polymer molecules arrange themselves in a regular fashion to attain a state of minimum free energy. There are a number of factors that influence the rate of crystallization and the resulting degree of crystallinity such as the rate of cooling from the melt, presence of nucleating agents, molecular weight and molecular weight distribution of the polymer, the amount of branching etc. If the cooling rate is very fast then the polymer may not crystallize at all, leading to a completely amorphous polymer. The process is in this case kinetically controlled.

By using X-ray diffraction techniques it is possible to determine the crystal structure of a polymer. Generally, in a crystal the polymer chains tend to align resulting in an orientation along a particular direction. A unit cell may consist of hundreds of atoms belonging to the repeating segments of a polymer chain, with several segments packed together in a crystal. The polymer chains fold back and forth in the crystal and a single chain can be part of two or more crystals giving rise to inter-crystallite links. The fold surface and the connectors or tie molecules form the amorphous regions in the polymer.

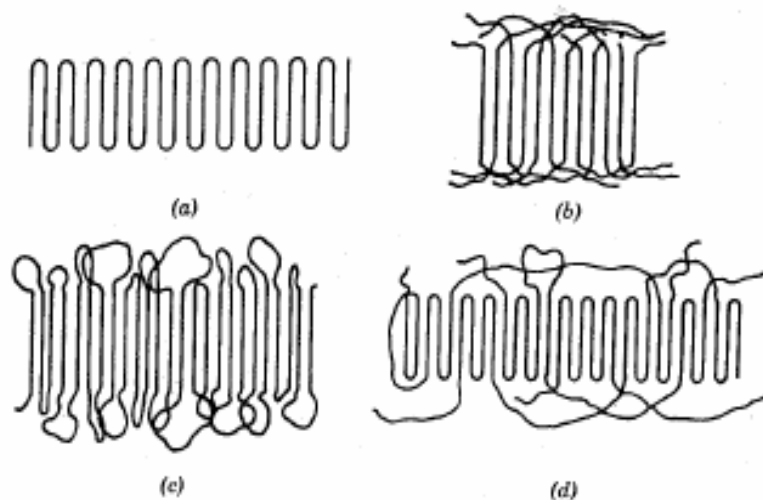


Figure 1.6 Schematic representation of models of the fold surfaces in polymer single crystals (a) sharp folds (b) switchboard model (c) loose loops with adjacent re-entry (d) a combination of several features.¹⁵

Crystallization of Polyethylene.

Polyethylene is one of the most studied polymers due to its wide application. Figure 1.6 shows different kinds of folds that arise at the surface of lamellae. Solution grown polyethylene crystals form plate-like lamellar single crystals. The chains in a lamellar single crystal are perpendicular to the plane of the lamella as shown in Figure 1.7b.¹⁶ The thickness of the lamella is of the order of 100 Å although the length of a polymer chain is of the order of several thousands of Ångstroms. Therefore the chains must fold back and forth between the top and bottom surface of the lamellae.¹⁷⁻²⁰ A linear polyethylene with a molar mass of 100,000 would require about seventy foldings for a lamellae with a thickness of 120 Å.¹⁸ Since linear high molecular weight polyethylene is more coiled than low molecular weight analogs, a higher temperature is required for crystallization from dilute solutions.²¹ Lamellar single crystals grown from dilute solutions are often accompanied by the formation of spiral structures called screw dislocations (see Figure 1.7a).²² Screw dislocations are believed to occur during collision between two growing single crystals.

Melt crystallized polymer consists of a ball like morphology called spherulites. Spherulites are formed by radial branching out of single folded chain lamellae in a three dimensional space and have more or less the same thickness as the solution grown crystals as shown in Figure 1.7c.

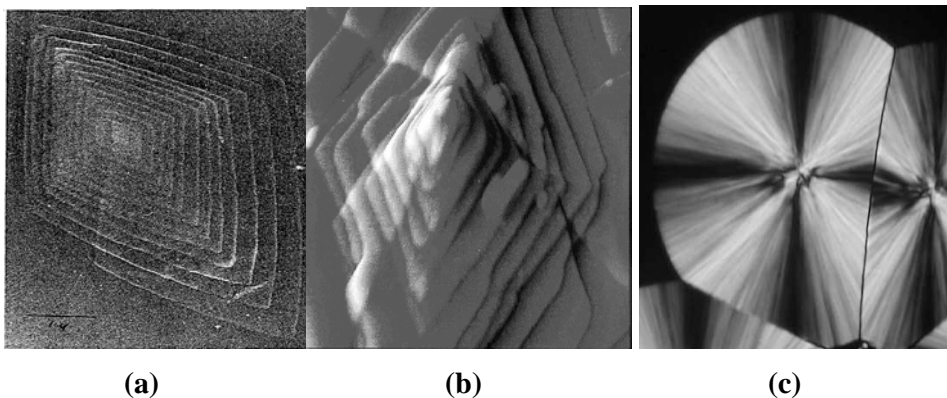


Figure 1.7 (a) Electron micrograph of lamellar growth of solution grown single crystal of polyethylene with screw dislocation.¹⁶ (b) AFM imaging of stacked array of lamellar single crystal of polyethylene.²³ (c) Optical micrograph showing spherulitic growth of melt crystallized polymer.²⁴

Solution grown lamellar crystals and melt crystallized spherulitic crystals of polyethylene have a completely different morphology. When synthesized in a solvent below the melt temperature, polyethylene will precipitate out. The nascent morphology, obtained upon polymerization, is considerably influenced by the polymerization conditions such as structure of the catalyst and co-catalyst and by the polymerization temperature. Various morphologies have been reported in the literature such as fibrillar, globular, cobweb, ribbon like, worm like, nodular, and lamellar depending on the polymerization conditions for the polymer produced by Ziegler- Natta catalyst.²⁵ Another striking feature of nascent polyethylene is the destruction of this unique morphology on annealing or melting and re-crystallization. The nascent UHMWPE crystals have a higher melting point than the solution or melt crystallized samples.²⁶ A remarkable advantage of using nascent powders is that the processability and the flow characteristics of the polymer can be influenced by the synthesis conditions. The significant discovery that some nascent UHMWPE could flow below the melting point on compression, whereas other samples of nascent UHMWPE could only be sintered, was assigned to a lower degree of entanglement of the former.²⁷

1.4 Processing of Polyolefins.

Generally polymers are shaped into final products by molding, extrusion or casting, which can be accomplished at much lower temperature than required for shaping steel, aluminum or glass and hence are cost effective. The common processing techniques usually employed for polyolefins are film extrusion (LDPE, LLDPE, HDPE, PP) ram extrusion (UHMWPE), blow molding (HDPE, PP), injection molding (HDPE, PP) compression molding (UHMWPE, PTFE) or fiber extrusion (PP).²⁸ Depending on the processing techniques and temperatures employed, the ultimate properties of the final product can be influenced. For instance, high performance fibers formed from polyethylene possess much better mechanical properties than polyethylene bottles when made from the same PE grade due to different processing techniques employed.

Processing of a polymer depends on its flow behavior which modifies the orientation of the long chain. The flow behavior of a polymer is in turn determined by the polymer architecture, degree of cross linking, molecular weight, molecular weight distribution, amount of entanglements, presence of additives and by the temperature and pressure at which they are pressed. Many of the above factors are influenced by the conditions employed during polymer synthesis. Therefore the flow behavior and hence the processability of a polymer can

be influenced considerably by the way it is synthesized. Semi-crystalline polymers are usually processed at high temperature, above their melting point and depending on the molecular weight, amount of entanglements and molar mass distribution exhibit high viscosities. The viscosity in the polymeric system increases considerably with molecular weight.²⁹

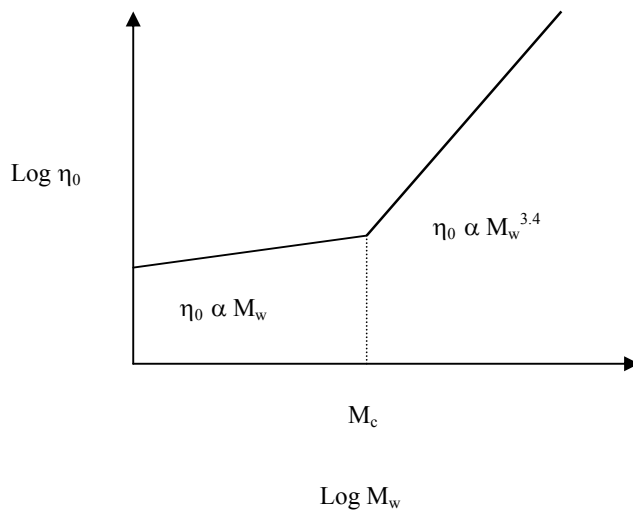


Figure 1.8 Plot representing the relation between zero shear viscosity (η_0) and molecular weight (M_w).

Up to the critical molar mass (M_c ; typically twice the length between entanglements M_e), the viscosity increases linearly with the molecular weight.²⁹ Above the entanglement molar mass the viscosity builds rapidly as shown in Figure 1.8 due to an increase in the amount of entanglements resulting in poor flow properties and difficult processability. Therefore, ultra high molecular weight polymers (UHMWPE) display poor processability and the finished products of UHMWPE possess fusion defects or grain boundaries. The presence of grain boundaries may lead to poor mechanical performance of the polymer.

Processing of UHMWPE.

UHMWPE has outstanding physical and mechanical properties such as high abrasion resistance, high impact toughness, good corrosion and chemical resistance, resistance to cyclic fatigue, and resistance to radiation.³⁰ Due to its excellent properties UHMWPE finds use in highly demanding applications³¹ including artificial implant materials.³²

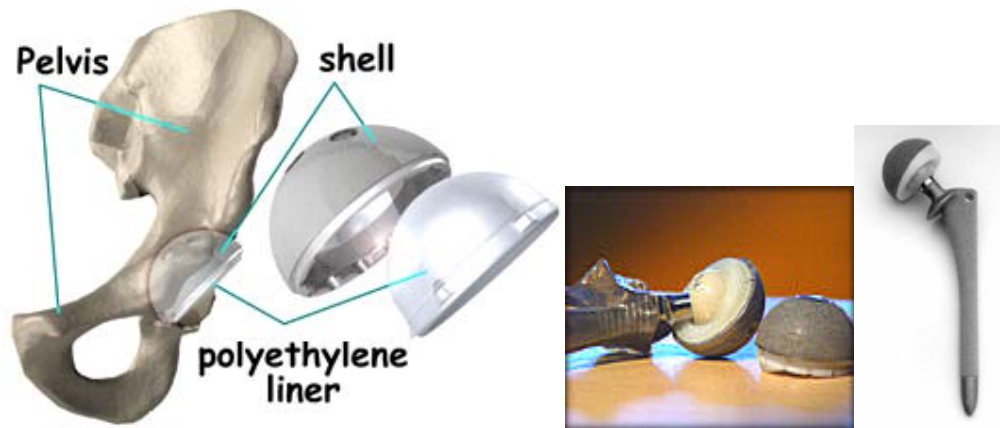


Figure 1.9 Picture shows the use of a UHMWPE component at the interface of metallic components in the artificial hip prosthesis.^{33,34}

The basic requirements for any medical implant material are: biological stability, biocompatibility, high toughness, high creep resistance, low friction, and low wear.³⁵ In the case of hip and knee joint prostheses, UHMWPE has been used at the interface of artificial joints. The hip cup is covered by a layer UHMWPE (10 mm thick) as shown in Figure 1.9. The use of a UHMWPE sheet in such an application reduces the friction when the hip cup moves against the artificial femoral head. Artificial joints made with UHMWPE can function well for twenty years if they are well-designed and well-implanted, but the use of UHMWPE in hip and knee prosthesis is often associated with major problems.^{30,36} One major problem associated with the hip prosthesis is the adhesive wear of this material. In the case of hip implants, sub-micron particles are released from the surface of the polyethylene (over 50,000 particles per step), leading to inflammatory response and subsequent loosening of the implant.³⁷⁻⁴¹ This is caused by cyclic articulation of the polymer cup against the metal, which in turn causes localized stress build up at the ball/socket interface. As a result, small fractions of UHMWPE adhere to the metal ball. These fractions break off in due course to form sub micrometer-sized particles. In the case of knee joints, failure of the implant generally occurs due to crack propagation through the existing fusion defects. For both hip and knee implants one of the possible causes for these problems have been poor processability and consequently poor homogeneity of the processed product obtained from such a high molecular weight material.

UHMWPE cannot be processed via conventional processing routes such as injection moulding, blow molding etc. UHMWPE is usually processed via compression molding or

ram-extrusion⁴² as the former methods would involve a very viscous melt. Regardless of the process applied, today all products of UHMWPE possess fusion defects or grain-boundaries due to which UHMWPE eventually fails in many applications.⁴³

The origin of grain boundaries can be traced back to the conditions during synthesis. In industry, UHMWPE is synthesized by a slurry process using a heterogeneous Ziegler-Natta catalyst with a hydrocarbon as diluent.⁴⁴ As the active sites in such catalyst systems are relatively close together, the chains grow in close proximity to each other. Due to the relatively high polymerization temperature of 60-100°C, crystallization of the polymer chains is relatively slow and the resulting polymer has a very high degree of entanglements. Due to the nature of this process, essentially every catalyst particle leads to a product polymer particle with (sub) millimeter dimensions (1 mg polymer particle of a polymer with a 1 million g/mol molecular weight contains 10^{14} entangled chains). Because of the high molecular weight and high degree of entanglements, the mobility of these chains is very limited and complete fusion of these polymer particles during processing is impossible to achieve. Thus the structure created during synthesis of the polymer affects the final properties of the polymer.

A considerable amount of research is being done to improve the wear life-time of these polymers for the hip prosthesis. Two different approaches have been reported in the literature to improve the mechanical performance of the UHMWPE products. One method involves addition of fillers, whereas the other approach focuses on improving the processability of UHMWPE. For example, Howdle *et al.*⁴⁵ have proposed the use of supercritical carbon dioxide to disperse silver particles in the UHMWPE matrix. Elsewhere they have reported blending of UHMWPE with polymethylmethacrylate (PMMA) as a possible solution to tackle the problem.⁴⁶ Another method described in the literature to improve the performance of this polymer is based on inclusion of multi-walled carbon nano-tubes, nano- Al_2O_3 particles or various other inorganic filler materials in the matrix.⁴⁷⁻⁴⁹ There are few main routes described in the literature to improve the processability of UHMWPE.

Rastogi, *et al.*⁵⁰ has tried to sinter the polymer via the hexagonal phase. With their study on a polymer obtained with a single site catalyst, they demonstrated how an initial lower entanglement density is crucial for obtaining a fully sintered material. In their study, they established a route to disentangle the chains by the intervention of the hexagonal phase at high temperature and pressure prior to melting. It was clearly shown that a fully fused material was obtained upon annealing of a less entangle metallocene grade polymer, at 4000

bars and 270°C for 12 hours. Another method involves dissolving the UHMWPE in a suitable solvent followed by ultra drawing (solution spinning), which affords highly aligned chains of UHMWPE fibers (Dyneema®).⁵¹

The commercial grade UHMWPE (broad MWD) is very suitable for some applications such as textiles, food and beverage industry, mining, ship building, transportation etc. However, thus obtained products suffer from serious disadvantages in medical applications where narrow molecular weight distribution⁵² and good homogeneity of the finished product are most desirable properties in order to improve the life-time of the artificial hip and knee prosthesis. In order to solve this problem, the challenge is to produce UHMWPE which not only has a narrow molecular weight distribution (for improving wear life time of hip cup) but also easy processability.

We here propose a novel route in which nascent UHMWPE with highly disentangled chains is synthesized by crystallization of the chains directly upon synthesis using homogeneous catalysts. We propose that when the temperature of polymerization is kept low, the chains begin to crystallize directly upon formation. Faster crystallization of the polymer chains upon formation in combination with sufficient dilution to keep the growing chains apart will facilitate the formation of polymers with highly disentangled chains. The use of homogeneous catalysts also allows the synthesis of polymers with narrow molecular weight distribution in addition to the unique morphology. The resulting polymer with highly disentangled chains can be processed into completely fused grain-boundary free material in the solid state and circumvents the use of high temperature and pressure as well as the use of large quantities of undesirable organic solvents. For highly demanding applications such as components of medical devices, where completely fused product is a pre-requisite, this new route is of significant importance. However, this new polymer production route has economical disadvantages over the existing production technology therefore may not be of interest for low end applications.

1.5 Scope of the Thesis.

Until now, UHMWPE has been synthesized using heterogeneous catalysts, where the active sites are not only relatively close to each other but also display different activities under a given set of polymerization condition leading to polymers with broad molecular weight distributions. In addition to that, since the growing chains are in close proximity to each

other, the resulting polymer has a very high degree of entanglement, raising the viscosity due to poor flow characteristics in the melt. In order to reduce the melt viscosity and hence improve the processability of the polymer we have investigated and proposed a new route to synthesize nascent UHMWPE with narrow molecular weight distribution which is discussed in detail in Chapters 2 & 3. Chapter 4 describes various characterization techniques such as drawing, compression molding, differential scanning calorimetry, and rheology used to study the effect of the polymerization conditions on the entanglement density. In addition, Chapter 4 describes the ease of processability of these polymers. A detailed investigation of the crystal structure of the nascent polymers and their crystallization behavior is discussed in Chapter 5. Finally the industrial relevance of the project is discussed.

1.6 References.

- (1) Fawcett, E. W.; Gibson, R. O.; Perrin, M. W.; Patton, J. G.; Williams, E. G. Imperial Chemical Industries Ltd. GB 471590, **1937**.
- (2) Hogan, J. P.; Banks, R. J. *United States Patent US2* **1958**, 825, 721.
- (3) (a) Ziegler, K.; Holzkamp, E.; Martin, H.; Breil, H. *Angew. Chem.* **1955**, 67, 541. (b) Ziegler, K. *Belgian Patent* **1954**, 533, 362. (c) Natta, G. *Angew. Chem.* **1956**, 68, 393. (d) Natta, G. *Mod. Plast.* **1956**, 34, 169. (e) Natta, G. *Angew. Chem.* **1964**, 76, 553.
- (4) Arlman, E. J.; Cossee, P. *J. Catal.* **1964**, 3, 99.
- (5) Hansjörg, S.; Walter, K.; Jürgen, V. H.; Rüdiger, W. *Angew. Chem.* **1980**, 92, 396.
- (6) (a) Brintzinger, H. H.; Fischer, D.; Mulhaupt, R.; Rieger, B.; Waymouth, R. M. *Angew. Chem. Int. Ed. Engl.* **1995**, 34, 1143. (b) Mahanthappa, M. K.; Cole, A. P.; Waymouth, R. M. *Organometallics*, **2004**, 23, 836-845.
- (7) Spaleck, W.; Kiiber, F.; Winter, A.; Rohrmann, J.; Bachmann, B.; Antberg, M.; Dolle, V.; Paulus, E. F. *Organometallics* **1994**, 13, 954.
- (8) Mise, T.; Miya, S.; Yamazaki, H. *Chem. Lett.* **1989**, 1853.
- (9) (a) Ewen, J. A.; Elder, M. J.; Jones, R. L.; Haspelslagh, L.; Atwood, J. L.; Bott, S. G.; Robinson, K. *Makromol. Chem., Macromol. Symp.* **1991**, 48-9, 253. (b) Ewen, J. A.; Jones, R. L.; Razavi, A.; Ferrara, J. D. *J. Am. Chem. Soc.* **1998**, 110, 6255.
- (10) Eberle, T.; Spaniol, P. T.; Okuda, J. *Eur. J. Inorg. Chem.* **1998**, 237.
- (11) Hasan, T.; Ioku, A.; Nishii, K.; Shino, T.; Ikeda, T. *Macromolecules* **2001**, 34, 3142.

- (12) Mitani, M.; Mohri, J. I.; Yoshida, Y.; Saito, J.; Ishii, S.; Tsuru, K.; Matsui, S.; Furuyama, R.; Nakano, T.; Tanaka, H.; Kojoh, S. I.; Matsugi, T.; Kashiwa, N.; Fujita, T. *J. Am. Chem. Soc.* **2002**, *124*, 3327.
- (13) Gibson, V.C.; Spitzmesser, S. K. *Chem. Rev.* **2003**, *103*, 283.
- (14) Fischer, E. W. *Nature* **1957**, *12a*, 753.
- (15) Billmeyer, F. W. Jr. *Text Book of Polymer Science*; John Wiley & Sons, Inc.: New York, 1984.
- (16) Ranby, B. G.; Morehead, F. F.; Walter, N. M. *J. Pol. Sci.* **1960**, *44*, 349.
- (17) Jaccodine, R. *Nature* **1955**, *176*, 305.
- (18) Till, P. H. *J. Pol. Sci.* **1957**, *17*, 447.
- (19) Keller, A. *Philos. Mag.* **1957**, *2*, 1171.
- (20) Stuart, H. A. *J. Pol. Sci.* **1959**, *34*, 721.
- (21) Holland, V. F.; Lindenmeyer, P. H. *J. Pol. Sci.* **1962**, *57*, 589.
- (22) Renekar, D. K.; Geil, P. H. *J. Appl. Phys.* **1960**, *31*, 1916.
- (23) <http://electron.mit.edu/~gsteale/mirrors/elchem.kaist.ac.kr/jhkwak/TopometrixWeb/apm mi01.htm>
- (24) Murayama, E. http://www.op.titech.ac.jp/lab/okui/murayam/ringed_en.pdf, **2002**.
- (25) Chanzy, H. D.; Revol, J. F.; Marchessault, R. H.; Lamandé, A. *Kolloid-Z. u. Z. Polymere* **1973**, *251*, 563.
- (26) Chanzy, H. D.; Bonjour, E.; Marchessault, R. H. *Coll. Pol. Sci.* **1974**, *252*, 8.
- (27) Smith, P.; Lemstra, P. J.; Booij, H. C. *J. Pol. Sci., Pol. Phys. Edn.* **1981**, *19*, 877.
- (28) Wilkinson, A. N.; Ryan, A. *J. Polymer Processing and Structure Development*; Kluwer Academic Publishers: Dordrecht, 1998.
- (29) Berry, G. C.; Fox, T. G. *Adv. Polym. Sci.* **1968**, Vol. 5, 261.
- (30) *Encyclopedia of Polymer Science and Engineering*; John Wiley & Sons: New York, 1985, Vol. 6, p 495.
- (31) Li, S.; Burstein, A. H. *Bone and Joint Surg.* **1994**, *76A*, 1080.
- (32) (a) Keller, A.; Hikosaka, M.; Toda, A.; Rastogi, S.; Barham, P. J.; Gooldbeck-Wood, G. *J. J. Mater. Sci.* **1994**, *29*, 2579; (b) Keller, A. *Philos. Trans. R. Soc. London* **1994**, *3*, A348.
- (33) <http://www.jointreplacement.com>
- (34) <http://www.aori.org/thr/thrwhat.html>
- (35) Barbour, P. S. M.; Stone, M. H.; Fisher, J. *Biomaterials* **1999**, *20*, 2101.
- (36) Kurtz, S. M.; Muratoglu, O. K.; Evans, M.; Edidin, A. A. *Biomaterials* **1999**, *20*, 1659.

-
- (37) Pazzaglia, U. E.; Ceciliani, L.; Wilkinson, M. J.; Dell'Orbo, C. *Arch. Orthop. Trauma Surg.* **1985**, *104*, 164-174.
- (38) Pazzaglia, U. E.; Wilkinson, M. J.; Dell'Orbo, C. *Arch. Orthop. Trauma Surg.* **1987**, *106*, 209.
- (39) Betts, F.; Wright, T.; Salvati, E. A.; Boskey, A.; Bansal, M. *Clin. Orthop.* **1992**, 276, 75.
- (40) (a) Huo, M. H.; Salvati, E. A.; Lieberman, J. R.; Betts, F.; Bansal, M. *Clin. Orthop.* **1992**, 276, 157. (b) McKellop, H. A.; Campbell, P.; Park, S. H.; Smalzried, T. P.; Grigoris, P.; Amstutz, H. C.; Sarmento, A. *Clin. Orthop. Relat. Res.* **1995**, *311*, 3.
- (41) Williams, R. P.; McQueen, D. A. *Clin. Orthop.* **1992**, 275, 174.
- (42) Cahn, R. W.; Hassen, P.; Kramer, E. J. *Materials science and Technology: Processing of polymers*; VCH: Weinheim, 1997; Vol 18.
- (43) Jenkins, H.; Keller, A. *Macromol. Sci. Phys. B* **1975**, *11*, 301.
- (44) Zwijnenburg, A.; Pennings, A. J. *Colloid Polym. Sci.* **1976**, *254*, 868.
- (45) Webb, P. B.; Marr, P. C.; Parsons, A. J.; Gidda, H. S.; Howdle, S. M. *Pure Appl. Chem.* **2000**, *72*, No. 7, 1347.
- (46) Busby, A. J.; Howdle, S. M. *Green Chemistry Network Symposium* **2002**.
- (47) Ruan, S. L.; Gao, P.; Yang, X. G.; Yu, T. X. *Polymer* **2003**, *44*, 5643.
- (48) Hongyan, G.; Chunxia, H. *China Plastic Industry* **2002**, *30*, 29.
- (49) Howard, E. G. *United States Patent* US 5352732, **1994**.
- (50) Rastogi, S.; Kurelec, L.; Lemstra, P. J. *Macromolecules* **1998**, *31*, 5022.
- (51) Smith, P.; Lemstra, P. J. *J. Mater. Sci.* **1980**, *15*, 505.
- (52) Tervoort, T. A.; Visjager, J.; Smith, P. *Macromolecules* **2002**, *35*, 8467.

Chapter 2

Synthesis of UHMWPE using a single site catalyst: bis[(pentamethyl)cyclopentadienyl] samarium (II) bis(tetrahydrofuran)

Synopsis: This chapter presents systematic investigation of a recently reported novel route to synthesize highly disentangled nascent UHMWPE with narrow molecular weight distribution. The effect of various polymerization conditions (dilution, temperature, pressure) on the activity of the catalyst and on the obtained molecular weight is presented. The mass transfer limitation of ethylene during the polymerization is also discussed.

2.1 Introduction.

In industry, UHMWPE is synthesized in a slurry process using a heterogeneous Ziegler-Natta catalyst with a hydrocarbon as diluent¹. The active sites in such a catalyst system are known to exist relatively close together, therefore the polymer chains grow in close proximity to each other. In addition a conventional heterogeneous catalyst contains different active sites which exhibit different activities thereby producing polymers with broad molecular weight distributions. Due to the relatively high polymerization temperature of 60-100°C in addition to the chains growing adjacent to each other, crystallization of the polymer chains is relatively slow and the resulting polymer has a very high degree of entanglement. Owing to the nature of this process, essentially every catalyst particle leads to a product polymer particle with (sub) millimeter dimensions (1 mg polymer particle of a polymer with a 1 million g/mol molecular weight contains 10^{14} entangled chains). High entanglement density poses restrictions to flow of the chains in the melt which results in improper fusion of the powder particles. Consequently, ultra high molecular weight polyethylene (UHMWPE) is difficult to process. Current processing techniques employed in the industry lead to products with non-homogeneous morphology and to the presence of grain boundaries.

One intriguing area of application of UHMWPE is in medical implants where a narrow molecular weight distribution (MWD) and a completely fused grain boundary free material are highly desirable for the ultimate performance under in-vivo conditions. The presence of grain boundaries leads to poor mechanical performance and insufficient lifetime of the artificial implants.

High entanglement density imparts excellent mechanical properties in the end application but causes restricted mobility of the polymer chains in the melt during processing. In order to improve the flow characteristics of the polymer chains and to reduce the melt viscosity, UHMWPE which has easy mobility in the melt is desired. Additionally, the molecular weight distribution should be low in order to improve the wear life-time of the artificial hip prosthesis.

Tervoort et al.² recently reported that monodisperse high molecular weight polyethylenes show a similar performance compared to UHMWPE with a broad molecular weight distribution. However, narrow MWD in HDPE will limit the processability of the material. In addition molecular weight distributions below 2 cannot be obtained in an economical process. Therefore we will focus on material with higher molecular weight (1-2 million g/mol) but

with slightly broader MWD (2-3). Polymers with this high molecular weight and relatively narrow MWD can be obtained in an economic fashion but their processability is poor. Therefore the challenge was to obtain easily processable UHMWPE by lowering the entanglement density as it has been shown that disentangled UHMWPE is well-processable.³ Lowering the entanglement density^{3,4} and thus the viscosity in the melt has been achieved by dissolving the polymer in a suitable solvent prior to polymer processing via solution spinning. This method is cumbersome and expensive.

Our strategy is to prevent entangling of polymer chains during the synthesis and hence to create a unique nascent morphology in UHMWPE. A remarkable advantage of nascent powders is that the morphology created during synthesis can have profound impact on processability and flow characteristics and subsequently on product properties such as improved mechanical performance of artificial implants.

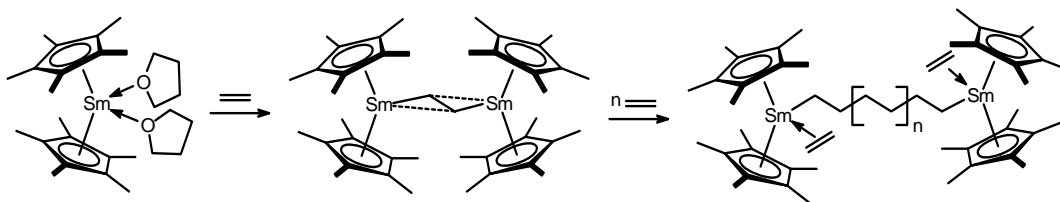
In order to control the molecular weight distribution, homogeneous complexes were used, which are single site in nature and hence display uniform activity and produce polymers with a narrow MWD.

It is proposed that when the temperature of polymerization is kept low, the chains will begin to crystallize during the polymerization when the crystallization rate is relatively fast compared to the polymerization rate ($R_{crys} > R_{polym}$). A sufficiently diluted system will result in greater separation of the active sites when compared to heterogeneous systems, leading to a unique morphology in the nascent state where the chains are highly disentangled. The resulting polymer with highly disentangled chains can be processed easily and subsequent curing should lead to completely fused grain-boundary free material.

The proper choice of catalyst and the appropriate polymerization conditions is crucial for the synthesis of UHMWPE with this unique morphology. Low temperature will facilitate high molecular weight and fast crystallization of polymer chains. To exclude any interference of molecular weight distribution, we preferred to use a living catalyst system. In a living catalyst chain transfer reactions do not occur and if all catalyst sites start polymerizing at the same time, a theoretical minimum MWD of 1 can be obtained. The major disadvantage of a living catalyst system is that only one polymer chain is produced by each catalyst site.

In the early eighties, it was discovered that organolanthanide complexes are highly active ethylene polymerization catalysts that typically do not create branches, nor incorporate α -olefins which results in completely linear polyethylenes.⁵⁻⁷ Several studies demonstrated that these lanthanocenes show living behavior, which in principle gives the opportunity to obtain

UHMWPE with a very narrow molecular weight distribution. Although lanthanocene hydrides of the type $\{\text{Cp}'_2\text{Ln}(\mu\text{-H})\}_2$ ($\text{Cp}' = \text{C}_5\text{Me}_5, \text{C}_5\text{H}_3(\text{CMe}_3)\text{SiMe}_3, 1/2 \text{Me}_2\text{Si}(\text{C}_5\text{Me}_4)_2$) are extremely active catalysts even at low temperature, the multi-step synthesis and extremely high reactivity of these species makes their use rather cumbersome. Evans and coworkers were the first to recognize that divalent lanthanide precursors $(\text{C}_5\text{Me}_5)_2\text{Ln}\cdot 2(\text{THF})$, available in a one step reaction of LnI_2 ($\text{Ln} = \text{Sm}, \text{Yb}$) with $\text{C}_5\text{Me}_5\text{K}$ in THF, could be oxidized to yield trivalent alkyl and hydride species.⁸ For example, $(\text{C}_5\text{Me}_5)_2\text{Sm}\cdot 2(\text{THF})$ reacts with ethylene via oxidative addition to form the dimeric trivalent complex $\{[(\text{C}_5\text{Me}_5)_2\text{Sm}]_2(\mu\text{-C}_2\text{H}_4)\}$, which with excess ethylene affords a living polymerization system that forms a polymer chain that grows at both ends (Scheme 2.1).^{7,9-13} These catalyst systems were found to be extremely active in the polymerization of ethylene without the use of any cocatalyst such as methylalumoxane.



Scheme 2.1 Activation of divalent precursor to trivalent active species by an ethylene molecule.

Yasuda¹⁴⁻¹⁸ used a related samarium system $\text{Me}_2\text{Si}[2(3),4\text{-(SiMe}_3)_2\text{C}_5\text{H}_2]_2\text{Sm}\cdot 2\text{THF}$ to homopolymerize ethylene to polyethylenes with a very high molecular weight ($M_n > 10^6$) and very narrow molecular weight distribution ($M_w/M_n = 1.6$).

As mentioned previously the samarocene catalyst does not require any cocatalyst and can be used as such in ethylene polymerization. As with aluminum alkyl scavengers a significant reduction in the molecular weight is observed. Therefore scavengers cannot be employed during polymerization when UHMWPE is the desired product. As a consequence, at the small scale we used, even with careful drying of solvents, a considerable fraction of the catalyst can be used up to scavenge impurities. Therefore the polymerizations require more catalyst than usual, especially due to the high dilution requirements.

2.2 Experimental Section.

2.2.1 General Comments.

All manipulations were performed under an argon atmosphere using a glovebox (Braun MB-150 GI) and Schlenk techniques. Solvents were distilled from Na/K alloy (petroleum-ether (40:60), and heptane), or dried over a Grubbs column (Al_2O_3 ; toluene) and stored under argon prior to use. The molecular weights and molecular weight distributions of the polymers were measured at 135°C by gel-permeation chromatography (GPC210, Polymer Labs) at the University of Groningen, the Netherlands, using 1,2,4-trichlorobenzene as solvent.

2.2.2 Catalyst synthesis.^{8,9}

Synthesis of $SmI_2 \cdot x(THF)$: A Schlenk flask was charged with Samarium metal (Aldrich) (1.94 g, 12.9 mmol) and THF (80 mL). To this suspension, a solution of ICH_2CH_2I in THF was added slowly (2.58 g, 9.1 mmol). To ensure complete reaction the mixture was refluxed for 17 hrs affording a blue THF solution of $SmI_2 \cdot x(THF)$ which was filtered to remove the excess of samarium and stored under argon prior to use.

Synthesis of C_5Me_5H : To a stirred solution of tetramethylcyclopentenone (15.27 g, 110.4 mmol) in diethyl ether (300 mL), CH_3MgCl (2.9M in THF) (38 mL, 110.2 mmol) was added dropwise at 0°C. The resultant solution was warmed to room temperature and stirred for 2 hours. The reaction was quenched slowly with ethanol after which water was added. The resultant milky white mixture was neutralized by adding concentrated hydrochloric acid. The organic layer was separated and dried over $MgSO_4$. Filtration and evaporation of the organic layer yielded an orange oil as the crude product. Distillation under reduced pressure afforded the pure compound in 60% yield.

Synthesis of C_5Me_5K : To a suspension of KH (1.77 g, 44.2 mmol) in THF (20 mL), C_5Me_5H (3.7 g, 27.15 mmol) was added dropwise at room temperature. The reaction mixture was stirred overnight and filtered. The white solid was washed with petroleum-ether (60:40) and dried under vacuum.

Synthesis of $(C_5Me_5)_2Sm \cdot 2(THF)$: A Schlenk flask was charged with C_5Me_5K (3.2 g, 18.35 mmol) and THF (30 mL). A THF solution of $SmI_2 \cdot x(THF)$ (80 mL) prepared as above was directly used as such and added to the suspension at room temperature. The color of the suspension immediately changed from dark blue to purple, and the reaction mixture was stirred overnight. The THF solvent was removed by vacuum to yield a gray solid. Toluene (100 mL) was then added and the resulting reaction mixture was stirred for 6 hours to yield a purple solution and a white precipitate. The white solid was separated by filtration and a clear purple filtrate was obtained. The solvent was removed under reduced pressure to yield a purple solid. Recrystallization of the solid from diethyl ether afforded the pure compound in 40% yield.

2.2.3 Polymerizations.

Polymerization (Pressure): To a stirred solution of ethylene in petroleum-ether (40:60 fraction; 80 mL), 14 μ mol of the catalyst $(C_5Me_5)_2Sm \cdot 2(THF)$ was added. The polymerizations were carried out in a 200 mL Büchi reactor, equipped with a mechanical stirrer, at 30°C and at different ethylene pressures: 1, 2 and 5 bar. The same experiment was repeated with toluene (80 mL) as solvent at an ethylene pressure of 5 bar at two different temperatures: 30°C and 50°C. The polymerizations were quenched after 15 minutes with methanol. The polymers were filtered, washed with acetone, and dried under vacuum at 60°C.

Polymerization (Dilution and Temperature): To a stirred solution of ethylene in petroleum-ether (40:60 fraction; 1 L), three portions of 14 μ mol each of the catalyst $(C_5Me_5)_2Sm \cdot 2(THF)$ were added with an interval of 5 minutes between the additions. The solvent was saturated with ethylene for 45 minutes prior to the addition of catalyst. The polymerization was performed using a magnetic stirring bar at 0°C at an ethylene pressure of 1 bar, with ethylene continuously bubbling through the solution. The polymerizations were carried out at different dilutions (42 μ mol of catalyst in 250, 500, and 1000 mL of solvent). The same polymerizations were repeated at a constant volume of 1 L at different temperatures (-10°C, 0°C, +10°C and +20°C) and ten times 2.8 μ mol of the catalyst $(C_5Me_5)_2Sm \cdot 2(THF)$ was added with an interval of one minute between the additions. The

polymerizations were quenched after 15 minutes with methanol. The polymers were filtered, washed with acetone, and dried under vacuum at 60°C.

2.3 Results and Discussions.

Since we anticipated that a lower temperature, low pressure and higher dilution would favor the synthesis of disentangled polymer chains, we studied the effect of dilution, temperature and pressure on the catalyst performance. The polymerizations were carried out in aliphatic hydrocarbon solvents as the polymer immediately precipitates out in this polymerization medium whereas in more polar solvents such as toluene it forms a gel, therefore enhancing the probability of the formation of highly disentangled chains. Since the dissolution of ethylene in the solvent is slow, ethylene was bubbled through the solvent with effective stirring. Preliminary polymerization results were anomalous with respect to the expected polymerization rates which appeared to be caused by mass transfer limitation.

2.3.1 Mass transfer of ethylene: preliminary polymerization experiments.

Mass transfer of ethylene plays an important role in obtaining a sufficiently high yield and molecular weight. Mass transfer of ethylene is affected by: (a) reaction temperature and pressure, (b) solubility of ethylene in the solvent, (c) degree of mixing in the reactors, (d) reactor geometry and (e) precipitated polymer in the medium.

The monomer concentration in solution is given by Henry's equation¹⁹:

$$C_M = K_H^0 \cdot \exp(E/RT) P_M \quad (1)$$

Where P_M is the monomer pressure (atm); $K_H^0 \cdot \exp(E/RT)$ is the Henry constant at temperature T ($\text{mol} \cdot \text{liter}^{-1} \cdot \text{atm}^{-1}$); C_M is the concentration of the monomer in solution ($\text{mol} \cdot \text{liter}^{-1}$); E is an empirical parameter ($\text{cal} \cdot \text{mol}^{-1}$) describing the dependence of K_H on temperature. For ethylene in heptane $K_H^0 = 1.15 \times 10^{-3} \text{ mol} \cdot \text{liter}^{-1} \cdot \text{atm}^{-1}$, $E = 2700 \text{ cal} \cdot \text{mol}^{-1}$.¹⁹ From the above equation it is clear that the dissolution and hence the concentration of ethylene will increase with decrease in polymerization temperature and increasing pressure. The concentration of ethylene drops from 0.2 M at -10°C to 0.1 M at +20°C. Therefore an

increase in temperature from -10°C to $+20^{\circ}\text{C}$ reduces the concentration of ethylene to 50% while at the same time the catalyst activity may have increased by one order of magnitude. Since catalysts can only react with the dissolved ethylene, the absolute amount of dissolved ethylene becomes very important when the propagation rate exceeds the dissolution rate. Thus at low solvent volume, although the molar concentration of ethylene dissolved in the polymerization medium is the same, the absolute amount of dissolved ethylene available at a given time will be lower compared to higher solvent volumes.

Table 2.1 *Effect of polymerization pressure and temperature.*

Entry	Temperature ($^{\circ}\text{C}$)	Pressure (bar)	Yield (g)	Concentration Of ethylene (moles/L)	M_w (kg/mol) ^b	D
1 ^a	30	1	-	0.1	-	-
2 ^a	30	2	0.4	0.2	1088	2.7
3 ^a	30	5	3.0	0.4	1428	1.5
4 ^b	30	5	1.2	0.5		
5 ^b	50	5	0.2	0.4	-	-

Polymerizations were carried out with (a) petroleum-ether (40:60) (80 mL). (b) With toluene (80 mL) as solvent.

In the first few minutes of the polymerization homogeneous catalysts are known to be extremely active, which at lower dilution and higher temperature and low pressure will quickly lead to monomer depletion. In order to demonstrate that ethylene dissolution in the polymerization medium indeed becomes the rate determining step, we carried out ethylene polymerizations at higher temperatures of 30°C and 50°C varying the pressure of ethylene from 1 to 5 bar using $(\text{C}_5\text{Me}_5)_2\text{Sm}\cdot 2(\text{THF})$.

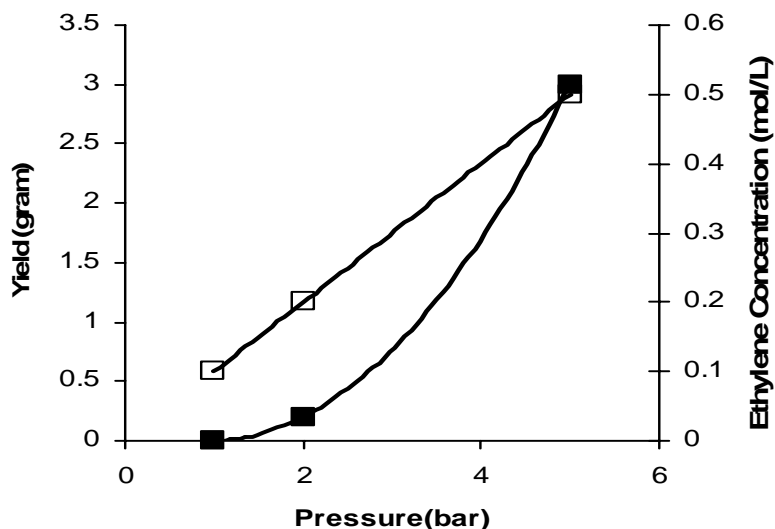


Figure 2.1 Influence of monomer pressure on the ethylene concentration (□) and the yield of the polymer (■) at 30 °C with 0.175 mM catalyst concentration.

Table 2.1 (entries 1-3) shows the results of ethylene polymerizations carried out at a constant volume of 80 mL with changing ethylene pressure at 30°C. It is seen that at low pressure (1-2 bar), the obtained yield is very low. When the pressure is raised to a higher value (Table 2.1, entry 3; Figure 2.1), the yield increases considerably. Changing the pressure from 1 to 5 bar at 30 °C the concentration of ethylene raises from 0.1 M to 0.5 M. The actual concentration of ethylene according to Henry's equation, at the beginning of polymerization drops from 0.5 M at 30°C to 0.4 M at 50 °C when the polymerization is carried out at 5 bar. With the increase in temperature from 30 to 50°C, the yield of the polymer drops drastically. Earlier reports on polymerization experiments using the same samarocene catalyst in a hydrocarbon solvent showed that the catalyst is thermally stable at higher temperature. Therefore, the drop in yield can only be explained by thermal decomposition of the catalyst in toluene. Therefore the samarium catalyst will only be used in hydrocarbon solvent in future experiments. Even though the amount of solvent used in the polymerizations is low (80 mL), the diffusion limitation can be overcome with the increase of pressure as shown in Table 2.1 where polymerization rate increases drastically with the increase of pressure. Although a clear trend relating the yield to varying temperature and pressure is seen, the yields obtained are quite low due to the low volume of solvent used. In order to avoid mass transfer limitations as well

as temperature overshoot in further experiments, we have used larger volume of solvent and low pressure.

2.3.2 Effect of Dilution during Polymerization.

Table 2.2 shows that with increasing amount of solvent, the yield and the molecular weight of the polymer obtained increases. Except for the amount of the solvent, all other conditions were maintained constant. Given that the dissolution of ethylene in the solvent is slower than the consumption of ethylene, mass transfer becomes the rate determining step at higher catalyst concentration and the system becomes diffusion controlled. Owing to higher molar concentration of the catalyst in a less diluted system (0.168 mM), the yield and the molecular weight of the polymer decrease. In a highly diluted catalyst system, the ethylene concentration will remain more or less constant and relatively high resulting in an increase in the yield and molecular weight (see Figures 2.2 & 2.3). The effect of dilution on the entanglement density is discussed in Chapter 4.

Table 2.2 Effect of dilution during polymerization.

Solvent (mL)	Yield (g)	M _w (kg/mol) ^a	D
250	0.4	1038	1.5
500	1.6	1769	1.6
1000	6.0	1700	4.2
1000*	9.0	2361	2.8

Polymerizations were carried out with (C₅Me₅)₂Sm-2(THF) (14 μmol × 3); ethylene (1 bar); 0°C; 15 minutes; petroleum-ether (40:60) (1 L); *with mechanical stirring. (a) Determined by GPC.

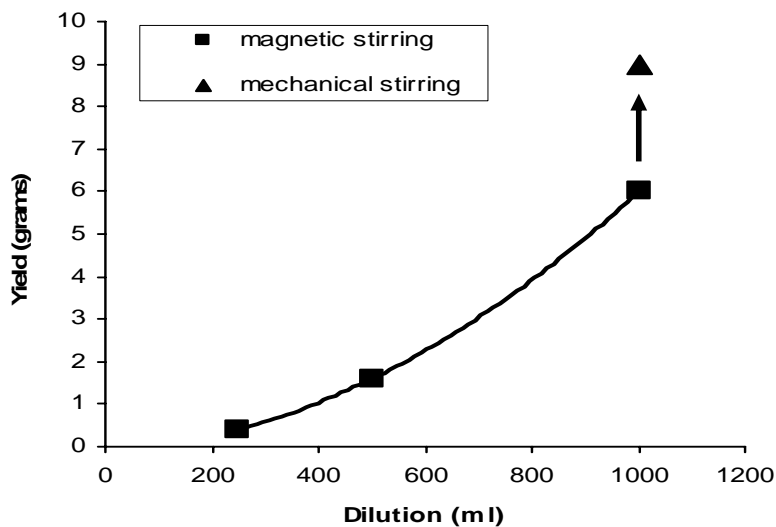


Figure 2.2 Influence of dilution on the yield of UHMWPE obtained using the $(C_5Me_5)_2Sm \cdot 2(THF)$ at $0^\circ C$.

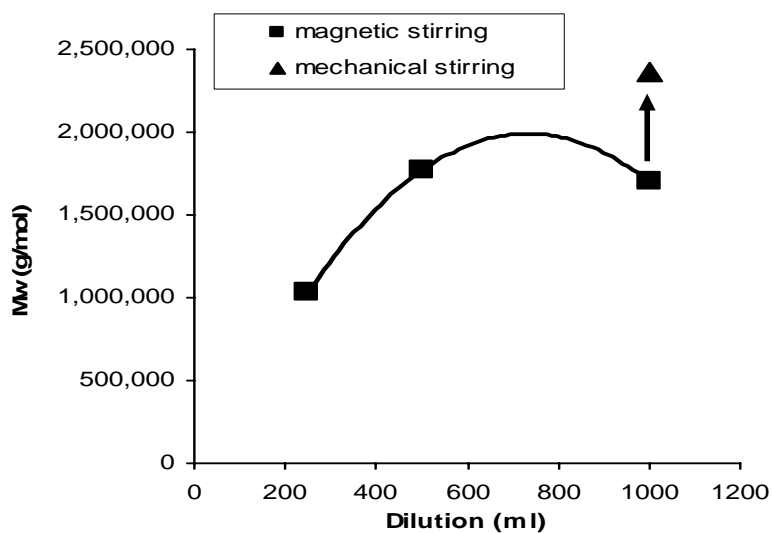


Figure 2.3 Influence of dilution on the M_w of UHMWPE obtained using the $(C_5Me_5)_2Sm \cdot 2(THF)$ at $0^\circ C$.

An important observation was that effective stirring plays a very important role in terms of yield, even at this small laboratory scale. When a mechanical stirrer was used instead of a magnetic stirring bar, the yield increased considerably. This observation prompted us to run the polymerizations using a mechanical stirrer for further studies. Another interesting

observation is that at low dilutions, e.g. 250 mL (0.168 mM) and 500 mL (0.084 mM), bubbling of ethylene through the solvent versus leading ethylene into the head space during the polymerization using magnetic stirring had no effect on the yield and molecular weight. In order to study as to how polymerization temperature affects the entanglement density which is discussed in chapter 4, the polymerization temperature was varied at constant dilution.

2.3.3 Effect of Polymerization Temperature.

Table 2.3 shows that, at -10°C , the catalyst activity is very low. This is evident from the low yield and molecular weight of the polymer, although the amount of dissolved ethylene is the highest at such low temperatures (according to equation 1). With a 10°C rise in temperature, the activity of the catalyst increases considerably.

Table 2.3 Effect of polymerization temperature.

Temperature ($^{\circ}\text{C}$)	Yield (g)	M_w (kg/mol) ^a	D
-10	2.4	1225	2.0
0	13.0	2040	2.5
+10	16.7	2265	2.7
+20*	14.0	1368	3.2

Polymerizations were carried out with $(\text{C}_5\text{Me}_5)_2\text{Sm}\cdot 2(\text{THF})$ ($2.8\ \mu\text{mol} \times 10$); ethylene (1 bar); petroleum-ether (40:60) (1 L); 15 minutes; * catalyst addition was $2.8\ \mu\text{mol} \times 7$ times. (a) Determined by GPC.

Figures 2.4 and 2.5 show that up to $+10^{\circ}\text{C}$ with the increase in temperature the catalyst activity increases, resulting in higher yield and higher molecular weight. At $+20^{\circ}\text{C}$ the lower yield and lower molecular weight may result from lower ethylene concentration and increased chain transfer, respectively.

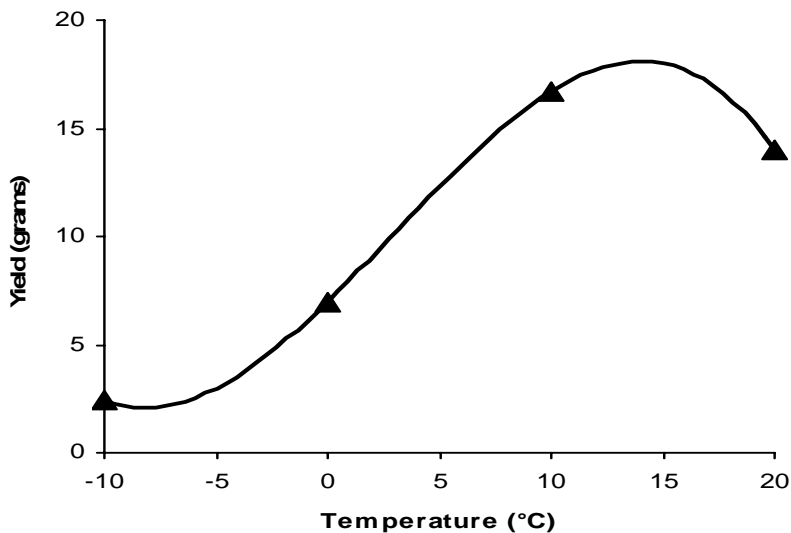


Figure 2.4 Influence of polymerization temperature on the yield of UHMWPE obtained using the $(C_5Me_5)_2Sm \cdot 2(THF)$.

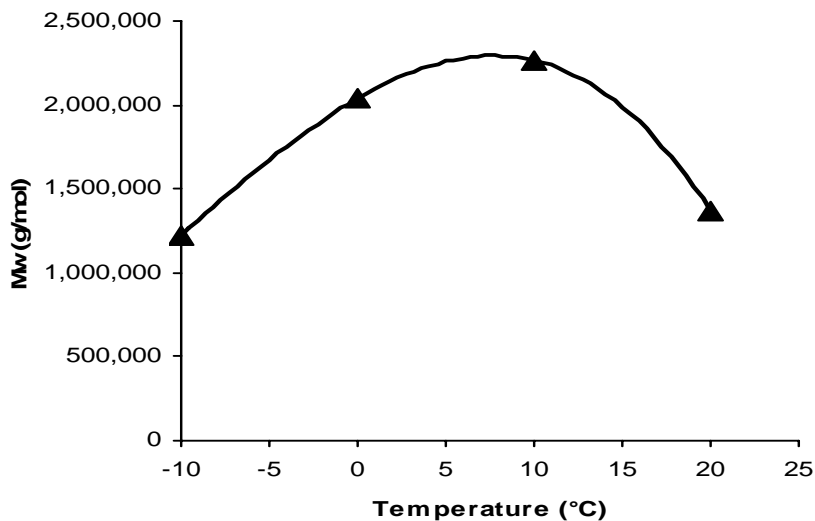


Figure 2.5 Influence of polymerization temperature on the M_w of UHMWPE obtained using the $(C_5Me_5)_2Sm \cdot 2(THF)$.

It is not surprising that the MWD of the UHMWPE synthesized with the samarocene is higher than expected for a truly living catalyst as shown in Table 2.3, due to heterogenization of the system during polymer synthesis.²⁰ The further broadening of MWD in combination with the lowering of molecular weight with increase in the polymerization temperature indicates that chain termination occurs at higher temperatures, transforming the catalyst from

a living system to non living catalyst system. Recently, Chirinos *et al.*²¹ reported a similar drop in the activity of their catalyst on increasing the temperature.

2.4 Conclusions.

In this chapter, the influence of varying the dilution and temperature on the activity of the catalyst and molecular weight of the produced polyethylene was investigated. It is shown that the polymers synthesized using $(C_5Me_5)_2Sm \cdot 2(THF)$ under various polymerization conditions are all UHMWPE with very narrow molecular weight distribution. The results presented in this chapter show that increasing the dilution results in an increase in the yield and molecular weight due to a larger initial (absolute) amount of dissolved ethylene in the system, whereas increasing the temperature results in increase in the yield and molecular weight up to +10°C. The drop in yield and molecular weight thereafter is related to diffusion limitation of ethylene and chain termination reactions that are likely to occur at higher temperatures. Besides it is also shown in this chapter that dissolution of ethylene can be a rate determining step in these polymerizations. It is expected that lower temperature and higher dilution favors the synthesis of highly disentangled UHMWPE which is necessary for the easy processability of the polymer. The influence of dilution and temperature on the entanglement density and hence the ease of processing of nascent UHMWPE will be discussed in Chapter 4.

Since this catalyst does not allow the use of scavengers, the catalyst precursor itself is used to scavenge the impurities in the polymerization medium which makes this catalyst very impractical. Therefore, other homogeneous catalysts were explored which allow the use of scavengers, polymerize ethylene to nascent UHMWPE at low temperature and are cost effective. It will be shown in Chapter 3 a different homogeneous catalyst that is capable of making UHMWPE at low temperature can produce nascent UHMWPE with narrow molecular weight distribution.

2.5 References.

- (1) Zwijnenburg, A.; Pennings, A. J. *Colloid Polym. Sci.* **1976**, *254*, 868.
- (2) Tervoort, T. A.; Visjager, J.; Smith, P. *Macromolecules* **2002**, *35*, 8467.
- (3) Rastogi, S.; Kurelec, L.; Lemstra, P. J. *Macromolecules* **1998**, *31*, 5022.
- (4) Smith, P.; Lemstra, P. J. *J. Mater. Sci.* **1980**, *15*, 505.

- (5) Watson, P. L.; Whitney, J. F.; Harlow, R. L. *Inorg. Chem.* **1981**, *20*, 3271.
- (6) Watson, P. L.; Herskovitz, T. *ACS Symp. Series*, **1983**, *212* (Initiation Polym.), 459.
- (7) Jeske, G.; Schock, L. E.; Swepstone, P. N.; Schumann, H.; Marks, T. J. *J. Am. Chem. Soc.* **1985**, *107*, 8103.
- (8) Evans, W. J.; De Coster, D. M.; Greaves, J. *Macromolecules* **1995**, *28*, 7929.
- (9) Gruter, G. J. M.; Wang, B.; van Beek, J. A. M. *European Patent Application* EP 1057837 A1 **2000**.
- (10) Evans, W. J.; Bloom, I.; Hunter, W. E.; Atwood, J. L. *J. Am. Chem. Soc.* **1981**, *103*, 6507.
- (11) Evans, W. J.; Grate, J. W.; Choi, H. J.; Bloom, I.; Hunter, W. E.; Atwood, J. L. *J. Am. Chem. Soc.* **1985**, *107*, 941.
- (12) Evans, W. J.; Bloom, I.; Hunter, W. E.; Atwood, J. L. *Organometallics* **1985**, *4*, 112.
- (13) Evans, W. J.; Hughes, L. A.; Hanusa, T. P. *Organometallics* **1986**, *5*, 1285.
- (14) Ihara, E.; Nodono, M.; Yasuda, H. *Macromol. Chem. Phys.* **1996**, *197*, 1909.
- (15) Yasuda, H.; Ihara, I.; Morimoto, M.; Nodono, M.; Yoshioka, S.; Furo, M. *Macromol. Symp.* **1995**, *95*, 203.
- (16) Matyjaszewski, K.; Gaynor, S. C.; Greszta, D.; Mardare, D.; Shigemoto, T.; Wang, J.-S. *Macromol. Symp.* **1995**, *95*, 217.
- (17) Yasuda, H.; Ihara, E. *Macromol. Chem. Phys.* **1995**, *196*, 2417.
- (18) Yasuda, H.; Ihara, E. *Bull. Chem. Soc. Jpn.* **1997**, *70*, 1745.
- (19) Kissin, Y. V. *Isospecific Polymerization of Olefins with Heterogeneous Ziegler-Natta Catalysts*; Springer-Verlag: New York inc., 1985, p 3.
- (20) Schaverien, C. J.; Ernst, R.; Schut, P.; Dall'Occo, T. *Organometallics* **2001**, *20*, 3436.
- (21) Chirinos, J.; Arévalo, J.; Rajmankina, T.; Morillo, A.; Ibarra, D.; Bahsas, A.; Parada, A. *Polym. Bull.* **2004**, *51*, 381.

Chapter 3

Nascent UHMWPE obtained using homogeneous catalysts: *exploring the versatility of the catalysts to generate UHMWPE with unique morphology.*

Synopsis: This chapter focuses on examining the potential use of different homogeneous catalysts to synthesize highly disentangled nascent UHMWPE with narrow molecular weight distribution. Two living homogeneous post metallocene catalysts were selected to generate the unique morphology in the nascent state which might benefit the processability of the material. Several polymerization conditions (dilution, temperature, pressure, cocatalyst) were varied to study their effect on the catalyst activity, molecular weight and the entanglement density.

3.1 Introduction.

The chemistry of catalytic olefin polymerization by various single site catalysts, especially the group 4 transition metal based compounds, has been of great importance in the past few decades.¹⁻³ Extensive studies on metallocene complexes involving cyclopentadienyl ligands have contributed towards greater understanding of catalyst design in terms of ligand structure and orientation surrounding the active center. The effect of ligand design on stabilizing the active center, selectivity and activity of the catalyst has been explored significantly.

MAO is the most widely used cocatalyst, able to activate a large number of metallocenes and non-metallocene complexes. Due to the high cost of MAO and relatively large amount needed to activate the catalyst ($Al/M=10^3-10^4$) (that might also lead to chain transfer to the $AlMe_3$ present in the MAO), alternative stoichiometric cocatalysts have been developed such as $B(C_6F_5)_3$; $NR_3H^+B(C_6F_5)_4^-$ and $Ph_3C^+B(C_6F_5)_4^-$.⁴⁻⁵ These systems can be used in close to equimolar amounts with either metallocene alkyl derivatives or with the chloride analogues together with trialkyl aluminum species such as $Al(i-Bu)_3$ and $AlEt_3$ that scavenge impurities and alkylate the catalyst precursor.

For a living single site catalyst, the chain termination is virtually absent and the polymers obtained have very narrow molecular weight distribution. Therefore stability towards scavengers employed during the polymerization is one of the main requirements for a living catalyst. Only a limited number of catalysts have been cited in the literature to be living at room temperature and above for the polymerization of ethylene. This is because at higher temperature various chain transfer reactions take place such as β -hydride- and β -alkyl elimination or chain transfer to cocatalyst (trans alkylation to aluminum), resulting in lower molecular weights and a MWD of 2. The earliest catalyst reported to be living at $-78^\circ C$ was based on vanadium acetylacetonate.⁶ Nakamura *et al.*⁷ discovered the diene complexes of tantalum to be living for the polymerization of ethylene below $-20^\circ C$. McConville *et al.*⁸ reported the first living polymerization at room temperature. The titanium diamido complex $[(2,6-Me_2C_6H_3)N(CH_2)_3N(2,6-Me_2C_6H_3)]TiMe_2$ was found to exhibit living polymerization of 1-hexene in the presence of $B(C_6F_5)_3$ as activator. However, the living complex deactivates in the absence of monomer yielding an inactive compound in quantitative yield. Nickel catalysts based on α -diimine ligands have been reported to be living for the polymerization of α -olefins at $-10^\circ C$.⁹ Schrock, *et al.*,¹⁰ Kim, *et al.*,¹¹ and Shiono, *et al.*¹² have independently reported catalysts that exhibit living polymerization of 1-hexene. The catalyst $[(t-BuN-o-$

$C_6H_4)_2O]ZrCl_2$ ¹³ also exhibits living behavior for hexene at 0°C. Sita, *et al.*¹⁴ found dimethylmonocyclopentadienylzirconium acetamidates to exhibit living stereospecific polymerization of α -olefins. Last decade has seen a growing interest in exploiting various soluble non-metallocene catalysts based on transition metals and lanthanides for the polymerization of olefins as well as α -olefins. Recently, Coates, *et al.*¹⁵ have demonstrated the living syndiospecific polymerization of propylene using bis(salicylaldiminato)titanium complex whereas, Kol *et al.*¹⁶ showed that the nonmetallocene C_2 -symmetric di(alkoxo) $ZrBn_2$ promotes living polymerization of 1-hexene at room temperature. Brookhart *et al.*¹⁷ reported a palladium catalyst based an aryl α -diimine ligand to be living for the polymerization of ethylene at 5°C. They have also reported a complex based on Co(III) to be living for ethylene.

In Chapter 2, a method to synthesize nascent UHMWPE with very narrow molecular weight distribution, using a metallocene catalyst $(C_5Me_5)_2Sm \cdot 2(THF)$ ¹⁸ was presented. The major drawback of this catalyst is that only in the absence of scavengers it polymerizes ethylene to UHMWPE, which makes its use expensive and cumbersome. Scavengers act as chain transfer agents for this catalyst and hence the desired molecular weight cannot be achieved. Due to these drawbacks, alternative catalyst systems were explored which will be discussed in this chapter. It will be investigated if the synthesis of highly disentangled UHMWPE with narrow molecular weight distribution is limited only to one exotic catalyst $(C_5Me_5)_2Sm \cdot 2(THF)$ or that different kinds of homogeneous catalysts can be employed to synthesize similar grades of polymer simply by controlling the polymerization conditions. In order to prove that, a non-metallocene single site catalyst based on group 4 transition metal, commonly referred to as Mitsui's bis(phenoxy-imine)titanium catalyst $[3-t-Bu-2-O-C_6H_3CH=N(C_6F_5)]_2TiCl_2$ ¹⁹ activated with MAO was used to synthesize UHMWPE by solution polymerization. In addition, another single site catalyst based on a group 3 metal $[PhC(N-2,6-i-Pr_2C_6H_3)_2]Y(CH_2SiMe_3)_2(THF)$ activated with $[PhNMe_2H]^+ [B(C_6F_5)_4]^-$ was tested to prove the principle of obtaining nascent disentangled UHMWPE at slightly higher temperatures. This catalyst was reported to be living and yield UHMWPE with very narrow MWD at 50°C.²⁰

3.2 Experimental Section.

3.2.1 General Comments.

All manipulations were performed under an argon atmosphere using a glovebox (Braun MB-150 GI) and Schlenk techniques. Solvents were distilled from Na/K alloy (petroleum-ether (40:60), and heptane) or dried over a Grubbs column (Al_2O_3 : toluene) and stored under argon prior to use. The catalysts were either prepared according to literature procedure²⁰ or obtained from Sabic Euro Petrochemicals. The molecular weights and molecular weight distributions of the polymers were measured at 135°C by gel-permeation chromatography (GPC210, Polymer Labs) at the University of Groningen, using 1,2,4-trichlorobenzene as solvent.

3.2.2 Polymerization with $[3\text{-}t\text{-Bu-2-O-C}_6\text{H}_3\text{CH=N(C}_6\text{F}_5)]_2\text{TiCl}_2$.

Polymerization (Pressure): To a mechanically stirred 200 mL Büchi reactor containing a solution of ethylene in petroleum-ether (40:60 fraction; 80 mL), MAO (16.6 mmol) and the catalyst (1 μmol) were added. The polymerizations were performed at 30°C at ethylene pressures of 1 and 5 bar. The same experiment was repeated with toluene (80 mL) as solvent at an ethylene pressure of 5 bar at 50°C. The polymerizations were quenched after 5 min with acidified methanol. The polymers were filtered, washed with acetone and dried under vacuum at 60°C.

Polymerization (Reaction Time): To a 1 L round bottom flask containing a solution of ethylene in heptane (500 mL), MAO (16.6 mmol) was added. The solution was stirred for a while before adding the catalyst (1 μmol). The solvent was saturated with ethylene for 45 minutes prior to the addition of catalyst and cocatalyst. The polymerizations were carried out at 8°C at an ethylene pressure of 1 bar, using a mechanical stirrer with ethylene bubbling through the solution. The polymerizations were quenched after different time intervals (5, 10, 15, 20 minutes) with acidified methanol. The polymers were filtered, washed with acetone and dried under vacuum at 60°C.

Polymerization (Dilution and Temperature): To a 2 L round bottom flask provided with a magnetic stirring bar/mechanical stirring, containing a stirred solution of ethylene in petroleum-ether (40:60 fraction; 1 L), MAO (33.2 mmol) was added followed by addition of

the catalyst (1 μmol). The solvent was saturated with ethylene for 45 minutes prior to the addition of catalyst and cocatalyst. The reaction was carried out at 8°C and an ethylene pressure of 1 bar, with ethylene continuously bubbling through the solution. The polymerizations were carried out at different dilutions (1 μmol of catalyst in 250, 500, 1000 and 2000 mL). The polymerizations were repeated using a mechanical stirrer at different temperatures (-10°C, 0°C, +10°C, +20°C, +50°C and +68°C). The polymerizations were quenched after 20 minutes with acidified methanol. The polymers were filtered, washed with acetone and dried under vacuum at 60°C.

Polymerization (MAO Concentration): To a stirred and saturated (for 20 minutes) solution of ethylene in petroleum-ether (40:60 fraction; 250 mL), different amounts of MAO (8.3, 16.6, 33.2, 66.4, 132.8 mmol) were added. The polymerization was performed in a 500 mL round bottom flask using a magnetic stirring bar at 8°C at an ethylene pressure of 1 bar for 10 minutes. Subsequently, the reactions were quenched with acidified methanol, the polymer products were filtered, washed with acetone and dried under vacuum at 60°C.

3.2.3 Polymerization with $[\text{PhC}(\text{N-2,6-}i\text{-Pr}_2\text{C}_6\text{H}_3)_2\text{Y}(\text{CH}_2\text{SiMe}_3)_2(\text{THF})$.

To a stirred solution of ethylene in toluene (250 mL), the catalyst (50 μmol) and activator (50 μmol) were added. The polymerizations were carried out in a 1 L Büchi reactor provided with a mechanical stirrer at 25 and 50°C, respectively, and at ethylene pressures of 5 bar for 30 minutes. After 15 minutes the reactions were quenched with acidified methanol and the polymers were filtered, washed with acetone and dried under vacuum at 60°C.

3.3 Results and Discussions.

3.3.1 Polymerization with $[\text{3-}i\text{-Bu-2-O-C}_6\text{H}_3\text{CH}=\text{N}(\text{C}_6\text{F}_5)_2\text{TiCl}_2$.

The post-metallocene catalyst system $[\text{3-}i\text{-Bu-2-O-C}_6\text{H}_3\text{CH}=\text{N}(\text{C}_6\text{F}_5)_2\text{TiCl}_2/\text{MAO}$ polymerizes ethylene in a living fashion at room temperature which, under controlled polymerization conditions might lead to easily processable polymer. The turnover frequency of the catalyst is very high ($\text{TOF} > 20,000 \text{ min}^{-1}\cdot\text{atm}^{-1}$) which is higher than that of the zirconocene catalyst system $\text{Cp}_2\text{ZrCl}_2/\text{MAO}$.¹⁹ The high activity is a result of a combination of steric and electronic factors. Systematic studies on the $[\text{3-}i\text{-Bu-2-O-}$

$C_6H_3CH=N(C_6F_5)_2TiCl_2$ /MAO system with varying amounts of fluorine substituents has demonstrated that the fluoro atoms play a crucial role in turning the titanium center more electrophilic. The presence of fluorine atoms on the phenyl ring prevents β -hydride elimination in the titanium catalyst.¹⁹ Moreover, a *tert*-butyl group at the 3-position of the phenoxy moiety diminishes the probability of other chain termination reactions and at the same time enhances effective ion separation between the cationic metal center and the counter ion of the co-catalyst resulting in an increase in the activity of the catalyst.²¹

During the polymerization, ethylene was constantly bubbled through the polymerization medium with effective stirring to minimize the diffusion limitation as discussed in Chapter 2. In order to study the effect of temperature, dilution, pressure and reaction time on the molecular weight and entanglement density, these parameters were varied and polymerization runs were carried out. All other conditions were kept constant.

Influence of Monomer Pressure.

Table 3.1 clearly shows that the activity of the catalyst increases drastically with the increase in pressure at 30°C (entry 1 and 2) because of a higher concentration of the dissolved monomer.

Table 3.1 *Effect of monomer pressure.*

Entry	Temperature (°C)	Pressure (bar)	Yield (g)	Concentration of ethylene (moles)	M_w^* (kg/mol)	D
1	30	1	0.8	0.1	736	1.3
2	30*	5	7.0	0.5	2688	1.3
3	50*	5	5.0	0.4	1158	1.8

Polymerizations performed using the $[3-t-Bu-2-O-C_6H_3CH=N(C_6F_5)_2TiCl_2$ (1 μ mol); *3 minutes; 5 minutes; toluene (80 mL); MAO (16.6 mmol); *Determined by GPC.

Even though the amount of solvent used is low (80 mL) in the polymerizations, the diffusion limitation can be overcome with the increase of pressure.

At 5 bar of ethylene, the polymerization rate was very high due to which the polymerizations had to be quenched after 3 minutes as the reactor content nearly solidified and a high exotherm was observed.

Therefore further experiments were carried out at low ethylene pressure (1 bar) to guarantee good control over the reaction. Moreover, the dilution (amount of solvent) was kept high to increase the absolute amount of ethylene in the medium and to prevent diffusion limitation and overshooting of temperature during the polymerization.

Influence of Polymerization Time.

Despite the living nature of the catalyst, there seems to be a limit for the maximum attainable molecular weight. In other words, even though UHMWPE is produced within the first few minutes of polymerization, the molecular weight does not increase linearly with the polymerization time and a relatively high MWD is obtained as shown in Table 3.2. However, as we can see from the duplicate measurements of the molecular weight of the 10 minutes experiment, the reproducibility of the molecular weight determination of UHMWPE using high temperature GPC is low.

Table 3.2 *Influence of polymerization time.*

Time (min)	Yield (g)	M _w (kg/mol)*	D
5	1.2	1067	1.7
10	1.5	772 1101	1.7 1.3
15.2	1.9	1426	1.7
20.5	2.0	1355	1.7

Polymerizations performed using the [3-*t*-Bu-2-O-C₆H₃CH=N(C₆F₅)₂ TiCl₂ (1 μmol); heptane (500 mL); MAO (16.6 mmol); 8°C; ethylene (1 bar);* Determined by GPC.

If not all the chains start to grow at the same time, a molecular weight distribution will result that is higher than the theoretical value of 1.0 expected for a perfectly living system. Among many other reasons that can lead to broad MWD in living systems, it was shown in Chapter 2 that heterogenization of the catalyst was a plausible cause for obtaining high MWD with the samarocene catalyst. Due to this encapsulation of the catalyst, the monomer diffusion through the polymer to the active center becomes increasingly difficult and the chain stops growing.

Influence of Dilution during Polymerization.

It is anticipated that a highly diluted homogeneous system would enhance effective separation of the growing chains which should lead to less entangled polymer chains. An increase of polymerization temperature is thought to increase the number of entanglements per unit chain. Moreover, in more diluted systems, the heat dissipation is more effective, resulting in less local temperature overshoot at the catalyst active sites. It has to be taken into account that when going to high dilution while keeping the absolute amount of catalyst and cocatalyst constant the reduced molar concentration of MAO may affect the catalyst activity which will be discussed in the section where effect of cocatalyst is described. Table 3.3 shows that the yield and molecular weight of the polymer does not increase appreciably with the increase in the amount of solvent used for the polymerization.

Table 3.3 *The influence of dilution during polymerization on molecular weight and yield.*

Solvent (mL)	Yield (g)	M _w (kg/mol) ^a	D
250	1.0	882	1.3
500	2.5	1378	1.4
1000*	2.0	1321	1.2
2000*	2.7	1525	1.2

Polymerization performed using the [3-*t*-Bu-2-O-C₆H₃CH=N(C₆F₅)₂TiCl₂]; MAO (33.2 mmol); ethylene (1 bar) 20 minutes, 8°C; *With mechanical stirring; (a) Determined by GPC.

Except at the lowest dilution (250 mL), a molecular weight of 1 million g/mol is achieved in all reactions regardless of the amount of solvent used. This means that diffusion of ethylene into the solvent is not critical for these polymerizations and that the yield and M_w are not

affected by the initial absolute amount of dissolved ethylene which increases as the amount of solvent used increases. The propagation rate is fast and a molecular weight of 1 million g/mol is achieved in a very short period and further growth of the chain is slow probably because of the encapsulation of active catalyst in the polymer matrix, which prevents the diffusion of ethylene to the catalyst active site.

Only for the lowest dilution (250 mL), the yield and M_w are relatively low. When the amount of solvent used is low, the molar concentration of the catalyst in the polymerization medium is relatively high (0.004 mM), resulting in consumption of all the dissolved ethylene faster than the dissolution while the absolute amount of dissolved ethylene is also low. This effect was also seen earlier when the polymerizations were performed at 1 bar with 80 mL of solvent at 30°C (entry 1, Table 3.1). The collective effect of high catalyst concentration, less amount of dissolved ethylene in the solvent at lower dilutions, leads to reduction in the yield and molecular weight as shown in Figure 3.1 and 3.2. The influence of dilution on the entanglement density is discussed separately in Chapter 4.

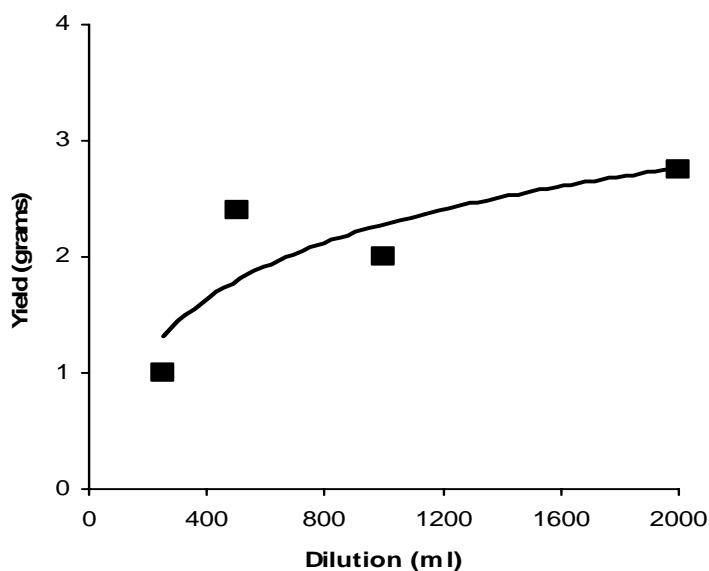


Figure 3.1 Effect of dilution on the yield of UHMWPE obtained using the [3-*t*-Bu-2-O- $C_6H_3CH=N(C_6F_5)_2TiCl_2/MAO$ catalyst system at 0 °C.

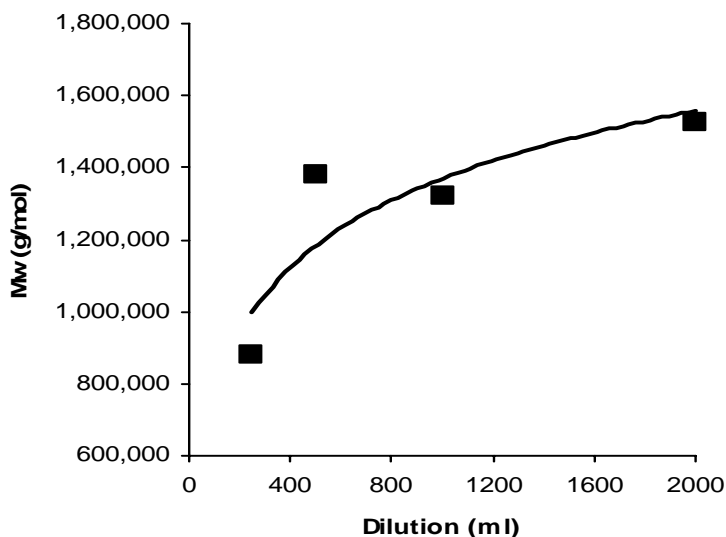
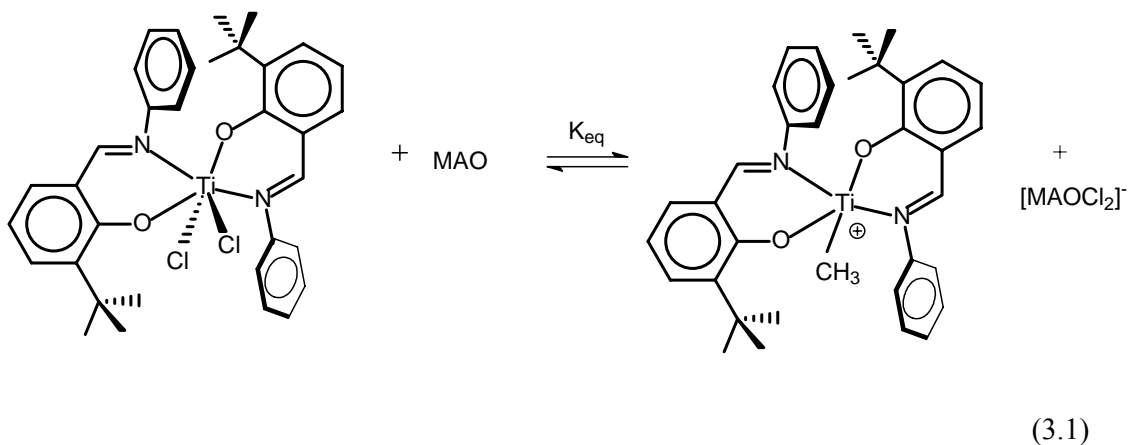


Figure 3.2 Effect of dilution on the M_w of UHMWPE obtained using the [3-*t*-Bu-2-*O*- $C_6H_3CH=N(C_6F_5)]_2TiCl_2/MAO$ catalyst system 0 °C.

Influence of Cocatalyst Concentration.

Since the catalyst is only active in the presence of MAO, the molar concentration of MAO in the medium might affect the activity of the catalyst, when an equilibrium exists between the catalyst precursor and the cationic active species formed upon reaction with MAO as shown in equation 3.1.



The concentration of MAO in the polymerization medium becomes increasingly important in dilution experiments, where the amount of solvent used for polymerization is varied. It is

well-known that besides generating an active cationic metal center, the trimethylaluminum (TMA) present in the MAO can cause various side reactions such as chain transfer or deactivation reactions.²² To study if the molar concentration of methylalumoxane is important for obtaining the same activity of the catalyst in the dilution experiments, the effect of cocatalyst to catalyst ratio on the yield, molecular weight and molecular weight distribution of the polymers was studied.

Table 3.4 clearly shows that the catalyst produces UHMWPE even at a very high cocatalyst to catalyst ratio of 132,000 (entry 5). In addition, the molecular weight continuously increases whereas the MWD stays very low with the increase in the concentration of MAO. This means that the chain transfer to aluminum is minimal even at such high concentration of trimethylaluminum (in MAO) in the polymerization medium. Therefore, it can be concluded that the catalyst shows living behavior even at high concentration of MAO, strengthening the information reported in the literature that the *tert*-butyl group at the 3-position of the phenoxy moiety effectively diminishes the probability of chain transfer reactions.²¹ The increased amount of MAO is accompanied by an increased amount of toluene. The increase in yield with the increase in the concentration of MAO can be explained by an increase in the polarity of the medium resulting in higher catalyst activity (solvent separated ion pairs versus contact ion pairs).²³ The increase in M_w with increased amount of MAO will result from reduced catalyst deactivation via bimolecular interactions leading to dormant sites and from the increased scavenging of impurities.

Table 3.4 The influence of MAO concentration.

Entry.	catalyst (μmol)	MAO (μmol)	Yield (g)	M_w (kg/mol) ^a	M_n (kg/mol)	D	No. chains/ Metal center*
1	1	8,300	0.9	785	584	1.4	1.5
2	1	16,600	1.3	886	634	1.4	2
3	1	33,200	2.3	1290	1005	1.3	2.3
4	1	66,400	3.0	1572	1220	1.3	2.5
5	1	132,800	4.6	1601	1244	1.3	3.6

Polymerization performed using the $[3\text{-}t\text{-Bu-2-O-C}_6\text{H}_3\text{CH=N(C}_6\text{F}_5)_2\text{TiCl}_2]$; heptane (250 mL); MAO (8.3, 16.6, 33.2, 66.4, 132.8 mmol in toluene, respectively); ethylene (1 bar); 10 minutes, 8°C; *With mechanical stirring; (a) Determined by GPC; * Assuming all metal centers are active.

For a true living system, each metal center should produce one chain. Obviously, Table 3.4 shows that this is not the case, which means that under the polymerization conditions employed, the catalyst does not exhibit truly living behavior and can produce more than one chain per metal center and still maintain very low poly-dispersity which is possible only if the propagation rate stays very high until a molecular weight of approximately 1 million g/mol is achieved. At that point diffusion limitation may lead to competing chain transfer reactions. Alternatively, assuming that the catalyst is truly living and that it produces one chain per metal center, the value of M_n for entry 4 of Table 3.4 should have been 3 million g/mol instead of 1.2 million g/mol. In order to verify the GPC results, the same polymer sample was sent to two different labs for GPC analysis. The results obtained were very surprising. For example for a polymer made with this catalyst was shown to have a M_n of 795 kg/mol in the laboratory where we did most of our measurements, while the same polymer was shown to have a M_n of 2000 kg/mol in another laboratory. The yield of this specific experiment was 3.7 grams of polymer obtained with 1 μ mol of catalyst. This corresponds to 4.6 chains per metal center for the 795 kg/mol molecular weight measurement and to 1.8 chains per metal for the 2000 kg/mol molecular weight measurement. Based on these explanations and Table 3.4, it can be stated that the catalyst is probably truly living and any discrepancy observed is due to chain transfer at high molecular weight and/or unreliable M_n values.

Influence of Polymerization Temperature.

Since it was expected that low polymerization temperature would favor the synthesis of disentangled chains of UHMWPE due to faster crystallization of the chains and lower polymerization rate, the influence of polymerization temperature on the catalyst activity, molecular weight and number of entanglements in the polymer chain was studied. The polymerization was performed at constant but higher dilution as discussed before. Table 3.5 shows the influence of the polymerization temperature. With the increase in temperature the observed productivity of the catalyst increases to a maximum which is close to +28°C (see Figure 3.3), after which the yield decreases with increasing temperature.

Irrespective of the synthesis temperature the molecular weight in all cases is above a million but as there is no trend in the molecular weight as a function of temperature, the accuracy of the GPC results are questionable as discussed before. In all cases, even at the highest temperature, UHMWPE is obtained. As expected for a living catalyst system, at low

temperatures the MWD is narrow. Only at higher temperature the MWD is broader which indicates that chain transfer reactions are starting to become competitive.

Table 3.5 The influence of polymerization temperature.

Temperature (°C)	Yield (g)	M _w (kg/mol) [*]	D
-10	1.8	1001	1.3
0	2.7	1397	1.4
+10	2.8	1131	1.3
+20	3.7	1089	1.4
+50	3.0	1788	1.7
+68	1.3	1099	2.7

Polymerizations performed using the [3-*t*-Bu-2-O-C₆H₃CH=N(C₆F₅)₂]₂TiCl₂ (1 μmol); petroleum-ether(40:60) (1 L); MAO (33.2 mmol); 20 minutes ; ethylene (1 bar); * Determined by GPC.

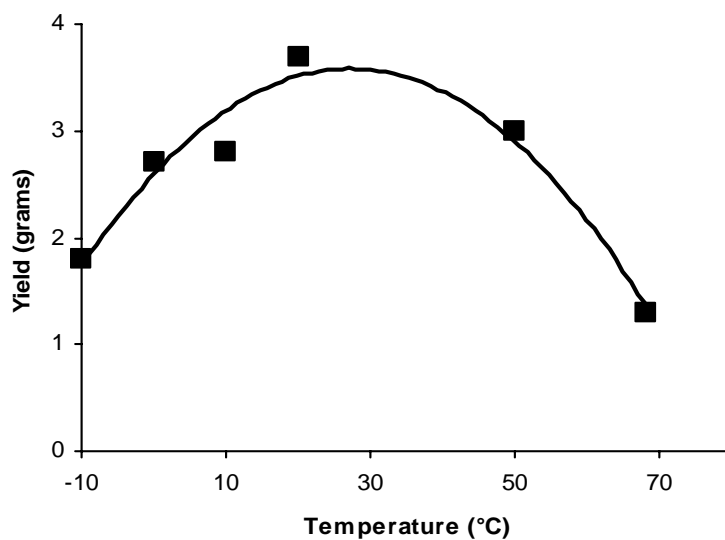


Figure 3.3. Effect of polymerization temperature on the yield of UHMWPE obtained using the [3-*t*-Bu-2-O-C₆H₃CH=N(C₆F₅)₂]₂TiCl₂/MAO catalyst system.

Like most titanium alkyl species, the intermediate (di)alkyl species are expected to be thermally unstable, which leads to catalyst deactivation and a lower yield at higher

temperature. In contrast, at low polymerization temperature, slow activation of the catalyst leads to lower yield. We would like to emphasize here that these experiments cannot be compared with the high pressure experiments as the above experiments were performed at optimal controlled conditions.

3.3.2 Polymerization with $[PhC(N-2,6-i-Pr_2C_6H_3)_2]Y(CH_2SiMe_3)_2(THF)$.

Since we wanted to investigate if a different homogeneous catalyst can be used for the synthesis of UHMWPE with narrow molecular distribution, polymerizations were carried out using the yttrium catalyst. The single site yttrium catalyst $[PhC(N-2,6-i-Pr_2C_6H_3)_2]Y(CH_2SiMe_3)_2(THF)^{20}$ upon activation with $[PhNMe_2H]^+[B(C_6F_5)_4]^-$ has been reported to polymerize ethylene to UHMWPE. With this catalyst, scavengers cannot be used as through chain transfer to aluminum the molecular weight drops significantly, similar to the samarocene catalyst discussed in Chapter 2. The catalyst, when activated with $[PhNMe_2H]^+[B(C_6F_5)_4]^-$, has been reported to be living and to polymerize ethylene rather slowly.²⁰ This feature allows us to tune the M_w of the polymer made with this living system by varying the polymerization time.

The polymerizations were carried out in a stainless steel autoclave as the catalyst was not active at low monomer pressure. As shown in Table 3.6, a large amount of catalyst was required for the reaction since most of it is consumed to scavenge the impurities. Although it was possible to obtain UHMWPE the molecular weight distribution that was obtained from these experiments is bimodal.

Table 3.6 Results of polymerization with $[PhC(N-2,6-i-Pr_2C_6H_3)_2]Y(CH_2SiMe_3)_2(THF)$.

Temperature (°C)	Yield (g)	M_w (kg/mol)*	D	No chains/Metal center
25	1.5	1339	5.2	bimodal
25	3.5	1145	4.2	bimodal
50	10.5	625	1.7	

Catalyst (50 μ mol); toluene (250 mL); activator (50 μ mol); 30 minutes; ethylene (5 bar); * Determined by GPC.

As the UHMWPE powders were found to be completely entangled even at 25°C, no further attempts were made to improve these results. The fact that UHMWPE obtained with the [3-*t*-Bu-2-O-C₆H₃CH=N(C₆F₅)₂TiCl₂ at 25°C with toluene as the diluent are highly disentangled is remarkable.

3.4 Conclusions.

In this chapter, it was investigated if different homogeneous catalysts with high molecular weight capability can be used to synthesize highly disentangled nascent UHMWPE with narrow molecular weight distribution by simply controlling the polymerization conditions. Two living homogeneous post-metallocene catalysts, [3-*t*-Bu-2-O-C₆H₃CH=N(C₆F₅)₂TiCl₂/MAO and [PhC(N-2,6-*i*-Pr₂C₆H₃)₂]Y(CH₂SiMe₃)₂(THF) were selected for this study. Only with the titanium catalyst the desired nascent disentangled UHMWPE with narrow molecular weight distribution was obtained. With the [3-*t*-Bu-2-O-C₆H₃CH=N(C₆F₅)₂TiCl₂/MAO, it is shown that the yield and molecular weight of the polymer does not increase appreciably with the increase in the amount of solvent used for the polymerization. The propagation rate is fast and a molecular weight of 1 million g/mol is achieved in a very short period of time and further growth of the chain is slow probably because of the encapsulation of active catalyst in the polymer matrix, which prevents the diffusion of ethylene to the catalyst active site. Only for the lowest dilution (250 mL) the M_w and yield obtained were low and it was attributed to the diffusion limitation of ethylene in the solvent, which becomes less severe when the amount of solvent used is high.

It is also shown in this chapter that the yield of the polymer continuously increases with increasing MAO concentration. This effect can be explained by an increase in the polarity of the medium resulting in higher catalyst activity (solvent separated ion pairs versus contact ion pairs). The increase in M_w with increased amount of MAO will result from reduced catalyst deactivation via bimolecular interactions leading to dormant sites and from the increased scavenging of impurities.

Similar to the dilution experiments it was shown that the M_w is hardly affected by the increase in the synthesis temperature, providing additional evidence of fast polymerization and catalyst encapsulation in the polymer matrix as stated earlier. However, the yield does increase with the increase in the temperature to a maximum at +28°C and then starts to decrease.

In order to investigate the influence of polymerization conditions on the entanglement density, various characterization techniques have been employed to ascertain the entanglement density of UHMWPE synthesized in Chapters 2 and 3 which are presented in Chapter 4.

3.5 References.

- (1) Fink, G.; Mülhaupt, R.; Brintzinger, H. H. *Ziegler Catalysts*; Eds.; Springer-Verlag: Berlin, 1995.
- (2) Kaminsky, W. *Metalorganic Catalysts for Synthesis and Polymerization*; Eds.; Springer-Verlag: Berlin, 1999.
- (3) Blom, R.; Follestad, A.; Rytter, E.; Tilset, M.; Ystenes, M.; Eds.; Springer-Verlag: Berlin, 2001.
- (4) Resconi, L.; Cavallo, L.; Fait, A.; Piemontesi, F. *Chem. Rev.* **2000**, *100*, 1253.
- (5) Bochmann, M.; Lancaster, S. J.; Hursthouse, M. B.; Malik, K. M. A. *Organometallics* **1994**, *13*, 2235.
- (6) Doi, Y.; Ueki, S.; Keii, T. *Macromolecules* **1979**, *12*, 814.
- (7) Mashima, K.; Fujikawa, S.; Nakamura, A. *J. Am. Chem. Soc.* **1993**, *115*, 10990.
- (8) Scollard, J. D.; McConville, D. H. *J. Am. Chem. Soc.* **1996**, *118*, 10008.
- (9) (a) Ittel, D. S.; Johnson, L. K.; Brookhart, M. *Chem. Rev.* **2000**, *100*, 1169. (b) Killian, C. M.; Tempel, D. J.; Johnson, L. K.; Brookhart, M. *J. Am. Chem. Soc.* **1996**, *118*, 11664.
- (10) Baumann, R.; Davis, W. M.; Schrock, R. R. *J. Am. Chem. Soc.* **1997**, *119*, 3830.
- (11) Jeon, Y-M.; Park, S. J.; Heo, J.; Kim, K. *Organometallics* **1998**, *17*, 3161.
- (12) Hagihara, H.; Shiono, T.; Ikeda, T. *Macromolecules* **1998**, *31*, 3184.
- (13) Schrock, R. R.; Baumann, R.; Reid, S. M.; Goodman, J. T.; Stumpf, R.; Davis, W. M. *Organometallics* **1999**, *18*, 3649.
- (14) Jayaratne, K. C.; Sita, L. R. *J. Am. Chem. Soc.* **2000**, *122*, 958.
- (15) Tian, J.; Phillip, H.; Coates, G. W. *J. Am. Chem. Soc.* **2001**, *123*, 5134.
- (16) Tshuva, E. Y.; Goldberg, I.; Kol, M.; Goldschmidt, Z. *Chem. Commun.* **2001**, 2120.
- (17) Gottfried, C. A.; Brookhart, M. *Macromolecules* **2001**, *34*, 1140.
- (18) Gruter, G. J. M.; Wang, B.; van Beek, J. A. M. *European Patent Application*, EP 1057837 A1, **2000**.

-
- (19) Mitani, M.; Mohri, J-I.; Yoshida, Y.; Saito, J.; Ishii, S.; Tsuru, K.; Matsui, S.; Furuyama, R.; Nakano, T.; Tanaka, H.; Kojoh, S-I.; Matsugi, T.; Kashiwa, N.; Fujita, T. *J. Am. Chem. Soc.* **2002**, *124*, 3327.
- (20) Bambirra, S.; Leusen, van D.; Meetsma, A.; Hessen, B.; Teuben, J. H. *Chem. Commun.* **2003**, 522.
- (21) Furuyama, R.; Saito, J.; Ishii, S-I.; Mitani, M.; Matsui, S.; Tohi, Y.; Makio, H.; Matsukawa, N.; Tanaka, H.; Fujita, T. *J. Mol. Catal. A: Chemical* **2003**, *200*, 31.
- (22) Bochmann, M.; Lancaster, S. J. *J. Organomet. Chem.* **1995**, *497*, 55.
- (23) Nishii, K.; Matsumae, T.; Dare, E. O.; Shiono, T.; Ikeda, T. *Macromol. Chem. Phys.* **2004**, *205*, 363.

Chapter 4

Characterization of Nascent UHMWPE as synthesized via Single Site Catalysts: *estimation of Entanglements in Nascent Powders.*

Synopsis: This chapter presents the results of various characterization techniques employed to estimate the entanglement density in the UHMWPE synthesized by the two different catalyst systems described in Chapters 2 and 3. The mechanical deformation tests performed on the UHMWPE support the success of the synthesis conditions as the films consolidated below the α -relaxation temperature are highly drawable. The high drawability is associated with a low entanglement density in the UHMWPE. Furthermore, valuable tools such as temperature modulated DSC studies combined with rheology are used to confirm this observation.

4.1 Introduction.

UHMWPE is difficult to process due to its high molar mass and the presence of entanglements.¹ High entanglement density imparts excellent mechanical properties but causes restricted mobility of the polymer chains in the melt. UHMWPE cannot be processed via conventional processing routes such as injection molding, blow molding, etc. and is usually processed via compression molding or ram-extrusion.² The high viscosity is due to the presence of entanglements and the long reptation time needed for these chains to renew their position within the melt and relax. Regardless of the process applied, today all products of UHMWPE possess fusion defects or grain-boundaries due to which they have limited lifetime when applied in highly demanding applications such as components for medical implant.³

The extremely high viscosity of UHMW polymer melts results from the entanglements of the polymer chains following the relation $\eta_0 \propto M_w^{3.4}$. Therefore, lowering the number of entanglements per unit chain⁴⁻⁵ is one of the prime requirements to improve the flow characteristics of the UHMWPE, both below and above the melting temperature of the polymer.

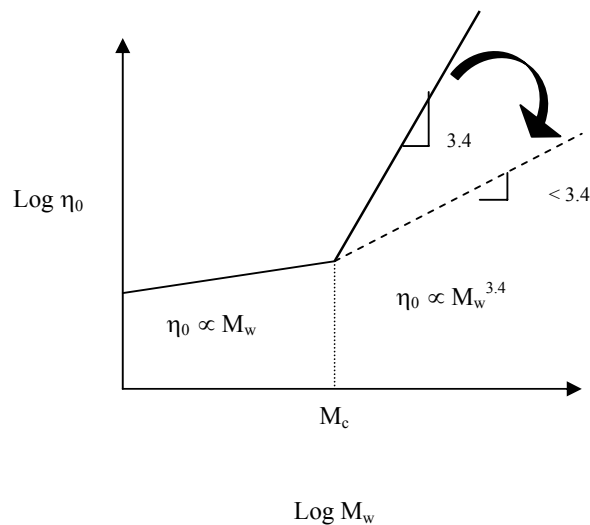


Figure 4.1 Hypothetical representation of lowered melt viscosity of UHMWPE with highly disentangled morphology.

For a thermodynamically labile state in which the material is not fully entangled, the fundamental relation between zero shear viscosity and molecular weight of the polymer does not follow the universally accepted model. Instead, the slope will be lower than the value of 3.4 in the plot of $\log \eta_0$ versus $\log M_w$ as shown schematically in Figure 4.1.

As described in the previous chapters, it is proposed that when homogeneous catalysts are used in diluted systems and the temperature of polymerization is kept low, the chains will begin to crystallize during the polymerization due to a faster crystallization rate compared to the polymerization rate ($R_{\text{crys}} > R_{\text{polym}}$). In order to establish if the as synthesized UHMWPE are disentangled, various characterization techniques have been used which are discussed in detail in this chapter. The quantitative determination of entanglement density poses great challenges since there is no direct method available to measure the entanglement density. Hence, combinations of different techniques are essential to obtain and support a qualitative estimation of the amount of entanglements. In this chapter, it is shown how a variety of techniques such as drawing, DSC and rheology have been used effectively to estimate relative variation in the entanglement density. Another purpose of this chapter is to compare polymers obtained with the two different homogeneous catalysts described in Chapters 2 and 3 in order to verify the universal behavior of homogeneous catalysts under similar polymerization condition to yield polymer with similar properties.

4.2 Results and Discussions.

4.2.1 Mechanical Deformation of Polymers.

Polymers when subjected to deformation are known to show yielding, necking, strain hardening and eventually they will fracture. Depending on the type of the polymer (structure and morphology) the manner in which they behave may differ. For instance, a ductile polymer when subjected to tensile testing shows a linear increase in the stress with increasing strain according to Hooke's law⁶ up to the yield point. Beyond the yield point, necking takes place, which extends as the strain is further increased resulting in a drop in the stress. When the process of necking is complete, strain hardening occurs whereby the stress increases until the polymer fractures (Figure 4.2a).

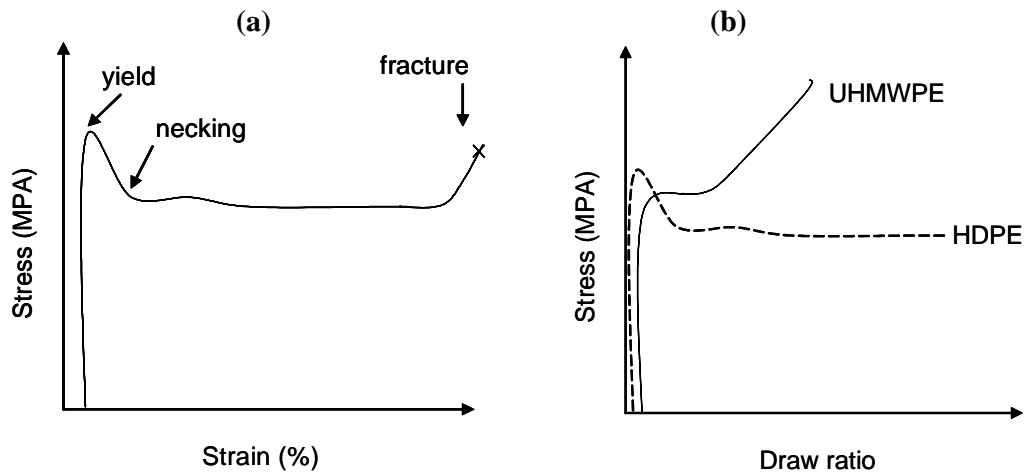


Figure 4.2 (a) Stress-strain behavior of polymers (b) Role of entanglements on the draw ratio of polyethylene.

On the other hand a stiff polymer fractures much faster and necking is drastically reduced.⁷ The degree of necking in the polymer is characterized by the draw ratio (length of fully necked sample/original length). Post yield behavior in polymers is directly related to the entanglement density and hence the chain stiffness. As the entanglement density increases the stiffness of the polymer chain increases resulting in a lower draw ratio⁸

It is well known that with the increase in the molar mass the number of entanglements per unit chain increases and consequently the draw ratio decreases. For instance, UHMWPE has a considerably lower draw ratio compared to HDPE as shown in Figure 4.2b. The drawing experiments, however, are strongly affected by the temperature at which they are performed. If the drawing temperature is too high, chain slippage might occur instead of chain extension. Therefore drawing should be performed at temperatures close to but still below the melting temperature of the polymers.

Figure 4.3 shows the difference in the drawing behavior between melt crystallized (upon compression molding) and solution crystallized UHMWPE as a function of temperature.⁹ In the region 1, below the melting temperature T_m^1 , the solution crystallized samples (S) are highly drawable compared to the melt crystallized samples (M). The drawability of solution crystallized samples drops considerably above the melting temperature due to entangling of the chains. The apparent increase in the drawability in region 2 for both melt- and solution crystallized samples is the result of chain slippage and -relaxation. At very high temperature (region 3) the drawability is completely lost due to the onset of the hexagonal phase.⁹

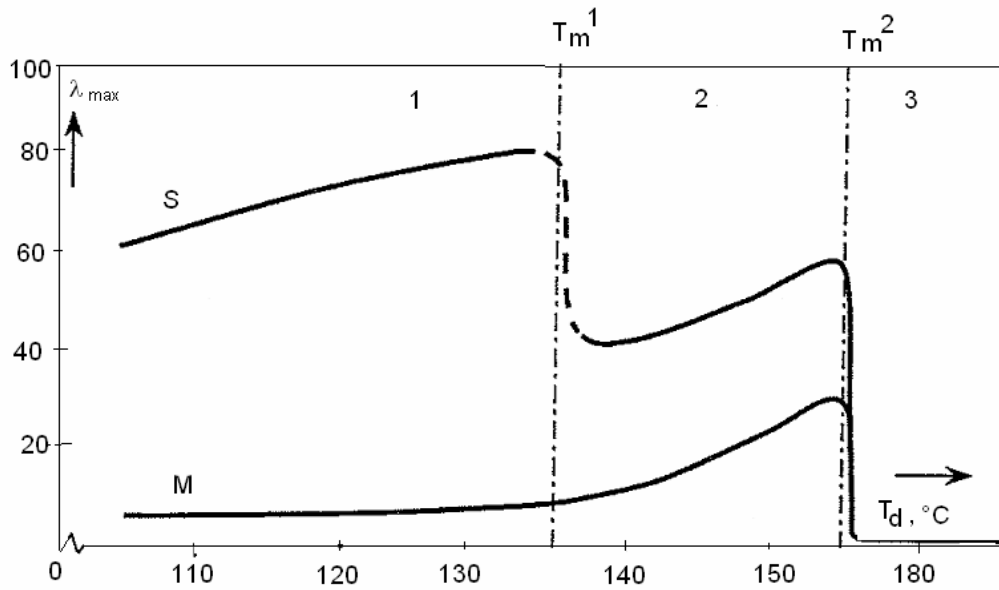


Figure 4.3 Drawing behavior of UHMWPE at different temperature. (M) Melt crystallized (S) solution crystallized.⁷

Whether or not a polymer is drawable is strongly dependent on the initial morphology and the processing conditions. The maximum draw ratio (λ_{\max}) was found to depend on the chain conformation.¹⁰ In case of single crystal mats of polyethylene consisting of regularly stacked folded chain crystals, i.e. disentangled state, the λ_{\max} is given by equation 1

$$\lambda_{\max} = L_f / \delta \quad (1)$$

where L_f is the fold length δ is the chain diameter. The maximum draw ratio is 30-60.

On the other hand, for melt crystallized polyethylene, i.e. entangled state, where chain conformation is random-coil, the maximum draw ratio is given by equation 2

$$\lambda_{\max} = K (M_e)^{1/2} \quad (2)$$

where M_e is the molar mass between entanglements and K is the proportionality constant. For UHMWPE, the maximum draw ratio is found to be 4-5.

Smith *et al.*¹¹ also reported that less entangled UHMWPE films prepared by depositing a vanadium catalyst on a glass slide followed by polymerization of ethylene at relatively low

temperatures, could be drawn in the solid state to a draw ratio of 60. This draw ratio corresponds to the theoretical value for disentangled UHMWPE. The drawability of the same polymer was lost upon melt crystallization suggesting entangling of the polymer chains. A possible explanation for the immediate loss in drawability upon melting was proposed by Barham and Sadler¹² by proposing immediate increase in radius of gyration using the concept of “chain explosion”.

Drawing by hand proved to be a simple method to qualitatively determine the draw ratio of UHMWPE films, which in turn is an effective tool to estimate the entanglement density in polymers. The samples¹³ were compression molded at 120°C/200 bar to form films prior to drawing. The drawing experiments on the films were performed in air at 120°C using a hot plate. The draw ratios were determined from the separation of ink markers pre-printed on the surface of the samples.

The solid state drawability of commercial nascent UHMWPE synthesized with a heterogeneous Ziegler-Natta catalyst is restricted due to the presence of entanglements, and was found to be less than 10.¹⁴⁻¹⁵ However, when entangled commercial grade UHMWPE is dissolved and subsequently crystallized from a suitable solvent the draw ratio dramatically increases. In contrast to the commercial grade polymer, polymers synthesized and obtained directly from the reactor through controlled polymerization conditions by using either one of the catalysts $(C_5Me_5)_2Sm \cdot 2(THF)$ or $[3-t-Bu-2-O-C_6H_3CH=N(C_6F_5)]_2TiCl_2$ showed remarkable solid state drawing characteristics. The draw ratios of the polymers produced at different temperatures (-10°C up to +68°C) were all found to be well above 120. This is much higher than the theoretical value of 60 which was discussed above. This means that the UHMWPE's synthesized under such conditions are highly disentangled when compared to the commercial grade UHMWPE.

It was expected that with the increase in the polymerization temperature the amount of entanglements per unit chain in the UHMWPE would increase and consequently the drawability would decrease. For the polymers synthesized using $(C_5Me_5)_2Sm \cdot 2(THF)$, increasing the polymerization temperature from -10°C up to +20 °C has no effect in terms of drawability of the polymers, indicating that the polymers are highly disentangled even at higher polymerization temperatures. Also the polymers synthesized using the catalyst $[3-t-Bu-2-O-C_6H_3CH=N(C_6F_5)]_2TiCl_2$ at temperatures ranging from -10°C up to +68°C show high draw ratios, suggesting that even at higher polymerization temperatures disentangled polymers can be obtained. From the fact that the drawability is similar in all these polymers,

it can be concluded that the number of entanglements per unit chain is similar in every case. Moreover, the formation of disentangled UHMWPE does not seem to be restricted to one particular catalyst but can be obtained by various homogeneous catalysts that are able to produce UHMWPE. As discussed in Chapter 3, the yttrium catalyst does not show this behavior.

4.2.2 Compression Molding.

The results from the drawing experiments show that the disentangled UHMWPE's are ductile and can be deformed in the solid state. Smith *et al.*¹¹ demonstrated that under extreme shear conditions at temperatures as low as 50°C, the specially synthesized UHMWPE powder (using a vanadium catalyst) can result into a transparent film. Using similar concepts, the powders synthesized as reported in Chapters 2 and 3 were subjected to shear deformation at 50°C and 200 bars. Figure 4.4 shows two films prepared under similar shear conditions. Unlike the film obtained by the commercial grade (Figure 4.4 a), the film prepared from the samples using the homogeneous catalysts $(C_5Me_5)_2Sm \cdot 2(THF)$ and $[3-t-Bu-2-O-C_6H_3CH=N(C_6F_5)]_2TiCl_2$ are translucent (Figure 4.4 b).

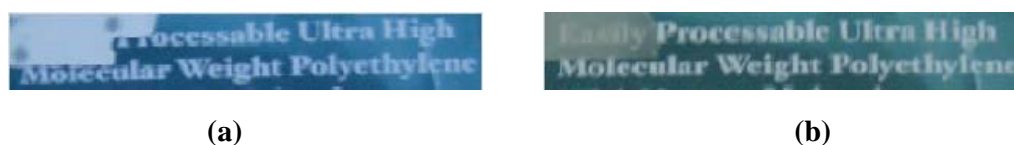


Figure 4.4 Compression molded samples of (a) entangled UHMWPE (opaque film) (b) highly disentangled UHMWPE (transparent film).

The commercial grade entangled polymer could not be pressed into completely fused transparent films, not even above the α -relaxation temperature (above 90°C). Compression molding experiments performed on UHMWPE samples synthesized at different temperatures using the two homogeneous catalysts described in Chapters 2 and 3, showed that clear polymer films could be obtained at temperatures much below the melting point. These observations are in good agreement with the high draw ratios for all samples obtained during mechanical deformation.

4.2.3 Differential Scanning Calorimetry.

An exciting phenomenon that has resulted in considerable debate about its occurrence is the fact that the melting peak in the first DSC scan of nascent UHMWPE appears around 141°C. On subsequent cooling from the melt and reheating, the material now melts at 135°C corresponding to the melting temperature of melt crystallized PE. This first melting peak of 141°C corresponds to the equilibrium melting temperature of polyethylene that can be theoretically calculated using the Gibbs-Thompson equation.¹⁶

$$T_m = T_m^\circ \left[\left(1 - \frac{2\sigma_e}{l \cdot \rho \cdot \Delta H_m} \right) - \left(\frac{2\sigma}{A \cdot \rho \cdot \Delta H_m} \right) - \left(\frac{2\sigma}{B \cdot \rho \cdot \Delta H_m} \right) \right] \quad (3)$$

Where T_m is the experimentally determined melting point, T_m° is the equilibrium melting point for infinite perfect crystals (141.5°C for polyethylene),¹⁷ σ_e is the surface free energy of the fold planes, σ is the surface free energy of the lateral planes, l is the crystal thickness in the chain direction (fold length), ΔH_m is the heat of fusion, A and B are the lateral crystal dimensions and ρ is the crystal density.

Engelen *et al.*¹⁸ showed that the small, irregularly stacked, folded chain crystals in nascent UHMWPE powder undergo fast reorganization upon heating. Therefore it was thought that this high first melting point of 141°C is due to the fast reorganization of small metastable folded chain crystals during heating leading to thickening of the lamella. Later it was shown by Kurelec¹⁹ that such a process cannot explain this high melting point as the thickness of the lamella does not increase to such an extent that the T_m would approach T_m° .

In a recent article Chirinos *et al.*²⁰ described the synthesis of UHMWPE using the homogeneous catalyst $(C_5H_5)_2Ti(O_2CC_6H_5)_2$ below room temperature. They observed a similar melting behavior and attributed the occurrence of the first melting peak at 141°C to the presence of disentangled chains that upon melting resulted in melt crystallized UHMWPE with a melting temperature of 135°C. However, the conclusion is false as the difference in the melting temperature has no correlation to the entanglement density (although the polymers synthesized at low temperatures could have low entanglement density). In order to verify the above assumption, the DSC of a fully entangled nascent UHMWPE sample was measured. Since a similar high melting peak was observed, it can be excluded that the first high melting peak originates from disentangled UHMWPE.

As a part of our study on disentangled UHMWPE, we investigated the melting behavior of UHMWPE (both entangled and disentangled) in more detail. Clearly the morphology of nascent crystals is different when compared to that of a reheated sample. Furthermore, both disentangled and entangled nascent UHMWPE exhibit a high melting temperature in the first scan in DSC, which suggests that the melting behavior of disentangled and entangled nascent UHMWPE are comparable. As the first experiment, the effect of the heating rate on the melting temperature was evaluated. When the heating rate is lowered from $10 \text{ K}\cdot\text{min}^{-1}$ to $1 \text{ K}\cdot\text{min}^{-1}$ the first melting peak shifts from 140°C to 138°C . The drop in the melting point observed is most probably due to the thermal lag in heating the sample at higher heating rate and certain degree of superheating. For convenience, a heating rate of $10 \text{ K}\cdot\text{min}^{-1}$ was used in further experiments.

As mentioned before, both entangled and disentangled UHMWPE show a high first melting temperature which in subsequent heating runs drops to the value corresponding to melt crystallized UHMWPE. It might be expected that the kinetics of this process are different for entangled and disentangled UHMWPE. To investigate the kinetics of melting of entangled and disentangled polymers, we performed annealing experiments with the polymers synthesized as described in Chapters 2 and 3 and with the commercial Montell 1900LCM polymers.

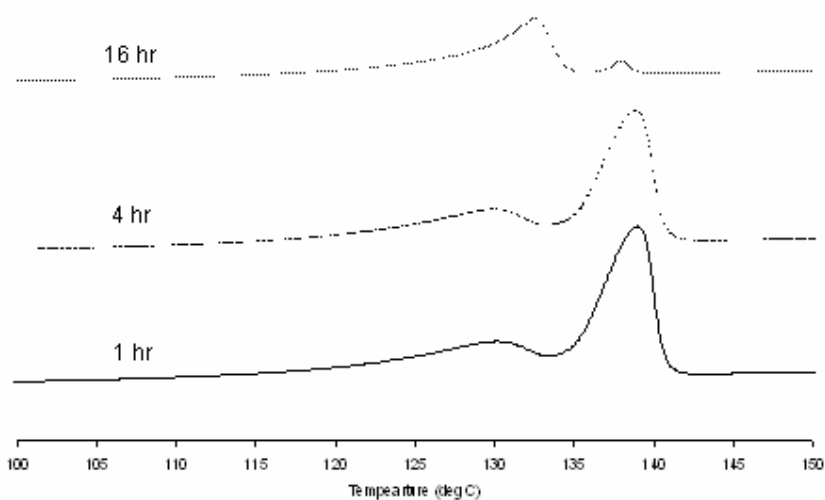


Figure 4.5 Effect of annealing time on the ratio of the two peaks at 135°C and 141°C for UHMWPE synthesized using $(C_5Me_5)_2Sm\cdot 2(THF)$ and $[3-t-Bu-2-O-C_6H_3CH=N(C_6F_5)]_2TiCl_2$.

Samples of nascent UHMWPE were annealed for 1, 4 and 16 hours at a temperature just above the onset of melting. Subsequently, they were cooled and reheated above the melting temperature at the rate of $10 \text{ K}\cdot\text{min}^{-1}$. On doing this, two peaks were observed in the DSC as shown in Figure 4.5, one corresponding to the original nascent morphology (141°C), and the other corresponding to melt crystallized PE (135°C). From the ratio of the two peaks it is possible to estimate how much of the nascent morphology is lost after a certain time. The polymers synthesized with homogeneous catalysts showed an appreciable increase in the peak at 135°C at the cost of the peak at 141°C , with increasing annealing time. For the commercial grade polymer, there was hardly any effect of the annealing time on the ratio of the two peaks observed. This strongly supports our hypothesis that disentangled UHMWPE can indeed be obtained by carefully controlling the polymerization conditions in such a way that the polymer chains crystallize before they get entangled. Therefore, the time required for nascent crystals to melt seems to depend on the initial crystal topology.

A plausible explanation would be that during annealing at 136°C the UHMWPE chains have time to melt by reeling out of the chains from the crystal. It is obvious that this phenomenon would occur more readily for a disentangled system than for an entangled one. Hence, a disentangled system would melt significantly faster, resulting in a faster increase of the peak at 135°C compared to a fully entangled system. Even among the UHMWPE synthesized with $(\text{C}_5\text{Me}_5)_2\text{Sm}\cdot 2(\text{THF})$ and $[\text{3-}i\text{-Bu-2-O-C}_6\text{H}_3\text{CH}=\text{N}(\text{C}_6\text{F}_5)]_2\text{TiCl}_2$ a notable difference in the annealing behavior was observed. For the polymers obtained with the $[\text{3-}i\text{-Bu-2-O-C}_6\text{H}_3\text{CH}=\text{N}(\text{C}_6\text{F}_5)]_2\text{TiCl}_2$ catalyst, irrespective of the synthesis temperature all the polymers showed a similar increase in the peak at 135°C with increasing annealing time as shown in Figure 4.6. However, for the UHMWPE synthesized with the samarocene catalyst this was not the case. The polymers synthesized at -10°C and 0°C showed rapid increase in the peak at 135°C with increase in the annealing time. But as the polymerization temperature is increased the effect starts to decrease and the polymer synthesized at $+20^\circ\text{C}$ shows only a marginal effect as shown in Figure 4.7. Even on annealing this sample for a long period of time very close to its first melting temperature (annealing temperature of 134.5°C), the ratio of the peaks does not change significantly as seen with polymers synthesized at -10 and 0°C . Nevertheless, the solid state drawability of this sample is similar to that of all the other polymers synthesized with the samarocene at lower temperatures. In addition to that, the onset of melting is also considerably lower for this sample (130.5°C) as compared to other polymers synthesized in this series (134°C) with the samarium catalyst.

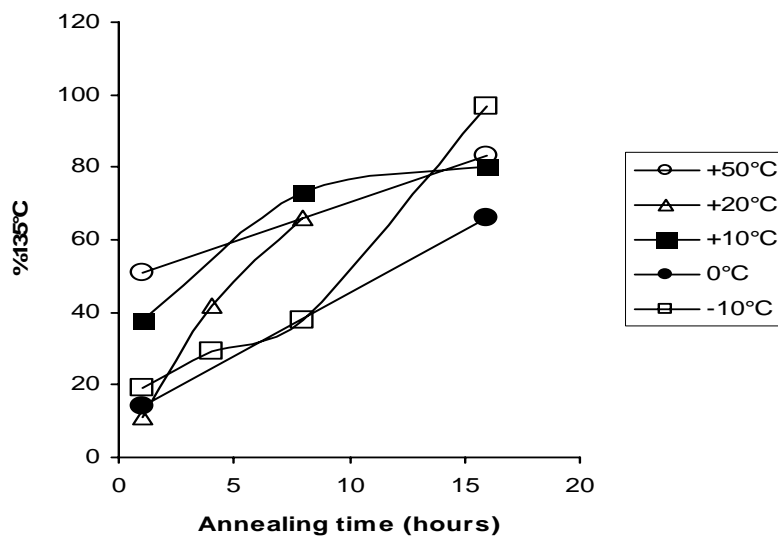


Figure 4.6 Relative increase of the 135°C peak with the annealing time for the UHMWPE synthesized with the $[3-t\text{-Bu-}2\text{-O-C}_6\text{H}_3\text{CH}=\text{N}(\text{C}_6\text{F}_5)_2\text{TiCl}_2/\text{MAO}]$ at different temperatures.

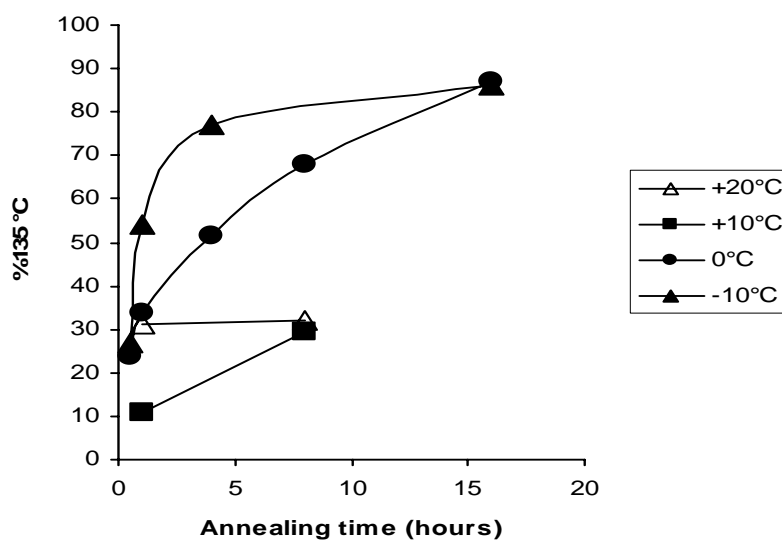


Figure 4.7 Relative increase of the 135°C peak with the annealing time for the UHMWPE synthesized with the $(\text{C}_5\text{Me}_5)_2\text{Sm}\cdot 2(\text{THF})$ catalyst at different temperatures.

One possible explanation for this behavior could be the difference in the entanglements present in the solid state obtained during the polymer synthesis.

The outcome of the annealing experiments is also very sensitive to the annealing temperature as shown in Figure 4.8, where the influence of annealing temperature at a fixed annealing time of 1 hour is demonstrated for the polymer synthesized with the samarocene catalyst at -10°C . A variation of even 0.5°C in the annealing temperature can have a considerable effect on the results.

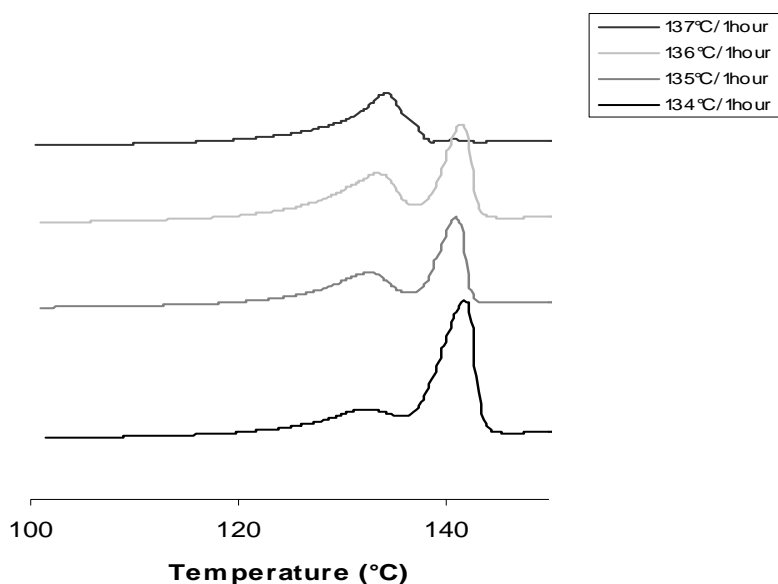


Figure 4.8 The effect of annealing temperature on the $135^{\circ}\text{C}/141^{\circ}\text{C}$ peak ratio for the UHMWPE synthesized using $(\text{C}_5\text{Me}_5)_2\text{Sm}\cdot 2(\text{THF})$ at -10°C .

While for the polymer synthesized at -10°C annealing for 1 hour at 134°C yielded two melting peaks, annealing the same polymer at a slightly lower temperature (133.5°C) did not lead to the appearance of the peak at 135°C . On the other hand, after the same sample was annealed for 1 hour at 136°C , the peak at 135°C had increased considerably. Annealing the sample at 137°C resulted in complete disappearance of the peak at 141°C , which clearly demonstrates the dynamic behavior of polymer chains at different temperatures. Annealing experiments are very useful for estimating the entanglement density but cannot be used as a quantitative technique.

4.2.4 Temperature Modulated DSC.

Recently, Höhne *et al.*^{21a} reported on the use of temperature modulated differential scanning calorimetry (TMDSC) to study the various processes taking place in UHMWPE below the actual melting point. It was found that TMDSC is an excellent tool to determine the time constants of processes such as α -relaxation and melting and dissolution of the polymer into the viscous melt. For disentangled UHMWPE the melting and dissolution was found to occur faster than for a fully entangled UHMWPE. Before describing the outcome of the TMDSC measurements on our samples, the technique will be briefly described.

A conventional DSC measures the heat flow (and heat capacity) and gives the net result of all kinds of transitions taking place in the sample during heating, making the study and evaluation of the individual changes taking place in the sample apart from the real melting and crystallization rather impossible. TMDSC is unique and provides the opportunity to separately measure the individual contributions to the heat capacity due to the various changes taking place in the sample and hence give a better understanding of these systems. We have exploited this technique to qualitatively assess the entanglement density in the polymers synthesized using the $(C_5Me_5)_2Sm \cdot 2(THF)$ and the $[3-t-Bu-2-O-C_6H_3CH=N(C_6F_5)]_2TiCl_2$ catalysts as presented in Chapters 2 and 3 and have subsequently compared the results with the completely entangled commercial grade UHMWPE.

Unlike in normal DSC, in TMDSC the actual temperature oscillates around an averaged temperature over one modulation cycle.²² As a result, the linear temperature program used for conventional DSC is superimposed with a sinusoidal temperature fluctuation according to the equation 4:

$$T(t) = T_0 + \beta_0 t + T_A \sin(\omega t) \quad (4)$$

where β_0 is the underlying heating/cooling rate, T_A is the temperature fluctuation amplitude and ω is the angular frequency of modulation ($\omega=2\pi f$). Some other types of periodical temperature fluctuations have been well-documented such as: saw-tooth, triangular, step like etc. When the average temperature is held constant ($\beta_0 = 0$), this is called a quasi-isothermal mode of measurement.

The apparent heating rate can be derived from equation 4 as

$$dT/dt = \beta_0 + T_A \omega \cos(\omega t) \quad (5)$$

Therefore, in TMDSC measurements the heating rate is not constant but fluctuates between $(\beta_0 + T_A \omega)$ and $(\beta_0 - T_A \omega)$. A conventional DSC provides information about the heat flow rate into the sample at a specific heating rate (equation 6).

$$\Phi(T, t) = C_p(T) dT/dt + \Phi^{ex}(T, t) \quad (6)$$

The first component on the right side represents the influence of the non-zero heat capacity of the sample, which does not change significantly during the small changes of temperature. The second component represents the heat flow in the sample due to various endothermic and exothermic changes taking place within the sample when heated or annealed at a particular temperature. A conventional DSC only measures the net heat flow rate of the processes that are taking place at the same time. The TMDSC method allows separating the heat capacity of these time dependent processes from the normal heat capacity and heat capacity associated with time independent or very fast processes.^{21a}

From equations 5 & 6 we obtain:

$$\Phi(T, t) = C_p(T) \beta_0 + C_p(T) \cdot T_A \omega \cdot \cos(\omega t) + \Phi^{ex}(T, t) \quad (7)$$

In the absence of processes $\Phi^{ex}=0$, and

$$\Phi(T, t) = C_p(T) \beta_0 + C_p(T) \cdot T_A \omega \cdot \cos(\omega t) \quad (8)$$

Therefore the measured heat flow rate consists of two parts as shown in Eq 8: the first term is the underlying part $\Phi_u(t)$ and is almost the curve that one would get from the conventional DSC. The second term is the periodic part $\Phi_{per.}(T, t)$ and fluctuates in time around zero.

Upon subtraction of the underlying part from the total signal, the periodic part is obtained (Φ_A) from where the heat capacity can be calculated using equation 9.

$$C_p = \Phi_A / T_A \omega \quad (9)$$

The apparent heat capacity calculated in this way should be identical to the thermodynamic (vibrational) heat capacity measured from the underlying curve or the conventional DSC measurement.

TMDSC experiments were carried out employing a modified Perkin-Elmer DSC-7 apparatus calibrated for cell constant and temperature using Indium standards. The instrument was modified using a commercial precision function generator to allow a sinusoidal temperature modulation. The measurements were carried out under nitrogen atmosphere to prevent degradation of the polymer samples. Typically for every measurement about 2 mg of a polymer sample was weighted out each time using a precision balance. Standard (crimped) aluminum pans of similar predetermined masses were used for all measurements. The masses of the pans on the reference side and the sample side were balanced to give a zero signal for the baseline. The experiments were carried out under quasi-isothermal mode at different temperatures (130°C, 135°C, 136°C and 138°C) at a frequency of 12.5 mHz (80 s period) and temperature amplitude of 0.06 K. The frequency used was low enough to measure the excess heat capacity associated with possible processes taking place in the pre-melting temperature region. If the processes are time dependent, they will not influence the periodic signal if the modulation frequency is too high and in that case the excess heat capacity will drop to zero. The measured modulated signal consists of two parts: The underlying part $\Phi_u(t)$ and the periodic part $\Phi_{per.}(T, t)$. Gliding integration over one period provided the underlying part $\Phi_u(t)$ which, when subtracted from the total measured signal, yielded the periodic part $\Phi_{per.}(T, t)$. The apparent heat capacity (magnitude and phase shift) was calculated using a mathematical procedure described in the literature.^{21b}

Höhne *et al.*^{21a} showed that the magnitude of heat capacity of nascent UHMWPE obtained by TMDSC in the pre-melting region was higher than the heat capacity obtained by conventional DSC indicating that there are some processes taking place in the pre-melting region. The magnitude of this excess heat capacity decreased on second heating suggesting that the process is irreversible in nature and is observed only on the first heating of the nascent crystals. Curve fitting on the data obtained from these measurements yields the time constants for the different processes taking place in the UHMWPE.

Table 4.1 Result of fitting $a_1 e^{-t/\tau_1} + a_2 e^{-t/\tau_2} + a_3 e^{-t/\tau_3}$ to the quasi-isothermal excess heat capacity for disentangled $(C_5Me_5)_2Sm \cdot 2(THF)$ based UHMWPE.

T(°C)	$a_1(Jg^{-1}K^{-1})$	$t_1(min)$	$a_2(Jg^{-1}K^{-1})$	$t_2(min)$	$a_3(Jg^{-1}K^{-1})$	$t_3(min)$
130	0.4	2.8	0.5	13.3	1.0	244.7
135	1.7	3.4	0.6	15.7	1.1	287.9
136	3.1	3.3	1.4	20.6	1.8	216.1
138	4.9	3.1	19.3	20.6	3.0	155.3

Figure 4.9 displays the results of two quasi-isothermal measurements carried out on UHMWPE synthesized with the samarocene catalyst. Curve fitting on the data obtained from each of these measurements at different temperatures affords three different time constants as reported in Table 4.1 and Figure 4.10. It can clearly be seen that there are three processes with different time constants operating at a given temperature.

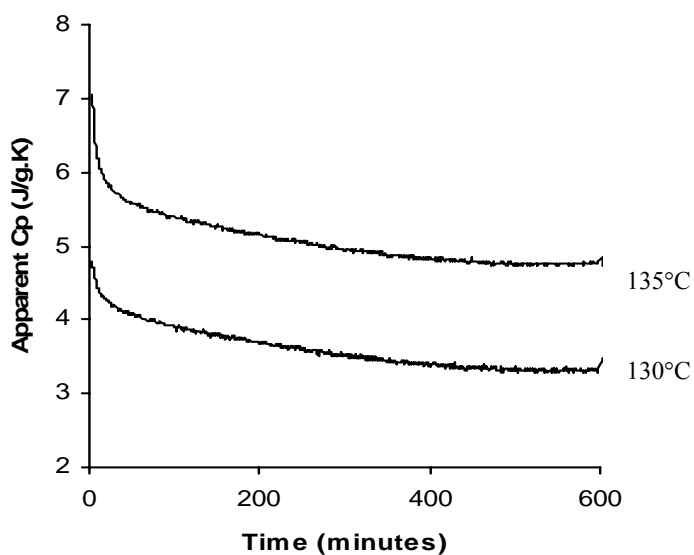


Figure 4.9 Plot representing apparent heat capacity versus time obtained from TMDSC quasi-isothermal measurements of nascent UHMWPE.

The polymer sample used in this study were similar to those previously investigated by Höhne *et al.*^{21a} As expected, the observed time constants are also comparable to those reported earlier.^{21a} A similar study conducted on the polymers synthesized using the

bis(phenoxy-imine)titanium catalyst is represented in Table 4.2 and Figure 4.11 and the results are in total agreement with those obtained with the samarocene catalyst. The data points with the lowest time constant (1-5 min) can be disregarded as artifacts assigned to the limited conductivity and the heat capacity of the measuring head of the DSC. The process with a time constant referred to as t_2 has been assigned to the ordering and perfection of the crystals (α -relaxation), which is exothermic in nature. From Tables 4.1, 4.2 and 4.3 and Figures 4.10, 4.11 and 4.12 it can be clearly seen that the time constant t_2 for commercial grade highly entangled UHMWPE is considerably higher than for the samples prepared using the homogeneous catalysts described in Chapters 2 and 3. The process with the highest time constant t_3 is assigned to the endothermic, slow melting and dissolution of the crystallites into the surrounding viscous liquid phase. The time constant of this process also differs considerably when comparing commercial grade samples with those prepared using the homogeneous catalysts.

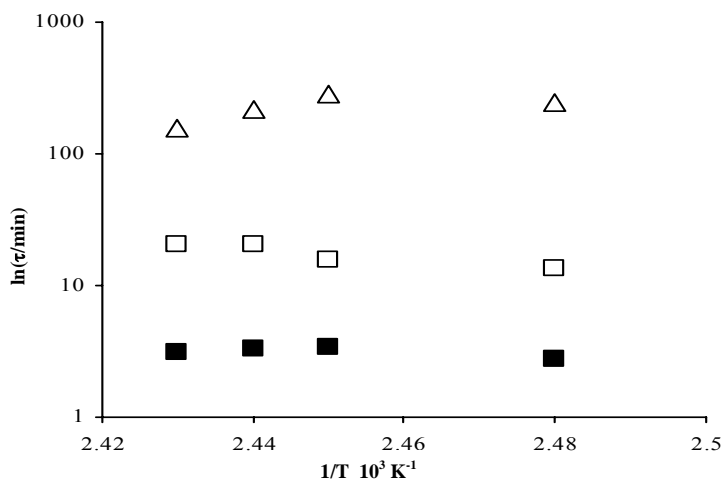


Figure 4.10 Plot representing different processes with different time constants listed in Table 4.1 for a disentangled UHMWPE synthesized at 0 °C using the $(C_5Me_5)_2Sm \cdot 2(THF)$ catalyst.

Table 4.2 Result of fitting $a_1 e^{-t/\tau_1} + a_2 e^{-t/\tau_2} + a_3 e^{-t/\tau_3}$ to the quasi-isothermal excess heat capacity for disentangled [3-*t*-Bu-2-*O*-C₆H₃CH=N(C₆F₅)₂TiCl₂ based UHMWPE.

T(°C)	a ₁ (Jg ⁻¹ K ⁻¹)	t ₁ (min)	a ₂ (Jg ⁻¹ K ⁻¹)	t ₂ (min)	a ₃ (Jg ⁻¹ K ⁻¹)	t ₃ (min)
130	0.1	5.53	0.4	11.0	0.9	320
135	1.7	3.9	0.6	14.5	1.1	303
136	4.0	2.8	1.3	15.3	1.37	198
138	8.4	1.8	4.9	6.2	1.2	34.2

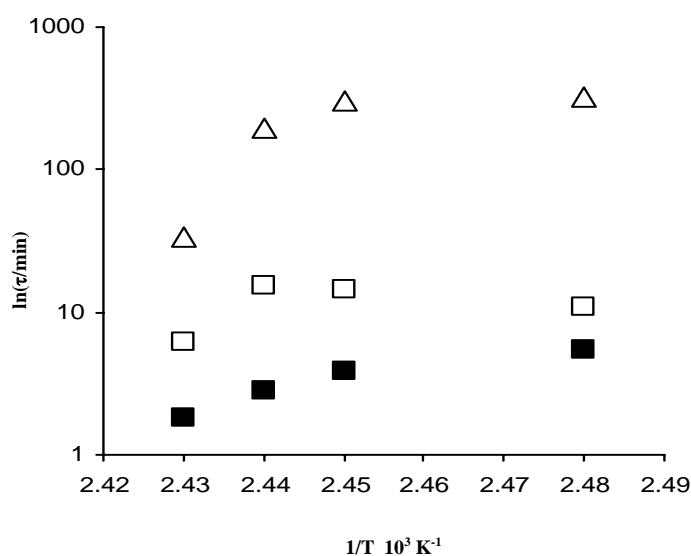


Figure 4.11 Plot representing different processes with different time constants listed in Table 4.2 for a disentangled UHMWPE synthesized at 0 °C using the [3-*t*-Bu-2-*O*-C₆H₃CH=N(C₆F₅)₂TiCl₂ catalyst.

Comparing Figures 4.10 and 4.11 with 4.12, it is seen that both entangled and disentangled polymers undergo an α -relaxation process and that the time constant t_2 for this process differs considerably especially at temperatures below the melting point. However, there is an appreciable difference for these polymer samples in the time constant for the process associated with the melting and dissolution. An entangled polymer exhibits much higher time constant (600 – 1000 minutes; Table 4.3, Figure 4.12) compared to a disentangled polymer (100 – 300 minutes; Tables 4.1 and 4.2, Figures 4.10 and 4.11). The results of TMDSC are in complete agreement with the annealing experiments. In other words, the processes of both α -

relaxation and melting and dissolution in the surrounding medium are much slower for an entangled material due to the highly viscous melt and the increased restriction to flow. Therefore TMDSC can be used to provide another qualitative measure to investigate entanglement density.

Table 4.3 Time constants obtained by curve fitting $a_1 e^{-t/\tau_1} + a_2 e^{-t/\tau_2} + a_3 e^{-t/\tau_3}$ to the quasi-isothermal excess heat capacity for entangled commercial UHMWPE based on heterogeneous catalyst.

T(°C)	t ₁ (min)	t ₂ (min)	t ₃ (min)
130	9.3	64.0	1000.0
135	5.8	22.0	477.0
136	4.3	25.0	559.0
138	2.3	13.9	195.0

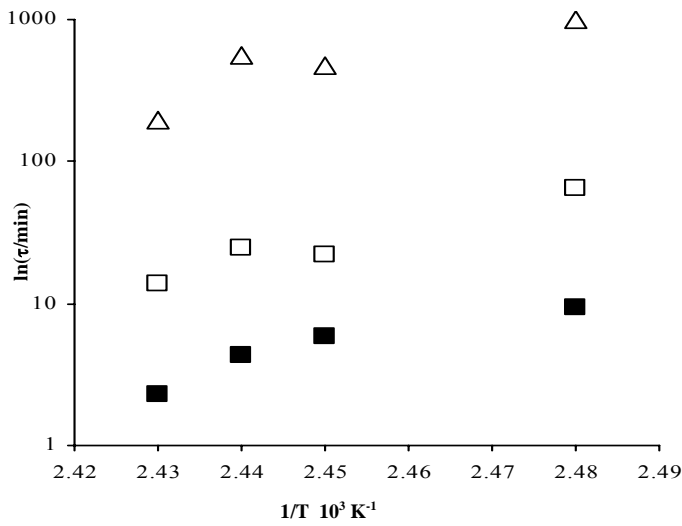


Figure 4.12 Plot representing different processes with different time constants listed in Table 4.3 for an entangled Montell grade UHMWPE.

4.2.5 Determination of Entanglements by Rheology

Another technique that provides information on the visco-elastic nature of a polymer melt is rheology. The graph of the zero shear viscosity versus the M_w is shown in Figure 4.1 (solid line). The graph shows that initially the viscosity of the polymer melt increases linearly with the increase in the molecular weight. Beyond a critical molar mass, M_c , an exponential increase in viscosity is observed. The exponential increase in viscosity results from entanglements between chains in the melt. A defined rheological experiment helps in the estimation of the plateau modulus G' . Figure 4.13 shows a typical plot of the storage modulus as a function of frequency at constant strain of a series of polystyrenes having different molecular weights and narrow MWD. The experimental findings are that the plateau spreads over wider frequency with increase in the molecular weight, while the modulus stays the same. This suggests that the modulus is independent of the molecular weight. The storage plateau modulus of the polymer is inversely related to the average molecular weight between entanglements (M_e) according to equation 10.²³

$$G'_{\text{plateau}} = g_N \rho RT / M_e \quad (10)$$

where g_N is a numerical factor, R is the gas constant, T is the temperature at which the measurement is carried out, M_e is the molecular weight between entanglements and ρ is the density of the polymer. Since G' is inversely related to the molar mass between entanglements M_e , it is clear that for the thermodynamically stable state of all polystyrene samples in Figure 4.13 the entanglement density is the same. So far rheology has been mainly used to study polymer melts in their thermodynamically stable state (i.e. fully entangled state). It is expected that the G' for a disentangled polymer will be lower than an entangled polymer and will increase to the level of the latter during the entangling process upon melting. Therefore we have exploited the versatility of this technique to ascertain the entanglement density of the polymer. Following the storage modulus at fixed frequency and temperature, dynamic changes in the number of entanglements with time can be followed.

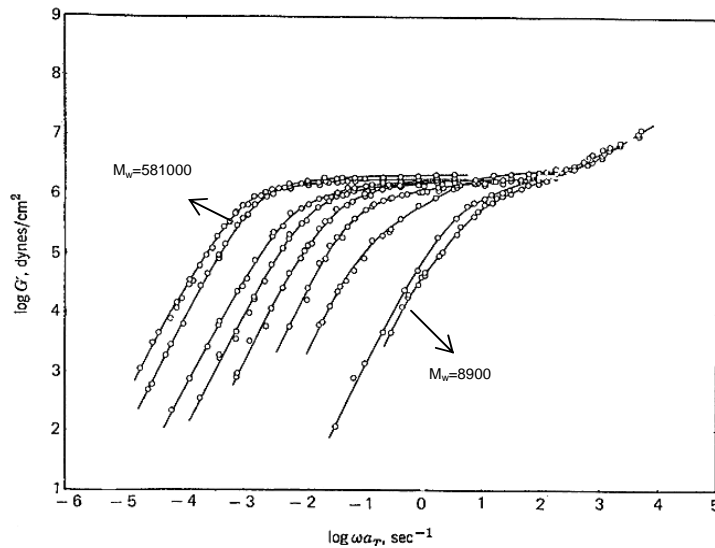


Fig 4.13 The storage modulus of a series of very narrow distributed polystyrenes having different molecular weight ranging from $M_w=8.9$ kg/mol to $M_w=581$ kg/mol . The plateau spreads over wider frequency with increase in the molecular weight, while the modulus stays the same.²³

Effect of Dilution and Temperature during Polymerization on the Storage Plateau Modulus.

Samarocene

The value of the storage plateau modulus of a fully entangled polyethylene is close to 2×10^6 Pa. In Chapter 1, it was proposed that at low polymerization temperatures, the polymer chains might begin to crystallize directly upon synthesis since the crystallization rate is expected to be faster than the polymerization rate at low temperatures. When the crystallization and polymerization rates are comparable, a sufficiently diluted system would keep the active sites apart, enhancing the formation of polymer with highly disentangled chains.

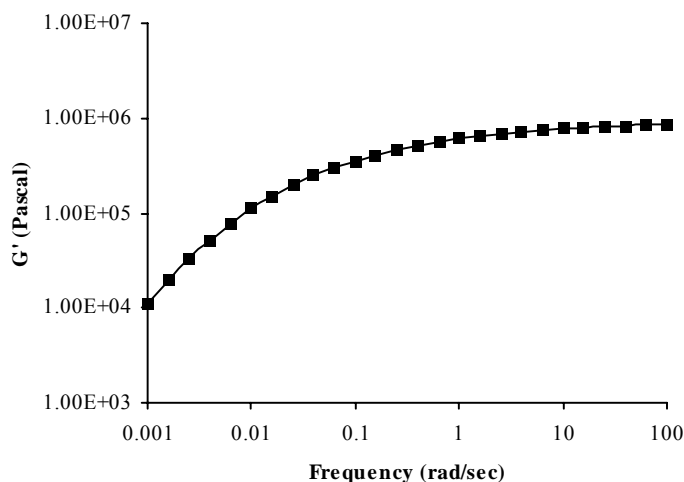


Figure 4.14 Plot representing the broad rubbery plateau exhibited by UHMWPE at higher frequency prepared at 0°C and a concentration of samarocene of 0.168 mM.

In order to study the possible influence of catalyst concentration and polymerization temperature on the storage modulus, frequency sweep measurements were carried out at 160°C using the UHMWPE synthesized with the $(C_5Me_5)_2Sm \cdot 2(THF)$ catalyst at varying dilutions (250 mL to 1000 mL) and temperatures (-10°C to +20°C).

Table 4.4 Effect of dilution during the polymer synthesis on the storage plateau modulus of UHMWPE synthesized using the $(C_5Me_5)_2Sm \cdot 2(THF)$.

Solvent (mL)	Yield (g)	T_m^a (°C)	M_w (kg/mol) ^b	D	G^{1c} ($\times 10^6$ Pa)
250	0.4	137.2	1038	1.5	0.9
500	1.6	141.2	1769	1.6	0.7
1000	9.0	141.2	2361	2.8	0.5

(a) Measured by DSC, Pyris 1 (b) Determined by GPC (c) Determined by rheology.

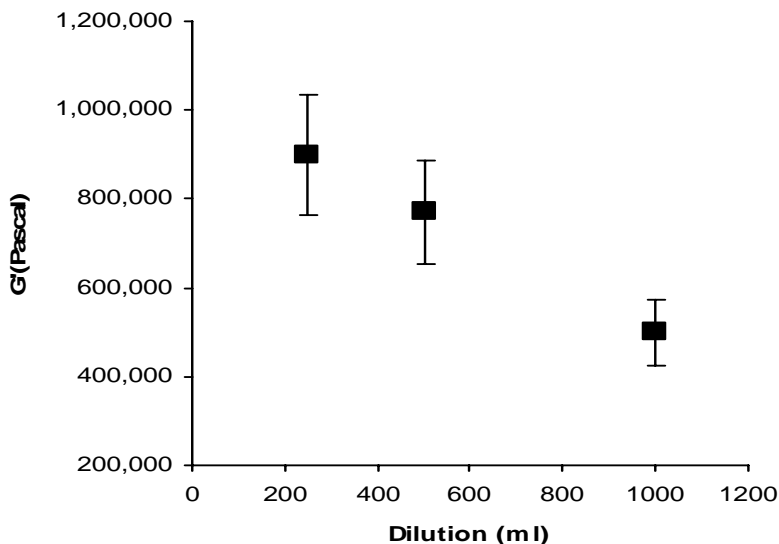


Figure 4.15 Influence of dilution during polymer synthesis on storage plateau of UHMWPE synthesized using the $(C_5Me_5)_2Sm \cdot 2(THF)$ at $0^\circ C$.

The polymer samples¹³ were compression molded at $50^\circ C/200$ bar into films. The plateau modulus was measured with an ARES 3LS-4A, of Rheometrics Inc. with a plate-plate geometry having a diameter of 8 mm. All measurements were performed in a temperature range of $160-180^\circ C$ in a nitrogen environment to prevent the degradation of polymer sample. The angular frequency dependence of the viscoelastic property G' (storage modulus) was determined in the range from 10^{-3} to 10^2 radians per second at $160^\circ C$. The dynamic strain applied was 0.5%. At this strain level all the tested materials were fully viscoelastic.

Tables 4.4 & 4.5 and Figures 4.15 & 4.16 display the effect of dilution and temperature on the value of the storage plateau modulus. For all samples, the value of the storage plateau modulus is significantly lower than 2×10^6 Pa suggesting a low entangled state. Moreover, the value of G' decreases from 0.9×10^6 Pa to 0.5×10^6 Pa on increasing the dilution from 250 mL to 1000 mL, respectively. As an example, the frequency sweep plot of the UHMWPE prepared at $0^\circ C$ and a concentration of samarocene of 0.168 mM is presented in Figure 4.14.

Table 4.5 Effect of temperature on the storage plateau modulus of UHMWPE synthesized using the $(C_5Me_5)_2Sm \cdot 2(THF)$.

Temperature (°C)	Yield (g)	T_m^a (°C)	M_w (kg/mol) ^b	D	G^c ($\times 10^6$ Pa)
-10	2.4	139.8	1225	2.0	0.6
0	13.0	140.3	2040	2.5	0.4
+10	16.7	141.6	2265	2.7	0.4
+20*	14.0	136.8	1368	2.2	0.5

* Catalyst addition was $2.8\mu\text{mol} \times 7$ times; petroleum-ether (40:60) 1 L; ethylene (1 bar)

(a) Measured by DSC, Pyris 1 (b) Determined by GPC (c) Determined by Rheology.

Also, with the average value²⁴ of 0.5×10^6 Pa the plateau modulus of polymers produced at different temperatures are much lower than that of the commercial grade entangled UHMWPE. Although it was expected that with the increase in the polymerization temperature the number of entanglements per unit chain would increase (as a result of an increase in the polymerization rate and a decrease in the crystallization rate), no significant change in the G' value was observed through out the temperature range. These results for the first time demonstrate that the entanglement density or M_e of the nascent polymer can indeed be tuned by changing the synthesis conditions, such as catalyst type and dilution.

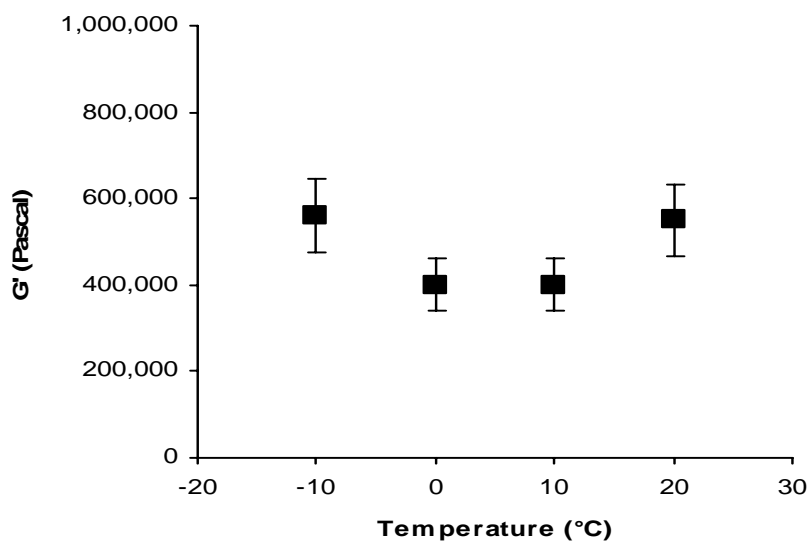


Figure 4.16 Influence of the polymerization temperature on the storage plateau of UHMWPE synthesized using the $(C_5Me_5)_2Sm \cdot 2(THF)$ at constant dilution (1 L).

Bis(phenoxy-imine)titanium catalyst.

Following the rheology experiments with the samarium catalyst, similar studies were performed on the polymers obtained with the catalyst $[3-t\text{-Bu-2-O-C}_6\text{H}_3\text{CH=N(C}_6\text{F}_5)_2\text{TiCl}_2$. Again it was observed that the value of G' is considerably lower than that for the commercial grade UHMWPE, and decreases even further upon dilution as shown in Table 4.6 and Figure 4.17. The results of rheology measurements on the UHMWPE synthesized using $[3-t\text{-Bu-2-O-C}_6\text{H}_3\text{CH=N(C}_6\text{F}_5)_2\text{TiCl}_2$ at different temperatures, ranging from -10°C to $+68^\circ\text{C}$ are shown in Table 4.7 and Figure 4.18. Like for the UHMWPE prepared by the samarocene the polymers synthesized with bis(phenoxy-imine)titanium show a low value of G' (0.6×10^6 Pa) throughout the whole temperature range of -10°C to $+20^\circ\text{C}$. The question at this point is what is the upper temperature limit at which disentangled UHMWPE can still be obtained. Although the G' value increases slightly, Figure 4.18 shows that the polymer prepared at $+50^\circ\text{C}$ still has a low storage plateau modulus (0.8×10^6 Pa) indicative for a less entangled morphology. Unfortunately, the storage plateau modulus of a UHMWPE sample prepared at $+68^\circ\text{C}$ could not be measured accurately due to slippage during the measurement. Nevertheless, the fact that this sample was highly drawable is very encouraging and strongly suggests that the production of a less entangled UHMWPE is feasible at temperatures as high as $+68^\circ\text{C}$.

Table 4.6 Effect of dilution during the polymer synthesis on the storage plateau modulus of UHMWPE synthesized using the $[3-t\text{-Bu-2-O-C}_6\text{H}_3\text{CH=N(C}_6\text{F}_5)_2\text{TiCl}_2/\text{MAO}$.

Solvent (mL)	Yield (g)	T_m^a ($^\circ\text{C}$)	M_w (kg/mol) ^b	D	G'^c ($\times 10^6$ Pa)
500	1.0	139.8	882	1.3	0.9
1000	2.0	140.4	1321	1.2	0.4
2000	2.8	140.0	1525	1.2	0.5

(a) Measured by DSC, Pyris 1 (b) Determined by GPC (c) Determined by rheology.

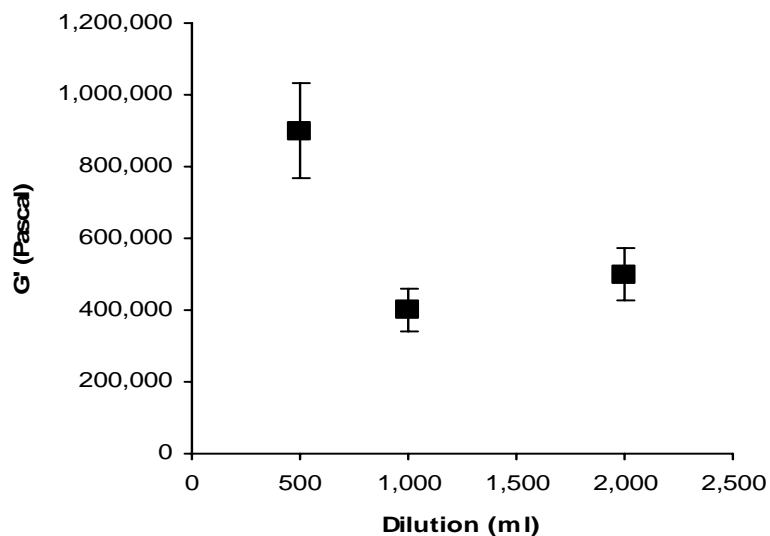


Figure 4.17 Influence of dilution during polymer synthesis on the storage plateau modulus of UHMWPE synthesized using the $[3-t-Bu-2-O-C_6H_3CH=N(C_6F_5)]_2TiCl_2/MAO$.

Table 4.7 Effect of the polymerization temperature on the storage plateau modulus of UHMWPE synthesized using the $[3-t-Bu-2-O-C_6H_3CH=N(C_6F_5)]_2TiCl_2/MAO$.

Temperature (°C)	Yield (g)	T_m^a (°C)	M_w (kg/mol) ^b	D	G^c ($\times 10^6$ Pa)
-10	1.8	140.4	1001	1.3	0.4
0	2.7	141.8	1397	1.4	0.6
+10	2.8	140.4	1131	1.3	0.5
+20	3.7	141.0	1089	1.4	0.6
+50	3.0	141.8	1788	1.7	0.8

Petroleum-ether (40:60) (1 L); ethylene (1 bar); (a) Measured by DSC, Pyris 1 (b) Determined by GPC (c) Determined by rheology.

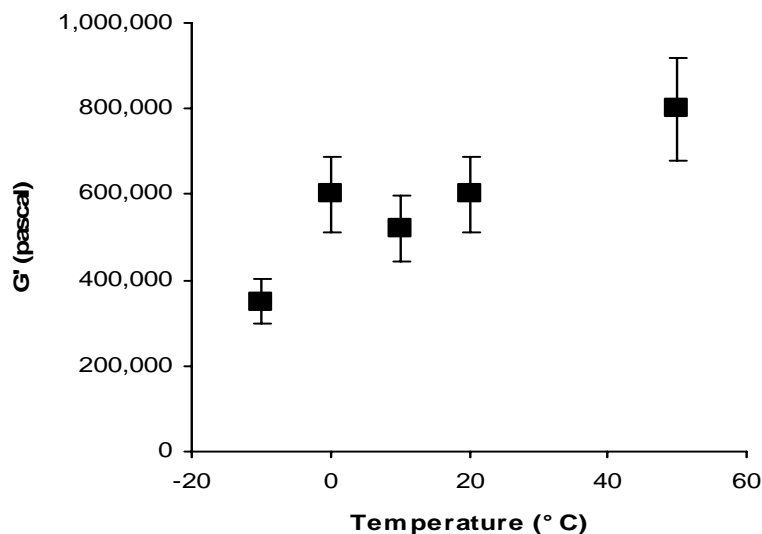


Figure 4.18 Influence of polymerization temperature on the storage plateau of UHMWPE synthesized using the $[3-t\text{-Bu-2-O-C}_6\text{H}_3\text{CH=N(C}_6\text{F}_5)_2\text{TiCl}_2\text{/MAO}$ at constant dilution (1 L).

Build Up of Storage Plateau Modulus with Time.

The results of the rheology experiments described above are in good agreement with those obtained from drawing, DSC and TMDSC experiments, and confirms that specific polymerization conditions such as choice of catalyst, temperature and dilution facilitate the synthesis of highly disentangled UHMWPE.

So far it has been shown that UHMWPE can be obtained that exists in a thermodynamically labile disentangled state. It was also shown that this state provides a material that can readily flow on compression even below the melting point. Although the disentangled state is advantageous for the processing, the mechanical properties of a polymer are very much dependent on the presence of entanglements. Therefore, the disentangled UHMWPE's must entangle fully at the end of the processing step in order to confer good mechanical properties to the final product. However, if the disentangled state could be maintained in the melt for a while, the low melt viscosity would result in better flow of the long chains and improved processability of the material. If disentangled polymers would entangle, it should result in the increase of modulus. This occurrence of the entanglement process was studied by time sweep rheology experiments²⁵ In such an experiment the build up of G' with time is followed at constant temperature (160°C), frequency (10 radians/second) and strain (0.5%).

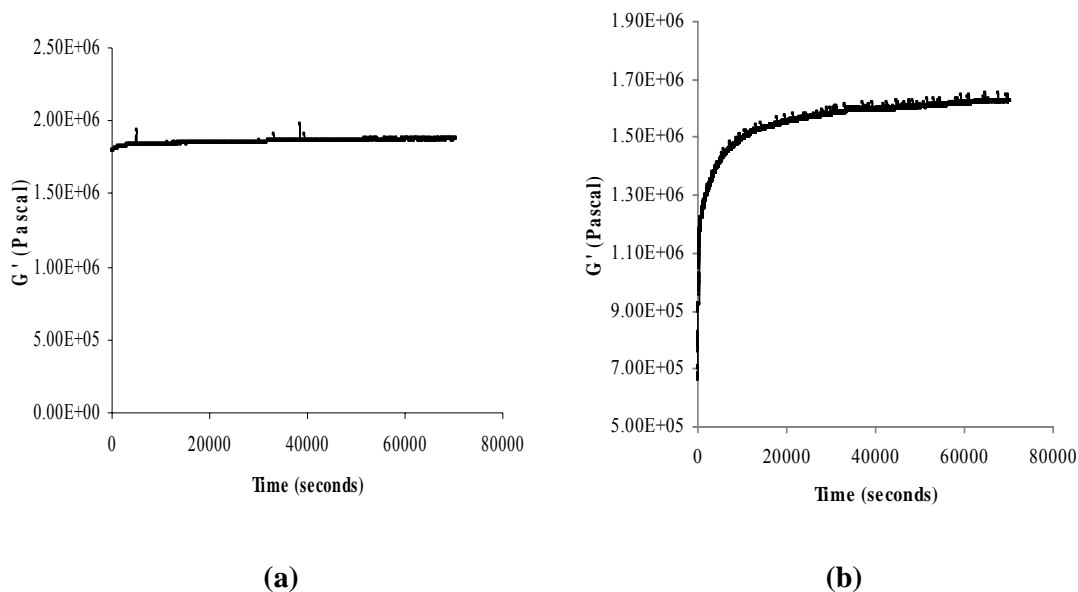
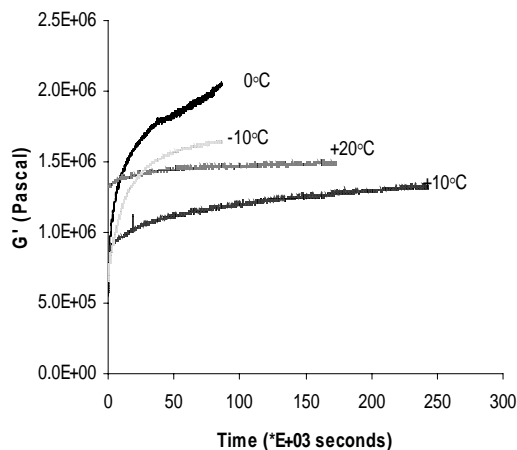


Figure 4.19 Time sweep test performed at 160°C on (a) commercial grade UHMWPE showing the absence of build up of the modulus with time (b) UHMWPE synthesized with the homogeneous catalysts showing build up of modulus with time.

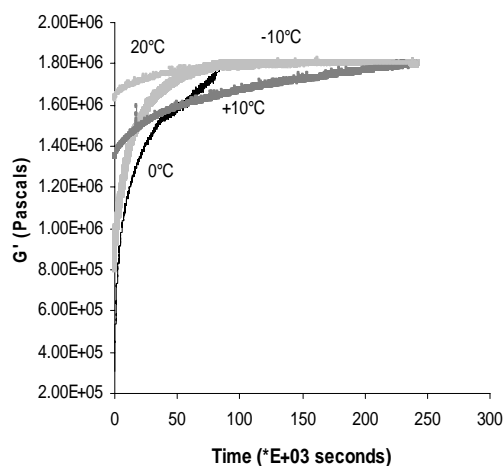
As expected, for an entangled commercial grade polymer there was no build up of modulus with time as shown in Figure 4.19a. The plateau value stays close to 2×10^6 Pa from the beginning to the end of the experiment. On the other hand, the polymers synthesized using samarocene catalyst at -10 and 0°C, showed a build-up of the storage plateau modulus (entanglements) from values around 0.5×10^6 Pa (which represent the disentangled state) to values close to 2×10^6 Pa, (representing the fully entangled state) as shown in Figures 4.19b and 4.20. It is also seen that under constant strain this build up occurs rather slow suggesting that the melt viscosity stays low for few hours before the polymer becomes fully entangled. Notably, when the same polymer films were left in the oven at 160°C for a few minutes without any strain, the polymers entangled within a few minutes. Obviously this behavior has far reaching consequences for processing.

Another interesting phenomenon was observed for the polymer samples synthesized at +10°C and +20°C using the samarocene catalyst. Although showing a low G' value during the frequency sweep experiments, the UHMWPE samples do not show a build up of modulus with time. A similar discrepancy was observed during annealing of these particular samples, which either showed slow or no increase of the melting peak at 135°C (see section 4.2.3).

Nevertheless, they formed clear films on compression (50°C/200 bar) that were highly drawable.



(a)

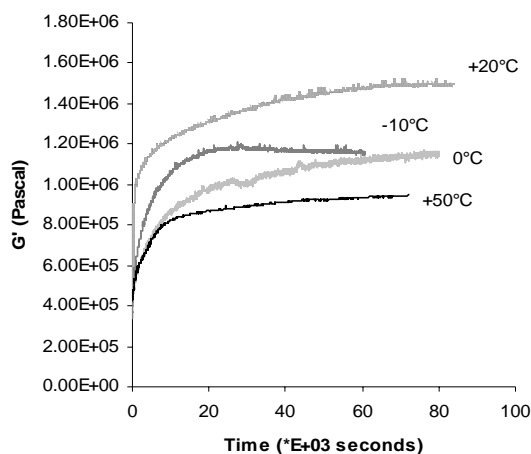


(b)

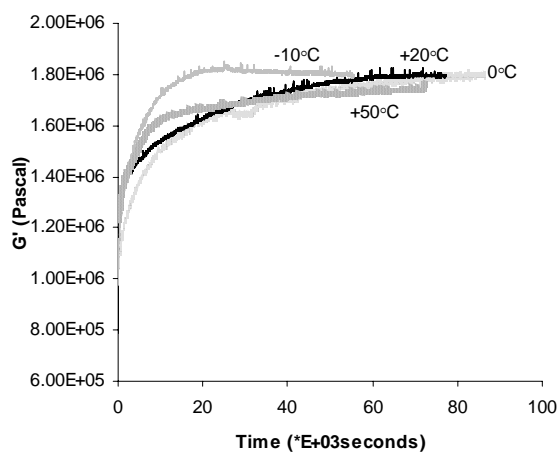
Figure 4.20 Plot representing the build up of modulus with time for UHMWPE synthesized at different temperatures using the $(C_5Me_5)_2Sm \cdot 2(THF)$ (a) not normalized (b) normalized

Interestingly, when the same polymer films were left in the oven at 160°C for a few minutes, the initial draw ratio (> 120) dropped drastically to values corresponding to that of commercial grade polymer. This means that the initial nascent material was highly disentangled, although rheology and annealing experiments gave inconclusive results. At this

stage we can only assume that the possible cause of the difference in the build up of modulus between samples synthesized at or below 0°C versus those formed at or above +10°C is likely resulting from small but significant differences in the number of entanglements in the solid-state obtained during polymer synthesis.



(a)



(b)

Figure 4.21 Plot representing the build up of modulus with time for UHMWPE synthesized at different temperatures using the $[3-t-Bu-2-O-C_6H_3CH=N(C_6F_5)]_2TiCl_2$ catalyst. (a) not normalized (b) normalized

Similarly, polymers synthesized at different temperatures using the bis(phenoxy-imine)titanium catalyst showed a build up of modulus with time indicating that the chains in

the disentangled state can be fully entangled when left in the melt for a significantly long time as shown in Figure 4.21.

Complexity of Rheology Measurements.

As has been demonstrated in the previous section, rheology proved to be a very useful technique to qualitatively estimate the relative entanglement density of a polymer. Unfortunately, there were problems encountered with respect to the accuracy of the measurements and the absolute values of G' could not be established easily. Therefore, the obtained values tend to show a reduced reproducibility. The origin of this problem is to a large extent due to anisotropic shrinkage of the sample during the measurement. The problem was more severe with the polymers obtained with the bis(phenoxy-imine)titanium catalyst system when compared to those obtained with the samarocene. An example of such a shortcoming is depicted in Figures 4.20 and 4.21 where the absolute value of G' for the polymer synthesized using the $(C_5Me_5)_2Sm \cdot 2(THF)$ and $[3-t-Bu-2-O-C_6H_3CH=N(C_6F_5)]_2TiCl_2$ catalyst system showed deviation on repeated measurements. There can be various reasons for the shrinkage in these UHMWPE samples. One reason could be the build up of stresses in the material during the preparation of a polymer film at a high pressure of 200 bar (and $50^\circ C$). When the polymer chains subsequently relax in the melt, the stresses are released resulting in the deformation of the material. In order to minimize the development of stresses, the films were prepared by compression molding at lower pressure. Therefore, a lower pressure of 50 bar was used instead of 200 bar and the temperature was doubled to $100^\circ C$ to retain easy flow of the material. Upon repeating the measurements, the experiments were reproducible to some extent but the problem still persisted.

Since the shrinkage was much more pronounced for polymers synthesized with $[3-t-Bu-2-O-C_6H_3CH=N(C_6F_5)]_2TiCl_2$ compared to $(C_5Me_5)_2Sm \cdot 2(THF)$ it was argued that the difference in catalyst system might play an important role. While samarocene is a single component catalyst that is active without the need of a cocatalyst, to activate the bis(phenoxy-imine)titanium catalyst large amounts of MAO is required. In order to investigate, if the MAO cocatalyst was responsible for the shrinkage in the material, UHMWPE was synthesized using the same bis(phenoxy-imine)titanium catalyst but activated with a different cocatalyst. Instead of 32,000 equivalents of MAO, triisobutylaluminum (TIBA; 100 equivalents) was used as the scavenger and alkylating agent in combination with

triphenylcarbeniumtetrakis (pentafluorophenyl) borate (1 equivalent) as the cation generating species. Upon performing the build up measurements on this polymer batch, shrinkage in the material was indeed absent. The MAO, present in large amount will probably be incorporated in the polymer during crystallization upon synthesis and hence influences the packing of the polymer significantly. Upon work-up of the polymer, the aluminum residues are washed away leaving voids in the material. When these voids are not fully removed during compression molding, they will disappear when the material relaxes in the melt causing shrinkage in the material.

Although with the samarocene system shrinkage was less pronounced, the absolute values are still not completely reproducible. To be able to compare a series of polymers synthesized at different temperatures, the curves were normalized by setting the final value of the modulus at the end of time sweep measurements at 1.8×10^6 Pa. This procedure is valid as it can safely be assumed that after 24 hours in the melt the material will be completely entangled. This was confirmed by drawing the polymer film before and after the time sweep measurement. By using this assumption, polymers can be more easily compared with respect to build up of modulus as shown in Figure 4.20 and 4.21. Obviously the initial values of G' in the normalized plots do no longer correspond to the values obtained from the frequency sweep measurements.

4.3 Conclusions.

Different characterization techniques ranging from common methods such as DSC and fiber drawing to more exotic ones such as TMDSC and rheology prove to be highly beneficial in the qualitative determination of the entanglement density of nascent UHMWPE. With these techniques, it was proven that UHMWPE synthesized using single site catalyst under controlled polymerization conditions can be highly disentangled. Furthermore, it was also shown that the approach of synthesizing nascent disentangled UHMWPE, processing it in the melt and subsequently curing to form fully entangled UHMWPE is indeed successful. Unfortunately, within the timeframe of this project the mechanical properties and the presence/absence of grain boundaries could not be studied.

In the following section we will draw the main conclusions from each of the techniques employed to qualitatively estimate the entanglement density. In addition, remarks are made pertaining to the simplicity of techniques for the estimation of entanglement density.

Mechanical Deformation.

Mechanical deformation experiments are fast, easy and highly illustrative for a qualitative estimation of entanglement density. The draw ratios of all the polymers synthesized using the homogeneous samarocene and bis(phenoxy-imine)titanium catalysts were found to be greater than 120 suggesting that each polymer is highly disentangled. In contrast, a commercial fully entangled UHMWPE could be drawn only to a draw ratio less than 10.

Compression Molding.

Compression molding is yet another rapid and simple technique that can provide a rough estimation of the presence of entanglements in the UHMWPE. Highly disentangled UHMWPE formed clear transparent films at 50°C and 200 bar when compared to the commercial grade entangled polymer which could not be pressed into films under these conditions. In contrast, deformation of UHMWPE produced using conventional production routes is impossible at such low temperature. The fact that the samarocene and bis(phenoxy-imine)titanium based UHMWPE can be formed into clear films below the α -relaxation temperature indicates that the polymer grains can be deformed easily below their melting temperature and made to flow.

DSC and TMDSC.

DSC annealing experiments performed on the UHMWPE synthesized with the homogeneous catalysts show faster increase in the intensity of the melt crystallized peak at 135°C with increasing annealing time when compared to an entangled commercial grade polymer which does not show any of such an effect. TMDSC undoubtedly demonstrates the ease of melting of polymer chains where an entangled polymer shows a much higher time constant (600-1000 minutes) for melting compared to a UHMWPE (100-300 minutes) synthesized using the homogeneous catalyst. The process of melting is believed to occur by first melting of the nascent crystals followed by dissolution into the surrounding viscous liquid, a process which is more complex for an entangled UHMWPE compared to disentangled UHMWPE. Therefore TMDSC again proves that the polymers synthesized with the homogeneous catalysts are highly disentangled. Although, DSC and TMDSC techniques provide a qualitative estimation of the number of entanglements but they are highly sensitive to small temperature variations and time consuming in contrast to the drawing and compression molding tests.

Rheology.

Rheology has been successfully and effectively applied to estimate the entanglement density in UHMWPE. UHMWPE synthesized using the homogeneous catalysts show low values of the storage plateau modulus ($G' = 0.6 \times 10^6$ Pa) when compared to the commercial grade entangled UHMWPE ($G' = 2 \times 10^6$ Pa) suggesting highly disentangled morphology. Moreover a disentangled polymer shows a build up of modulus with time when left in the melt at 160°C up to the value of 2×10^6 Pa for completely entangled UHMWPE. However, the drawback of this technique is that the initial value of G' is difficult to reproducibly establish. Differentiation between entangled and non-entangled UHMWPE and qualitatively estimation of the entanglement density is possible by extrapolation and normalization of the G' end-value (2×10^6 Pa). Despite these challenges, the exciting results bestow confidence that rheology can indeed be employed to qualitatively establish the entanglement density in UHMWPE.

4.4 References.

- (1) Berry, G. C.; Fox, T. G. *Adv. Polym. Sci.* **1968**, *5*, 261.
- (2) Cahn, R. W.; Hassen, P.; Kramer, E. J. *Materials Science and Technology: Processing of Polymers*; VCH: Weinheim, **1997**, 18.
- (3) Jenkins, H.; Keller, A. *Macromol. Sci. Phys. B* **1975**, *11*, 301.
- (4) Rastogi, S.; Kurelec, L.; Lemstra, P. J. *Macromolecules* **1998**, *31*, 5022-5031.
- (5) Smith, P.; Lemstra, P. J. *J. Mater. Sci.* **1980**, *15*, 505.
- (6) Christopher, W. M. *Rheology: Principles, Measurements and Applications*; VCH Publishers, Inc.: USA, 1994, p 1.
- (7) Young, R. J.; Lovell, P. A. *Introduction to Polymers*; Stanley Thornes (Publishers) Ltd: United Kingdom, 2000, p 358.
- (8) Lemstra, P. J.; Aerle, v. N. A. M. J.; Bastiaansen, C. W. M. *Polymer Journal* **1987**, *19*, 85.
- (9) Salem, D. R. *Structure Formation in Polymeric Fibers*; Hanser Publishers: **2000**, Chapter 5, p 209.
- (10) Peterlin, A. *Polym. Eng. Sci.* **1978**, *18*, 488.
- (11) Smith, P.; Chanzi, H. D.; Rotzinger, B. P. *Polym. Commun.* **1985**, *26*, 258.
- (12) Barham, P. J.; Sadler, D. M. *Polymer* **1991**, *32*, 393.

- (13) Physical and mechanical testing were exclusively carried out on UHMWPE samples containing the antioxidant (2, 6-di-tertbutyl-4-methyl-phenol).
- (14) Capaccio, G.; Ward, I. M. *Polymer* **1975**, *16*, 239.
- (15) Capaccio, G.; Crompton, T. A.; Ward, I. M. *J. Polym. Sci.* **1976**, *14*, 1641.
- (16) Hoffman, J. D.; Weeks, I. J. *J. Chem. Phys.* **1965**, 42.
- (17) Wunderlich, B. et al. ATHAS data bank. <http://web.utk.edu/~athas>.
- (18) Yvonne, M. T.; Tervoort, E.; Lemstra, P. J. *Polym. Commun.* **1991**, *32*, 343.
- (19) Kurelec, L. Ph.D Thesis; Eindhoven University of Technology, **2001**.
- (20) Chirinos, J.; Arévalo, J.; Rajmankina, T.; Morillo, A.; Ibarra, D.; Bahsas, A.; Parada, A. *Polym. Bull.* **2004**, *51*, 381.
- (21) (a) Höhne, G. W. H.; Kurelec, L.; Rastogi, S.; Lemstra, P. J. *Thermochim. Acta* **2003**, *396*, 97. (b) Höhne, G. W. H. *Thermochim. Acta* **1997**, *304/305*, 209.
- (22) Höhne, G. W. H.; Hemminger, W.; Flammersheim, H. J. *Differential Scanning Calorimetry*; Springer: Berlin, 2003.
- (23) Ferry, J. D. *Viscoelastic Properties of Polymers*; 3rd Ed; John Willey & Sons: 1980.
- (24) The outcome of the rheology measurement was significantly affected by the change in the shape of the sample. Based of multiple duplicate experiments the error in the measurements was estimated to be $\pm 0.1-0.2 \times 10^6$ Pa.
- (25) Rastogi, S.; Kurelec, L.; Cuijpers, J.; Lippits, D.; Wimmer, M.; Lemstra, P. J. *Macromol. Mater. Eng.* **2003**, *288*, 964.

Chapter 5

Structure determination of nascent morphology: a SAXS/WAXS study.

Synopsis: In the past, various attempts have been made to understand the high melting temperature of nascent UHMWPE. SAXS and WAXS studies combined with DSC techniques have often been used to investigate the nascent morphology and to correlate it with the melting temperature of 141°C observed during the first heating of the nascent sample. The absence of a SAXS pattern in the nascent samples at room temperature has been attributed to a wide dispersion in the lamellae thickness or to the formation of extended chain crystal during synthesis or to irregular stacking of the crystals. By performing a series of SAXS and WAXS studies, an attempt has been made in this chapter to establish a correlation between the polymerization conditions and the lamellae morphology obtained during the synthesis. Our observations are that a relatively sharp dispersion in the lamellae thickness exists for the samples that were synthesized at low temperatures, which gives rise to a well-defined SAXS pattern at room temperature. WAXD studies conclusively show the existence of a monoclinic reflection in the samples synthesized at or below 10°C. This reflection is absent in PE synthesized, using the same catalyst at temperatures higher than 20°C.

5.1 Introduction.

In previous chapters it has been shown that the morphology of the nascent powders can be strongly influenced by the polymerization conditions, which results into variation in melting behavior and thus the rheological aspects of the polymer melt. This chapter presents the X-ray diffraction study on the UHMWPE synthesized under various conditions. Wide angle X-ray scattering (WAXS) is used to investigate the crystal structure of UHMWPE synthesized using the homogeneous catalysts as reported in Chapters 2 and 3, while small angle X-ray scattering (SAXS) is used to explore the resultant morphology of the different grades.

Here we recall that the nascent UHMWPE is synthesized in such a way that the growing polymer chains crystallize directly upon synthesis. Therefore, the polymerizations are carried out at low temperature and high dilutions so that the crystallization rate is faster than the polymerization rate. As discussed in Chapter 4, the nascent UHMWPE (both entangled and disentangled) exhibit a melting peak at 141°C during first heating. However, the melting temperature decreases during second heating run. Chanzy *et al.*¹ attributed the high melting point of nascent UHMWPE to the formation of chain-extended crystals during polymerization. In view of the absence of any small angle X-ray diffraction pattern, Engelen *et al.*² concluded that the nascent crystals contain small, irregularly stacked crystals which reorganize upon heating resulting in the thickening of lamellae leading to the high melting peak. Recently, Kurelec *et al.*³ showed that in nascent UHMWPE's lamellar thickening does not occur to the extent that extended chain crystals are formed even when the crystals are subjected to the highly mobile hexagonal phase. It was also shown that lamellar thickening is strongly dependent on the initial entanglement density. These experimental findings contradict the explanation for the high melting temperature given by Engelen *et al.*² In Chapter 4 we showed that independent of the polymerization conditions the nascent UHMWPE normally exhibits high melting temperature. A possible explanation of this behavior is that a chain residing within the same crystal is sufficiently long to feel its length. In the past, X-ray studies have been performed to follow lamellar thickening in a range of nascent powders. It has been shown conclusively that thickening behavior strongly depends upon the synthesis conditions governing the entanglements.³⁻⁴ This existing know-how has been used to explore differences in the thickening behavior of thus synthesized well-characterized grades.

Another interesting feature of nascent powders is that the initial morphology depends strongly on the synthesis condition. Various morphologies have been reported in the literature depending on the catalyst and synthesis conditions applied.⁵ The use of single site catalysts at low temperatures usually results in highly disentangled UHMWPE's that are able to flow during compression below their melting points. This prompted us to investigate the morphologies of the nascent UHMWPE synthesized under varying conditions using different catalysts and cocatalysts.

5.2 Experimental.

X-ray Diffraction

Small and wide angle X-ray experiments were performed on nascent UHMWPE powders. Experiments were performed on beamlines ID02 and ID11 at the ESRF, Grenoble. Energy used for the experiments was 12keV, wavelength (1Å). For wide angle X-ray diffraction studies, a sample to detector distance of 40cm was maintained, whereas a 10 meter distance was used for small angle X-ray diffraction studies. For better resolution of WAXD patterns beamline ID11 at the ESRF was used. Unless specified an exposure time of 10 seconds was applied for data collection. Using the FIT2D program developed within the ESRF, 2D X-ray patterns were transformed into one dimensional patterns by performing integration along the azimuthal angle. Heating and cooling scans at atmospheric pressure were performed by placing a compressed sample on a silver block of a Linkam THMS600 hot-stage. All samples were compression molded at 50°C.

5.3 Results and Discussions.

Small Angle Diffraction

5.3.1 Time resolved SAXS during heating and cooling at atmospheric pressure on commercial grade UHMWPE (GHR1080).

Figure 5.1 shows a typical SAXS pattern of the commercial grade UHMWPE synthesized using a commercial heterogeneous catalyst at 80°C. As mentioned in Chapter 4, the chains within the polymer are completely entangled. It is clearly seen that at room temperature (27°C), the commercial entangled UHMWPE sample hardly shows any SAXS pattern (halo).

Upon heating at a rate of $10^{\circ}\text{C}\cdot\text{min}^{-1}$ to 170°C , the SAXS pattern develops till the sample melts completely. The complete absence of the halo at room temperature suggests that regular lamellar organization defining an average lamellar thickness does not exist in the nascent powder. The SAXS pattern disappears above 143°C due to complete melting of the polymer (not shown here). This observation is in complete agreement with earlier reported data on a similar class of commercial polymers in the literature.^{2,6} In other words, these nascent powders are characterized by irregular stacking of the crystalline lamellae.

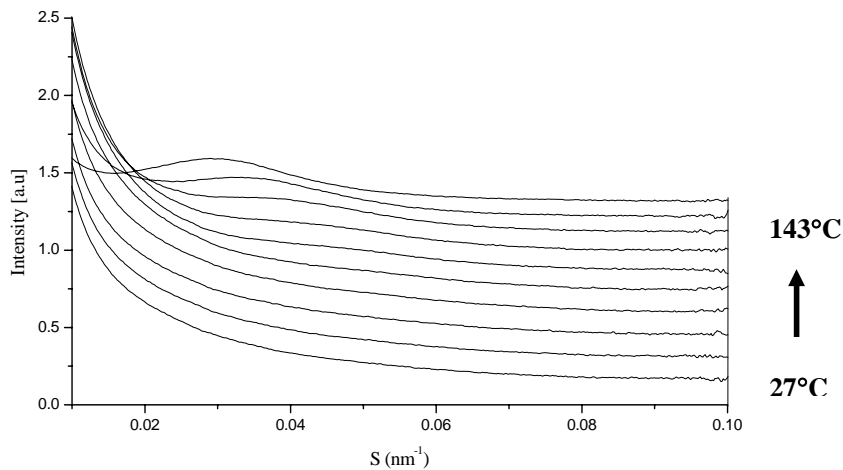


Figure 5.1 Lorentz corrected SAXS pattern of nascent commercial UHMWPE (GHR1080) recorded during heating at $10^{\circ}\text{C}\cdot\text{min}^{-1}$.

Ottani *et al.*⁶ have reported that even on annealing the nascent powder at 80°C for long duration (> 12 hrs), no regular lamellar stacking is observed. Following the heating run as described above, the sample was subsequently cooled to room temperature at the rate of $10^{\circ}\text{C}\cdot\text{min}^{-1}$ as shown in Figure 5.2a. It is clearly seen that at 148°C , the SAXS pattern is not observed due to the molten state of the polymer.

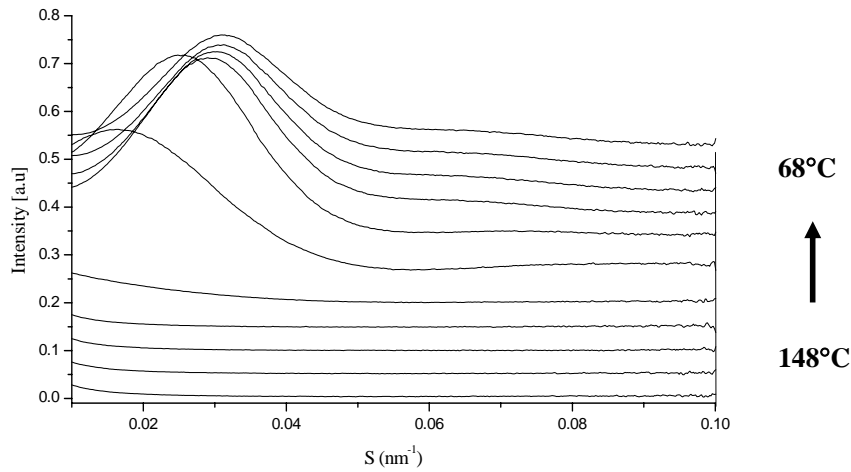


Figure 5.2a Lorentz corrected SAXS pattern of nascent commercial UHMWPE (GHR1080) recorded during cooling at $10\text{ }^{\circ}\text{C}\cdot\text{min}^{-1}$.

On cooling the sample, the halo starts to appear at 123°C indicating the development of ordering in the lamellar thickness. The increase in the intensity of the SAXS pattern strongly supports relatively regular stacking of the crystalline and non-crystalline layers compared to the starting material. Figure 5.2b clearly shows the difference between the SAXS pattern of a nascent material with the melt crystallized sample at room temperature. Therefore the SAXS intensity is retained even when the sample is cooled to room temperature.

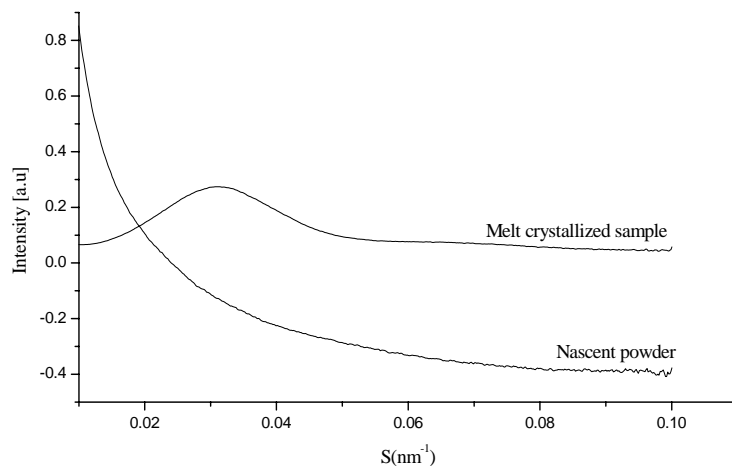


Figure 5.2b Comparison of the SAXS pattern of nascent (GHR1080) and the melt-crystallized commercial UHMWPE recorded at room temperature.

In contrast to the commercial grade, the polymers synthesized with the homogeneous catalysts show the presence of a well-defined SAXS signal at room temperature. The observed SAXS pattern strongly depends on the synthesis conditions. Table 5.1 shows four different grades of UHMWPE which were synthesized using two different homogeneous catalysts under different polymerization conditions. SAXS and WAXD studies were performed on these samples.

Table 5.1 Different grades of UHMWPE synthesized with homogeneous catalysts.

Entry	Grade	Catalyst	Cocatalyst	Polymerization temperature (°C)
1	BW*	$(C_5Me_5)_2Sm \cdot 2(THF)$	-	25
2	Samarocene	$(C_5Me_5)_2Sm \cdot 2(THF)$	-	0
3	Samarocene	$(C_5Me_5)_2Sm \cdot 2(THF)$	-	10
4	Bis(phenoxy imine) titanium	$[3-t-Bu-2-O-C_6H_3CH=N(C_6F_5)]_2TiCl_2$	MAO	10

*Obtained from DSM Chemical Research, The Netherlands; ethylene (1 bar).

5.3.2 Time resolved SAXS during heating and cooling at atmospheric pressure on BW grade UHMWPE.

Figure 5.3 shows the presence of a SAXS pattern at room temperature for the highly disentangled BW grade UHMWPE, indicating the presence of relatively well-defined lamellae thickness in the nascent material.

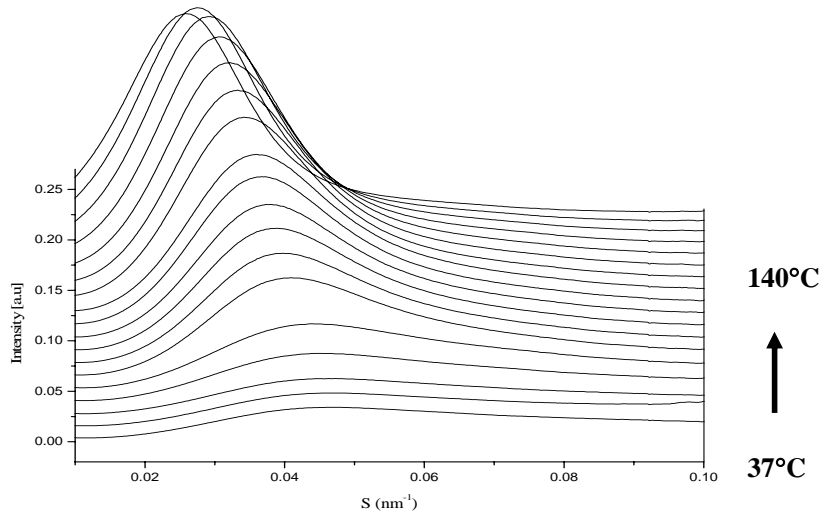


Figure 5.3 Lorentz corrected SAXS pattern of BW grade nascent UHMWPE (synthesized at +25 °C) recorded during heating at 10 °C·min⁻¹.

This observation is in contrast with the commercial grade UHMWPE as discussed above. On heating the nascent UHMWPE, the intensity of the SAXS pattern increases gradually to 140°C. With increase in the intensity the broad peak also sharpens suggesting a decrease in the dispersion of the lamellar thickness, which would be only possible when the chains are able to reorganize. The anticipated reorganization process during heating of the BW sample is in agreement with the experimental data collected by TMDSC in Chapter 4. Above 138°C, the intensity starts to decrease until the sample melts. Partial melting of the lamellae causes enhancement in the electron density fluctuation, which results into an increase in the SAXS intensity. Shift in the peak position can be a result of a partial melting process and lamellar thickening. The experimental data is, however, not conclusive to resolve the two factors in the peak shift.

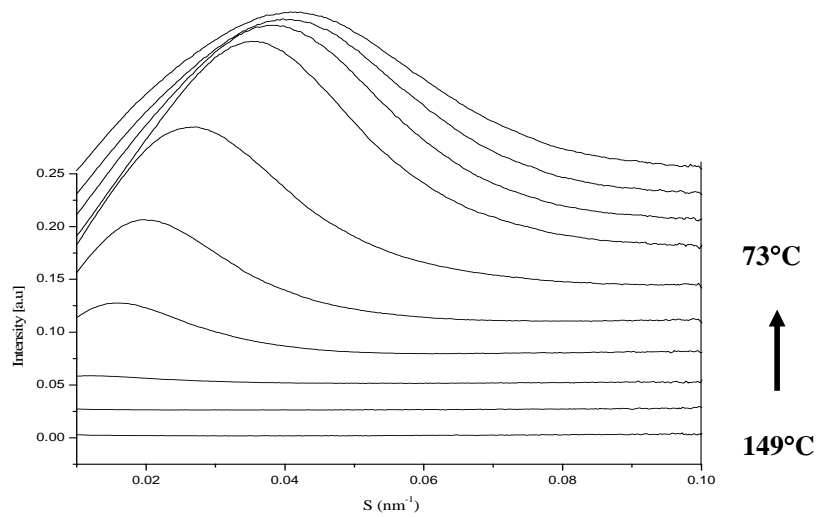


Figure 5.4a Lorentz corrected SAXS pattern of BW grade nascent UHMWPE (synthesized at +25 °C) recorded during cooling at 10 °C·min⁻¹.

On subsequent cooling to room temperature at the same rate, the halo starts to appear again at approximately 123 °C as shown in figure 5.4a. The SAXS pattern at room temperature of the thus melt crystallized BW sample is similar to that obtained by melt crystallization of the commercial grade UHMWPE.

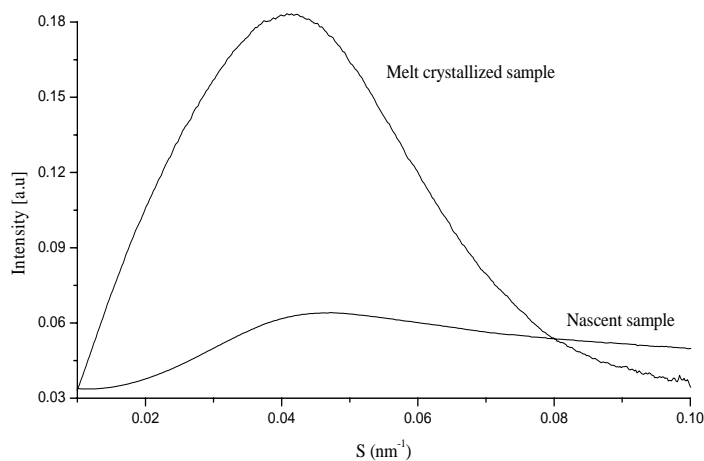


Figure 5.4b Comparison of the SAXS pattern of nascent and melt crystallized BW grade UHMWPE (synthesized at +25 °C) recorded at room temperature.

A comparison between the nascent and melt crystallized sample at room temperature is shown in figure 5.4b, where the presence of well-defined lamellar organization is confirmed even in the nascent material.

To compare between different grades of UHMWPE synthesized with homogeneous catalysts, the BW grade will be used as a model system for further discussions. This grade has been used for future discussions because this is the sample that has been well-studied in our laboratory, thus facilitating characterization of the morphology.

5.3.3 Time resolved SAXS during heating and cooling at atmospheric pressure on bis(phenoxy-imine)titanium grade UHMWPE.

Figure 5.5 shows a series of SAXS patterns for the highly disentangled bis(phenoxy-imine)titanium grade UHMWPE. SAXS patterns were recorded *in situ* during heating from room temperature to 170°C. Similar to the commercial grade UHMWPE, at room temperature a diffraction pattern is absent. An unusual feature in this sample is that the SAXS pattern develops when the sample is heated but fails to show any pattern on cooling from the melt.

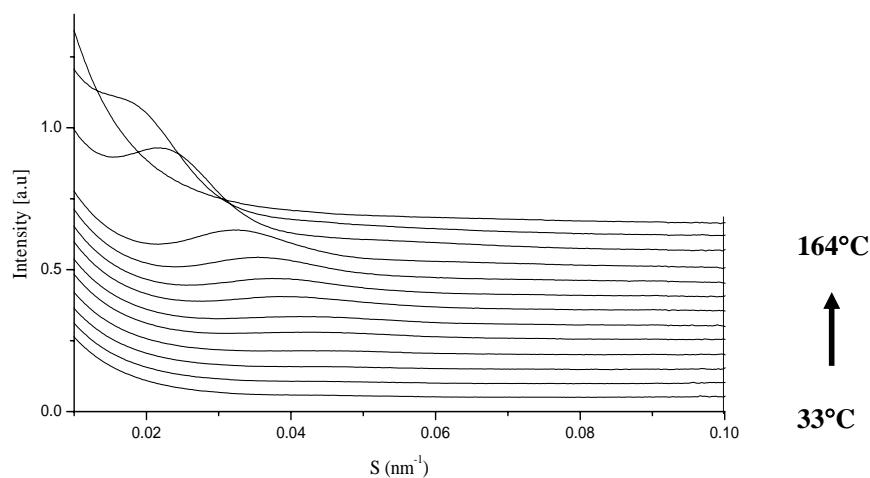


Figure 5.5 Lorentz corrected SAXS pattern of bis(phenoxy-imine)titanium grade nascent UHMWPE (synthesized at +10 °C) recorded during heating at 10 °C·min⁻¹.

Figures 5.6a and 5.6b show that even upon cooling from the melt the halo does not develop at all. Thus the sample behaves completely different from the others discussed so far. It has been recognized that bis(phenoxy-imine)titanium grade UHMWPE showed considerable shrinkage in rheological measurement (Chapter 4).

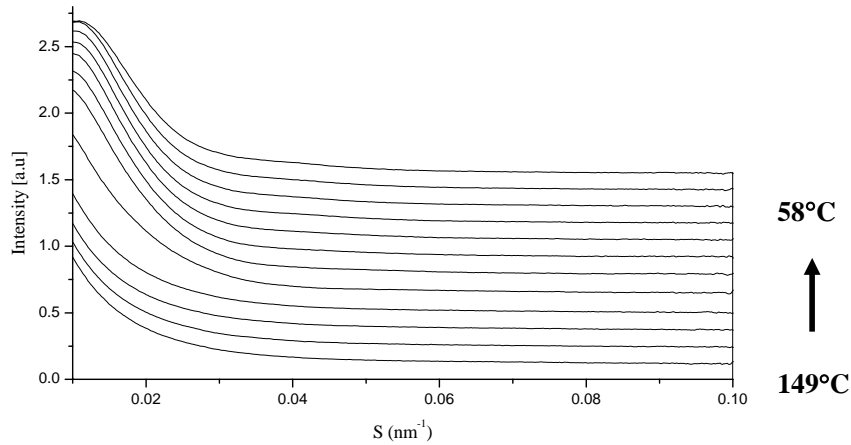


Figure 5.6a Lorentz corrected SAXS pattern of bis(phenoxy-imine)titanium grade nascent UHMWPE (synthesized at $+10\text{ }^{\circ}\text{C}$) recorded during cooling at $10\text{ }^{\circ}\text{C}\cdot\text{min}^{-1}$.

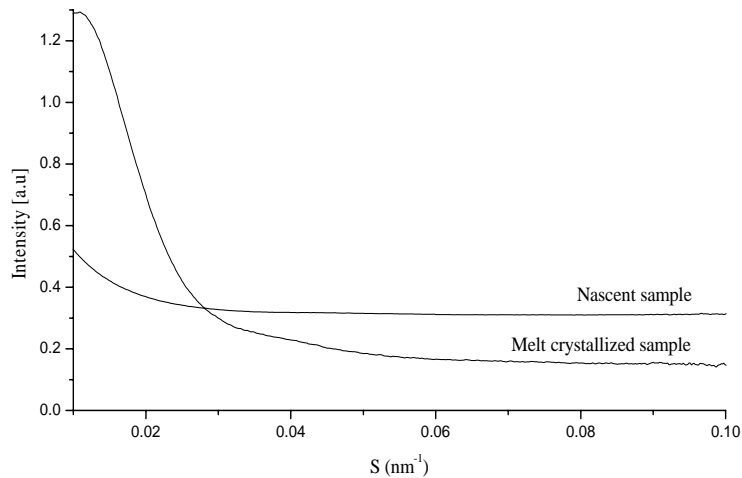


Figure 5.6b Comparison of the SAXS pattern of nascent and melt crystallized bis(phenoxy-imine)titanium grade UHMWPE (synthesized at $+10\text{ }^{\circ}\text{C}$) recorded at room temperature.

Therefore, during the synthesis a completely different kind of morphology has been created proving that the type of morphology is indeed affected by the polymerization conditions and the type of the catalyst.

5.3.4 Time resolved SAXS during heating and cooling at atmospheric pressure on samarocene grade UHMWPE.

Figure 5.7 depicts the SAXS diffraction pattern of a samarocene grade (highly disentangled), polymer synthesized under similar conditions as the BW grade but at lower temperature of 0°C. The BW grade was synthesized in a large reactor (10 L) under fully optimized condition compared to the samarocene grade (1 L). It is clearly seen that there is some order of the lamellae at room temperature (halo) which intensifies on heating the sample up to its melting temperature. The halo disappears once the polymer is completely molten above 160°C. Upon cooling the sample from the melt, a well-defined halo similar as was observed for the BW sample is seen.

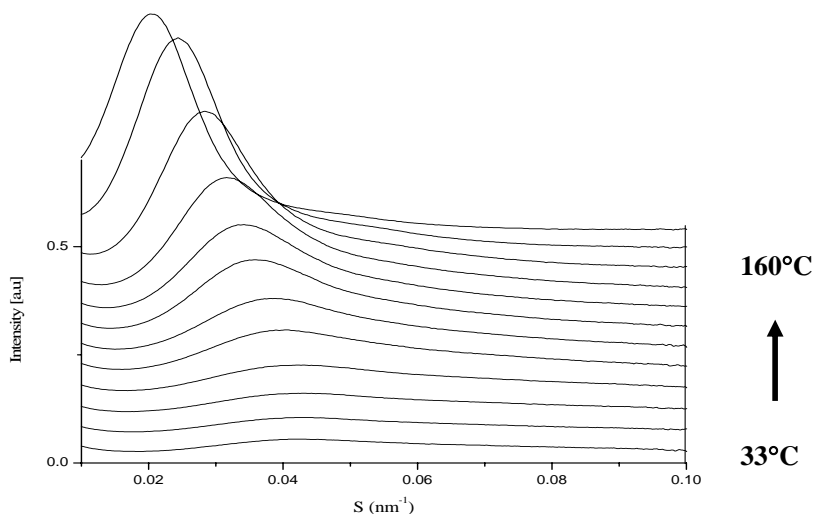


Figure 5.7 Lorentz corrected SAXS pattern of samarocene grade nascent UHMWPE (synthesized at 0°C) recorded during heating at 10 °C·min⁻¹.

UHMWPE synthesized at +10°C, also shows similar behavior as shown in Figures 5.7a and 5.7b.

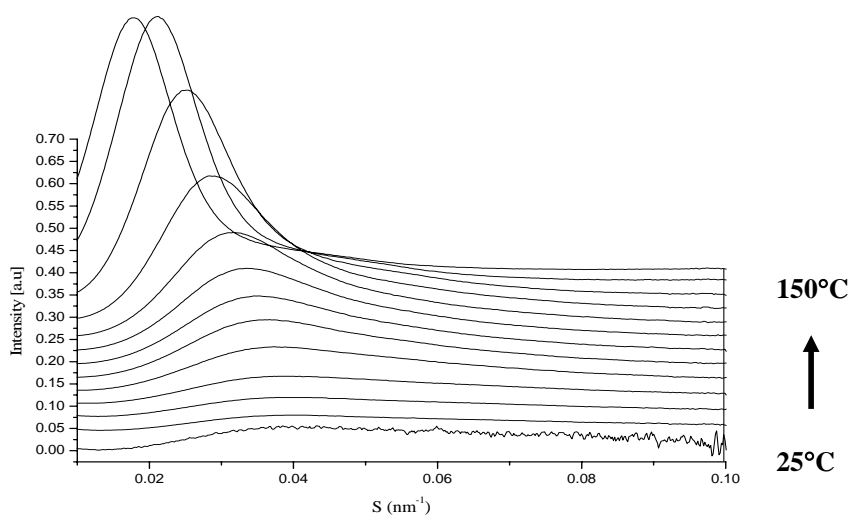


Figure 5.7a Lorentz corrected SAXS pattern of samarocene grade nascent UHMWPE (synthesized at $+10^\circ\text{C}$) recorded during heating at $10^\circ\text{C}\cdot\text{min}^{-1}$.

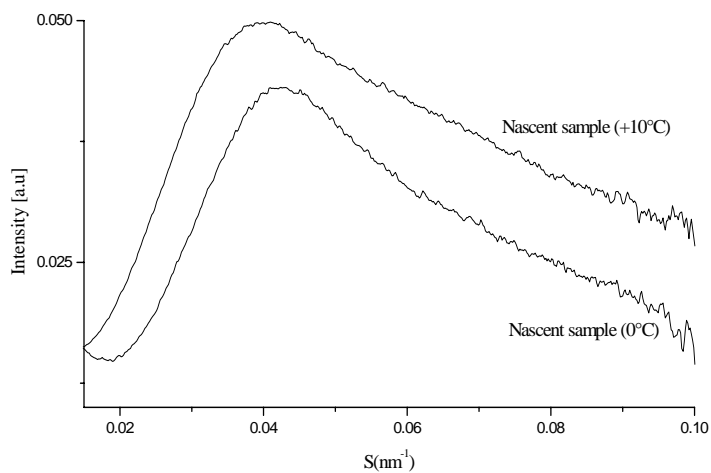


Figure 5.7b Comparison of the SAXS pattern recorded at room temperature of nascent UHMWPE synthesized with the samarocene catalyst at 0 and $+10^\circ\text{C}$ respectively.

Wide Angle X-ray Diffraction.

Wide angle X-ray scattering experiments were performed to investigate the crystal phase structure in the UMMWPE synthesized using single site catalyst at different polymerization conditions as described in Chapters 2 and 3. It is well-known that during crystallization upon polymer synthesis, especially at a large degree of supercooling, various kinds of imperfections are bound to occur. These defects could be present on the fold surface of the crystals (amorphous layer) or could exist within the crystalline lattice. The fold surface imperfections are formed when the polymerization temperature is low and crystallization rate is fast. On the other hand, the distortions in the lattice take place due to the mechanical deformation during polymer synthesis and preparation or due to the dynamics of chain folding during crystallization.⁶ It was shown in Chapter 4 that the defects or imperfections are removed during annealing the UHMWPE, where considerable reorganization of the polymer chain takes place resulting in removal of distortions and thickening of the lamellae. The crystal phase distortions are characterized by the presence of the monoclinic phase in addition to the thermodynamically stable orthorhombic phase, which might increase as the temperature is lowered. Removal of such imperfections are usually accompanied by reduction in the volume or shrinkage as the volume of the monoclinic unit cell is larger than the orthorhombic unit cell in addition to the perfecting of the fold surface in between two different crystalline phases. Chanzy *et al.*⁷ attributed the occurrence of the monoclinic phase to interference between growing crystallites.

Figure 5.8 shows the WAXD pattern of the polymers synthesized with the single site samarocene catalyst at different polymerization temperatures. It is clearly seen that the monoclinic reflection (100) exists in the nascent material, in addition to the usual orthorhombic reflections (110) and (200) at low temperature indicating shear in the crystalline lattice. The monoclinic reflection is very strong in the samples synthesized at low polymerization temperatures ranging from -10°C to +10°C. The reflection is absent in the polymer synthesized at +20°C. It is reported in the literature⁸ that a commercial grade nascent UHMWPE synthesized at +90°C does not exhibit any monoclinic reflection at room temperature.

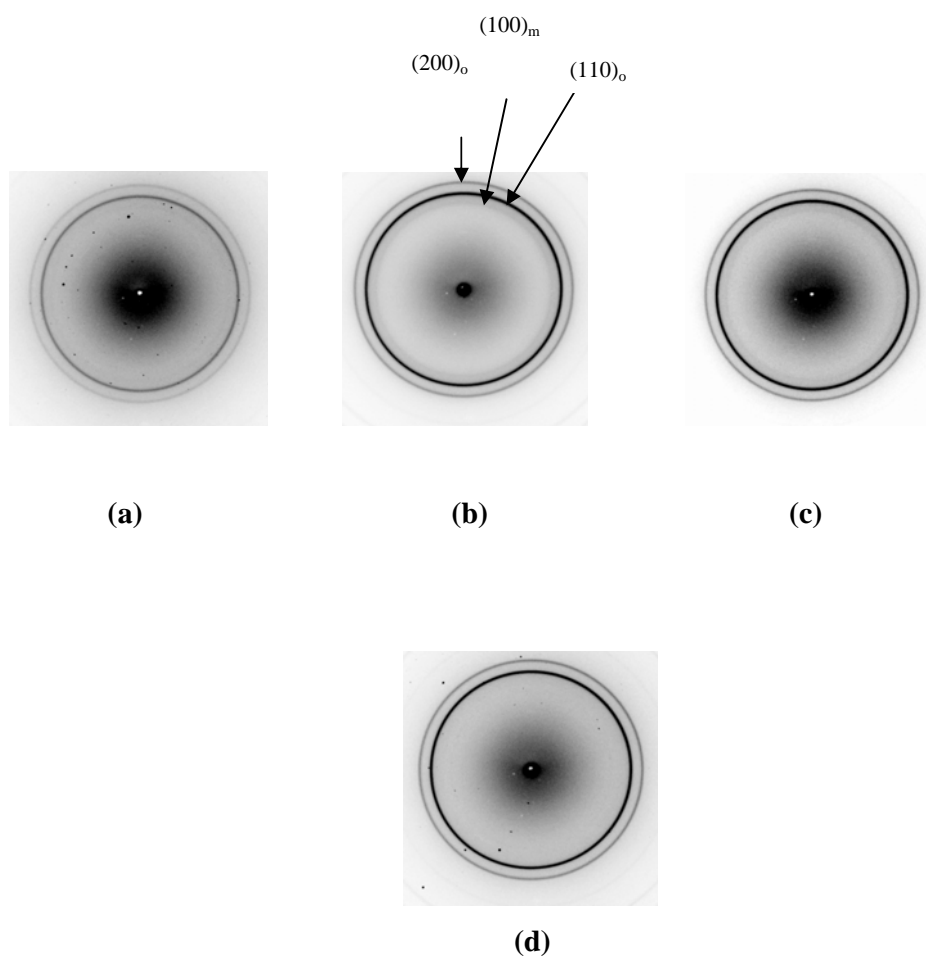


Figure 5.8 Wide angle X-ray patterns recorded at room temperature of nascent UHMWPE synthesized using the samarocene catalyst at different temperatures. (a) -10°C (b) 0°C (c) $+10^{\circ}\text{C}$ (d) $+20^{\circ}\text{C}$.

Figure 5.9 shows the X-ray pattern of the nascent UHMWPE synthesized using the bis(phenoxy-imine)titanium catalyst at different polymerization temperatures. Once again we observe a monoclinic reflection at low polymerization temperatures (0°C to $+10^{\circ}\text{C}$) and its non-existence for the polymer synthesized at $+50^{\circ}\text{C}$.

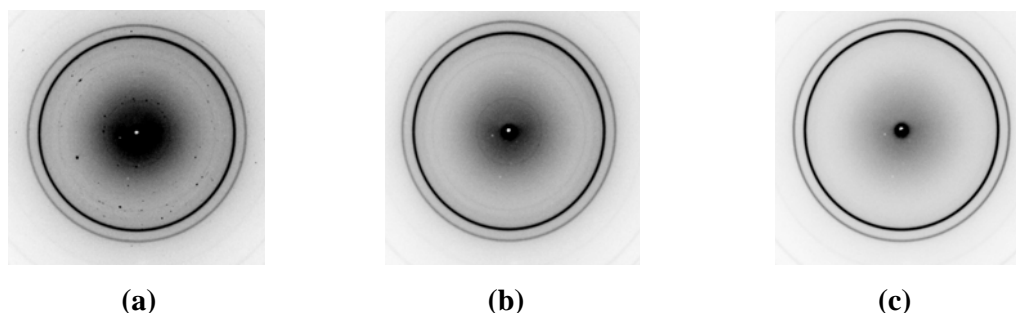


Figure 5.9 Wide angle X-ray patterns recorded at room temperature of nascent UHMWPE synthesized using the bis(phenoxy-imine)titanium catalyst at different temperatures. (a) 0°C (b) $+10^{\circ}\text{C}$ (c) $+58^{\circ}\text{C}$.

BW grade UHMWPE synthesized at $+25^{\circ}\text{C}$ also shows the presence of monoclinic phase as shown in Figure 5.10. Hence, it can be concluded that the formation of the monoclinic phase is strongly dependent on the polymerization conditions.

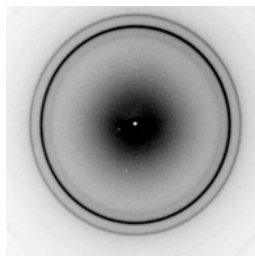


Figure 5.10 Wide angle X-ray patterns recorded at room temperature of BW grade nascent UHMWPE synthesized at $+25^{\circ}\text{C}$.

5.4. Conclusions.

In-situ SAXS studies performed on different grades of UHMWPE proved that the initial morphology of the nascent UHMWPE is considerably influenced by the synthesis conditions. It was shown in this chapter that changing the catalyst and cocatalyst results in different lamellar arrangements of the crystals, which changes during heating. WAXS experiments were conducted to probe the crystal phase structure of the UHMWPE synthesized at different temperatures using the samarocene and the bis(phenoxy-imine)titanium catalyst. WAXS patterns show the existence of the monoclinic phase in addition to the orthorhombic phase at

low temperature. However, the monoclinic reflection is absent in the nascent material synthesized using the same catalyst but at higher temperatures.

5.5 References.

- (1) Smith, P.; Chanzy, H. D.; Rotzinger, B. P. *J. Mater. Sci.* **1987**, *22*, 523.
- (2) Yvonne, M. T.; Tervoort, E.; Lemstra, P. J. *Polym. Commun.* **1991**, *32*, 343.
- (3) Kurelec, L. C., Ph. D. Thesis, Eindhoven University of Technology, 2001.
- (4) Rastogi, S.; Kurelec, L.; Cuijpers, J.; Lippits, D.; Wimmer, M.; Lemstra, P. J. *Macromol. Mater. Eng.* **2003**, *288*, 964.
- (5) Chanzy, H. D.; Revol, J. F.; Marchessault, R. H.; Lamandé, A. *Kolloid-Z. u. Z. Polymere* **1973**, *251*, 563.
- (6) Ottani, S.; Ferracini, E.; Ferrero, A.; Malta, V.; Porter, R. S. *Macromolecules* **1995**, *28*, 2411.
- (7) Smith, P.; Chanzy, H. D.; Rotzinger, B. P. *J. Mater. Sci.* **1987**, *22*, 523.
- (8) Joo, Y. L.; Han, O. H.; Lee, H. K.; Song, J. K. *Polymer* **2000**, *41*, 1355.

Technology Assessment

UHMWPE is usually intractable via conventional processing routes due to very high melt viscosity and today all products of UHMWPE possess fusion defects or grain boundaries. Among numerous application of this polymer, the use of UHMWPE for biomedical application mainly, hip joints has been the major focus in this work. One of the major problems with such application has been the adhesive wear of the polymer which causes osteolysis and loosening of the implant. Though, the incomplete fusion of the powder particles has been often regarded as one of the possible cause for insufficient lifetime of the hip joint, Kurelec¹ showed that complete fusion of the particles does not lead to substantial improvement in the adhesive wear of the material.

The remarkable effect of narrow molecular weight distribution towards reduced adhesive wear has been reported.² However, extraction of monodisperse fractions of UHMWPE from commercial grades is highly impractical. It has been clearly shown in this thesis that homogeneous catalysts can be used to directly synthesize disentangled nascent UHMWPE with very narrow molecular weight distribution by carefully controlling the polymerization conditions, which displays a significantly improved processability compared to commercial grade fully entangled UHMWPE. Although narrow molecular weight distribution for such a high molecular weight polymer is expected to hinder the processability, creating a less entangled state during polymer synthesis has been proved to significantly enhance the processability of the material. Thus processed material will, after curing, show improved mechanical performance.

It has been discussed in Chapter 4 that the solid state drawability of as synthesized disentangled polymers is very high. High performance UHMWPE fibers (Dyneema®) are commercially produced via disentangling the polymer chains by dissolving the UHMWPE in decalin followed by ultra-drawing (gel spinning). In contrast, the direct synthesis of highly disentangled UHMWPE by solution polymerization offers considerable advantages for polymer processing as it circumvents the drawbacks associated with gel spinning, where a relatively large quantity of solvent needs to be processed and high temperature and relatively long time is required to dissolve the polymer. However, this new polymer production route has economical disadvantages over the existing production technology and may therefore only be of interest for high demanding products with high end applications such as the components for artificial hip implant.

Solution polymerization using homogeneous catalysts is also useful to synthesize UHMWPE-CaCO₃ blends. Usually, the incorporation of inorganic fillers such as CaCO₃ in a polyolefin matrix is known to cause an increase in the impact strength, making them useful for various engineering applications. However, the elongation at break and the tensile strength are found to decrease as a result of the poor adhesion between the filler particles and the polymer matrix.³ In order to overcome this adhesion problem and to achieve high elongation at break, a uniform distribution of the filler particles at higher filler concentrations is needed, which can be obtained when the polymerizations are carried out in the presence of filler particles. Alternatively, a suspension of finely powdered CaCO₃ can be added to highly disentangled UHMWPE nascent powder to ensure homogeneous dispersion of the filler particles. Thus the solution polymerization can be of advantage to synthesize the composites directly in one step.

References.

- (1) Kurelec, L. C., Ph. D. Thesis, Eindhoven University of Technology, 2001.
- (2) Tervoort, T. A; Visjager, J; Smith, P. *Macromolecules* **2002**, 35, 8467.
- (3) Suwanprateeb, J. *J. Appl. Polym. Sci.* **2000**, 75, 1503.

Summary

The main objective of this work was to develop general procedures to synthesize highly disentangled easily processable ultra high molecular weight polyethylene (UHMWPE) with a narrow molecular weight distribution (MWD) for better end-properties. It is well-known that a narrow molecular weight distribution would hinder the processability of high molecular weight polymers. Hence, the challenge was to find a solution to tackle the issues addressed. In order to do so UHMWPE with highly disentangled chains was desired because a lower entanglement density is expected to improve the mobility of the polymer chains under processing conditions. Completely entangled UHMWPE exhibits a high melt viscosity and is intractable via conventional processing routes such as injection molding and blow molding. Due to the intractable nature of this polymer, irrespective of the processing technique employed, the final products obtained invariably show fusion defects or grain boundaries. The defects in the final products result in the poor mechanical performance and reduced lifetime of the polymer products, especially when UHMWPE components are used in highly demanding applications such as medical implants (hip and knee prosthesis).

Therefore, this thesis addresses the fundamental issue of improving the processability of UHMWPE starting from the synthesis of a polymer with a unique morphology to the use of various characterization techniques proving that the morphology created during polymer synthesis can be of considerable advantage to polymer processing.

The first objective was to synthesize UHMWPE with narrow molecular weight distribution. For this, homogeneous catalysts were sought because they yield polymer with uniform activity and produce polymer with a narrow MWD (≤ 2) owing to their single site character. The second requirement was to synthesize a highly disentangled UHMWPE. To synthesize

polymers with this unique morphology, the polymerization conditions such as catalyst concentration (dilution), temperature and pressure were varied. It was assumed that when the temperature of polymerization is kept low, the chains will crystallize upon their formation during the polymerization when the crystallization rate is faster than the polymerization rate ($R_{\text{crys}} > R_{\text{polym}}$). A sufficiently diluted system would enable greater separation of the active sites and thus of the growing polymer chains, leading to a unique morphology in the nascent state where the chains are highly disentangled.

The first catalyst system tested was the single component catalyst $(C_5Me_5)_2Sm \cdot 2(THF)$. The reactions performed by varying the dilution showed that the yield and molecular weight increases with the increase in the dilution due to the larger (absolute) amount of ethylene dissolved in the polymerization medium. The polymerizations performed at different temperatures (-10°C , 0°C , $+10^\circ\text{C}$ and $+20^\circ\text{C}$) show that increasing the polymerization temperature above $+10^\circ\text{C}$ results in a drop in the yield and the molecular weight and is attributed to due to diffusion limitation of ethylene in the solvent and chain termination reactions that become prominent at higher temperatures. It was also shown that mass transfer of ethylene becomes the rate determining step in the polymerization reactions at higher temperature. However, a major drawback of this catalyst is that only in the absence of scavengers it polymerizes ethylene to UHMWPE, which makes its use expensive and unpractical because a considerable amount of catalyst is used to scavenge the impurities. To overcome these shortcomings and to explore if a different homogeneous catalyst can be used to synthesize highly disentangled UHMWPE by controlling the polymerization conditions, Mitsui's bis(phenoxy-imine)titanium catalyst system $[3-t\text{-Bu-2-O-C}_6\text{H}_3\text{CH=N(C}_6\text{F}_5)_2\text{TiCl}_2/\text{MAO}]$ was used. Polymerizations performed at various conditions show that with the increase in dilution, reaction time and temperature the yield and molecular weights are hardly affected, which was attributed to the extremely fast polymerization and subsequent encapsulation of the catalyst in the polymer matrix. Unusually, a very large excess of MAO ($>100,000$ equivalents) was required to reach optimum activity, which was attributed to a relatively large number of active species resting in the dormant state at low MAO concentrations and an increase in reactivity with more MAO (in toluene) present as a result of the increased polarity of the solvent. In order to investigate the influence of polymerization conditions on the entanglement density, different tools were needed to characterize the polymer samples. The disentangled state of the UHMWPE obtained from homogeneous catalysts was proved using various characterization techniques such as drawing

in the solid state, compression moulding, differential scanning calorimetry (DSC), temperature modulated DSC (TMDSC) and rheology and compared with commercial grade UHMWPE. The UHMWPE synthesized by both the catalysts at different polymerization conditions were compression molded to films below their melting temperature (50°C/200 bar). Upon mechanical deformation in the solid state, the films exhibited a draw ratio greater than 120. In contrast, a commercial grade entangled UHMWPE exhibits a draw ratio of less than 10. Moreover, the films produced with the homogeneous catalysts were transparent unlike the films obtained from the commercial grade UHMWPE, confirming the ease of flow of the polymer chains upon shearing even much below the melting temperature in the former case. These observations are indicative for a lower entanglement density in the nascent material produced using homogeneous catalysts.

In order to further strengthen the results obtained from drawing and compression molding studies which prove that the polymers obtained with the homogeneous catalysts are highly disentangled, annealing experiments by DSC were performed on the UHMWPE. The polymers were annealed at a temperature close to the onset of melting of nascent UHMWPE. The samples when annealed for different durations at the said temperature, subsequently cooled and melted at the rate of 10 K·min⁻¹ resulted in the appearance of two peaks: one corresponding to the melting temperature of the nascent polymer (141°C) and the other corresponding to the melting temperature of the melt crystallized polyethylene (135°C). For the polymers synthesized with the homogeneous catalysts, increasing the annealing time results in increase of the melt crystallized peak. The observed increase is due to the continuous melting of nascent crystals during annealing which increases with increasing annealing time. On the other hand, the commercial grade polymer hardly shows any of such behavior strongly indicating that flowability and hence, melting is much slower for the fully entangled commercial grade UHMWPE compared to the the as-synthesized disentangled polymers due to reduced number of entanglements per unit chain of the latter.

TMDSC conclusively shows that the melting process is much faster for the UHMWPE synthesized with the homogeneous catalyst, since the time constant derived for melting are much lower (100-300 minutes) compared to the entangled commercial grade polymer which has a very high time constant (600-1000 minutes). As expected, even the α -relaxation process is much faster for polymers synthesized with the homogeneous catalysts when compared to the commercial grade UHMWPE especially at temperatures below the melting of the nascent polymers. From these experiments, it was concluded that the melting occurs by first melting of the nascent crystals followed by gradual dissolution into the surrounding viscous liquid, a

process which is more complex for an entangled UHMWPE and hence needs more time compared to a disentangled UHMWPE.

Finally, a powerful technique like rheology was used to quantify the number of entanglements per unit chain. Compared to a completely entangled UHMWPE which shows a storage plateau modulus of about 2×10^6 Pa, the polymers obtained with the two homogeneous catalysts exhibited much lower values ($G' = 0.6 \times 10^6$ Pa). Since the value of the plateau modulus is inversely related to the molar mass between entanglements (M_e), it was concluded that the polymers synthesized using homogeneous catalysts as described in Chapter 2 and 3, are highly disentangled. Additionally, a disentangled UHMWPE showed a build up of modulus from the initial low values (0.6×10^6 Pa) up to the value of 2×10^6 Pa for a completely entangled UHMWPE, when left in the melt at 160°C for a few hours. As expected, the commercial grade entangled UHMWPE does not show any build up of modulus. However, it was shown that rheology can only be used as a qualitative tool due to reduced reproducibility of the results. Nevertheless, each of the techniques described above provides a valuable and qualitative estimation of the number of entanglements per unit chain in the nascent polymers and prove the disentangled morphology of the UHMWPE synthesized with the homogeneous catalysts.

Additionally, *in-situ* SAXS experiments were performed to see the influence of polymerization conditions (heterogeneous versus homogeneous catalysts; type of homogeneous catalyst, type of cocatalyst) on the nascent morphology. It was shown that polymers synthesized with the homogeneous samarocene catalyst showed the existence of halo at room temperature in the nascent material, the intensity of which increases when the material is heated indicative of a long range order in the lamellar thickness. At room temperature for the polymers synthesized using the bis(phenoxy-imine)titanium, halo was not observed. The absence of the halo at room temperature in the commercial grade polymer and the UHMWPE synthesized with the bis(phenoxy-imine)titanium catalyst suggests a broad distribution of lamellar thickness, which becomes narrow as the sample is heated to the melt. A sharp difference between the commercial grade and polymer grade synthesized using the bis(phenoxyimine)titanium catalyst was that the halo is retained on cooling for the former whereas it is absent for the latter. WAXS experiments show the existence of a monoclinic phase in addition to the orthorhombic phase for the polymers synthesized at low temperatures up to 0°C . The monoclinic phase is absent for the polymers synthesized at higher temperature.

To conclude, the initial aim of the project as described in this thesis has been achieved successfully. UHMWPE with narrow molecular weight distribution was synthesized using different homogeneous catalysts and was proved by various characterization techniques to be highly disentangled. The resulting polymer exhibits an excellent processable material which after curing yields a fully entangled and completely fused product.

However, for the process to become commercially attractive a cheap, active, non-living catalyst would be required.

Samenvatting

Het belangrijkste doel van dit werk was het ontwikkelen van algemene procedures voor de synthese van uit sterk onverstrengelde ketens bestaand, eenvoudig verwerkbaar, ultrahog molgewicht polyetheen (UHMWPE) met een smalle molgewichtsverdeling voor betere producteigenschappen. Het is bekend dat de verwerkbaarheid van hoog molgewicht polyetheen afneemt met een smallere molgewichtsverdeling. Het was daarom een uitdaging om een oplossing voor dit dilemma te vinden. Hiervoor was UHMWPE met sterk onverstrengelde ketens gewenst omdat een verminderde ketenverstrengeling de mobiliteit van de ketens tijdens de verwerking zou verbeteren. UHMWPE met volledig verstrengelde ketens heeft een hoge smeltviscositeit en is niet verwerkbaar via conventionele verwerkingstechnieken zoals spuitgieten en folieblazen. Door deze stugheid vertonen de eindproducten van deze polymeren, onafhankelijk van de toegepaste verwerkingstechniek, versmeltingsdefecten of korrelgrenzen (grain boundaries). Deze defecten in de eindproducten resulteren in slechte mechanische eigenschappen en een gereduceerde levensduur van deze producten, vooral wanneer UHMWPE-componenten zijn toegepast in zeer veeleisende toepassingsgebieden zoals die van medische implantaten (heup en knie prothesen).

Om die reden wordt in dit proefschrift de fundamentele uitdaging om de verwerkbaarheid van UHMWPE te verbeteren beschreven, beginnend met de synthese van polymeren met een unieke morfologie tot het gebruik van verschillende karakteriseringstechnieken waarmee werd bewezen dat de morfologie die werd verkregen gedurende de polymeersynthese grote voordelen heeft voor de polymeer verwerkbaarheid.

De eerste doelstelling was om UHMWPE met een smalle molgewichtsverdeling te synthetiseren. Hiertoe werden homogene katalysatoren geselecteerd omdat deze door hun

single-site karakter polymeren met een smalle molgewichtverdeling (≤ 2) kunnen geven. De tweede doelstelling was om een UHMWPE met sterk onverstregelde ketens te maken. Om polymeren met deze unieke morfologie te bereiden werden de polymerisatie condities zoals katalysator concentratie (verdunding), temperatuur en druk gevarieerd. De aanname hierbij was dat wanneer de polymerisatie temperatuur laag werd gehouden, de ketens direkt na hun vorming zullen kristalliseren als de kristallisatiesnelheid groter is dan de polymerisatie snelheid ($R_{\text{crys}} > R_{\text{polym}}$). Een voldoende verdund systeem leidt tot een relatief grotere afstand tussen de katalysator sites en dus tussen de groeiende polymeerketens wat tot een unieke morfologie van de nascent toestand leidt waarbij de ketens sterk onverstregeld zijn.

Het eerste katalysatorsysteem dat werd getest was de single-component katalysator $(\text{C}_5\text{Me}_5)_2\text{Sm}\cdot 2(\text{THF})$. De reacties die bij verschillende verdunningen werden uitgevoerd lieten zien dat de productiviteit en het molgewicht toenamen met een toename in verdunning door de grotere (absolute) hoeveelheid opgelost etheen in het polymerisatie medium. Het verhogen van de polymerisatietemperatuur boven de $+10^\circ\text{C}$ leidt tot een productiviteits- en molgewichtsverlaging wat wordt toegeschreven aan diffusielimitatie van etheen in het oplosmiddel en aan ketenterminatie reacties die meer voorkomen bij hogere temperaturen. Ook is het aangetoond dat de massaoverdracht van etheen de snelheidsbepalende stap wordt voor de polymerisatiereacties bij hogere temperaturen. Een groot nadeel van deze katalysator is echter dat alleen hoge molgewichten kunnen worden verkregen in de afwezigheid van scavengers. Het feit dat een deel van de katalysator als scavenger wordt gebruikt vermindert de praktische toepasbaarheid van deze katalysator sterk. Om deze tekortkomingen te elimineren en om te evalueren of andere homogene katalysatorsystemen ook kunnen worden gebruikt om UHMWPE met sterk onverstregelde ketens te verkrijgen werd Mitsui's bis(fenoxyimine)titanium katalysatorsysteem $[3-t\text{-Bu-2-O-C}_6\text{H}_3\text{CH=N(C}_6\text{F}_5)_2\text{TiCl}_2/\text{MAO}$ bestudeerd. Polymerisaties, uitgevoerd onder verschillende condities, lieten zien dat verschillende verdunningen, reaktietijden en reaktietemperaturen nauwelijks invloed hebben op de productiviteit en op het molgewicht wat werd toegeschreven aan zeer snelle polymerisatie en volledige omhulling van de katalysatormolekulen door de polymere matrix. Het was opmerkelijk dat een zeer grote overmaat MAO ($>100,000$ equivalenten) nodig was om een optimale activiteit te bereiken. Dit werd toegeschreven aan de aanwezigheid van een relatief groot aantal "slapende sites" bij lage MAO concentraties. Een toename in reaktiviteit met meer MAO (in toluen) kan het gevolg zijn van de toegenomen polariteit van het reaktiemedium. Om het effect van de polymerisatie condities op mengingsdichtheid van de ketens te onderzoeken werden verschillende apparaten ingezet om de polymeer monsters te

analyseren. De toestand met onverstregelde UHMWPE ketens verkregen met homogene katalysatoren werd bewezen door gebruik te maken van verschillende karakterisatietechnieken zoals verstrekken in de vaste toestand, persen, differential scanning calorimetry (DSC), temperature modulated DSC (TMDSC) en rheologie en vergeleken met een commercieel monster. De UHMWPE die werd gesynthetiseerd met behulp van beide homogene katalysatoren onder verschillende polymerisatiecondities werden geperst tot films onder hun smelttemperatuur. (50°C/ 200 bar). Tijdens mechanische deformatie in de vaste toestand lieten de films een verstrekkingsgraad zien van meer dan 120. Daarentegen vertoont een commerciële kwaliteit UHMWPE (waarbij de ketens geheel verstrengeld zijn) een verstrekkingsgraad van 10. Bovendien waren alleen de films die werden verkregen met de homogene katalysatoren transparant, wat een gevolg is van de eenvoudigere vloeit van deze polymeerketens tijdens shearing, zelfs als dit ver beneden de smelttemperatuur wordt uitgevoerd. Deze waarnemingen zijn indicaties voor een lagere ketenverstregelingsdichtheid in de nascent materialen verkregen met de homogene katalysatoren.

Om de resultaten verkregen door de verstrekkingsexperimenten en de pers experimenten, welke aantoonde dat de polymeren sterk onverstregeld waren, verder te versterken werden DSC annealing experimenten met het UHMWPE uitgevoerd. De polymeren werden geannealed bij een temperatuur dicht bij het punt waar het nascent UHMWPE begint te smelten. De monsters werden gedurende verschillende tijden geannealed bij de bovengenoemde temperatuur, waarna ze werden afgekoeld en gesmolten met een snelheid van 10 K·min⁻¹ wat resulteerde in het optreden van 2 pieken: één welke overeenkomt met de smelttemperatuur van nascent polymeer (141°C) en de andere welke overeenkomt met de smelttemperatuur van smelt gekristalliseerd PE (135°C). Voor de polymeren die werden gesynthetiseerd met de homogene katalysatoren resulteerde een langere annealingtijd tot een toename in de 135°C piek. De waargenomen toename is het gevolg van het continue smelten van nascent kristallen gedurende de annealing. Aan de andere kant liet het commerciële monster nauwelijks dergelijk gedrag zien, wat een sterke indicatie is dat vloeit en dus smelten veel langzamer is voor het volledig verstregelde materiaal in vergelijking met het niet verstregelde UHMWPE.

Met TMDSC werd eenduidig aangetoond dat het smeltproces veel sneller is voor UHMWPE gesynthetiseerd met de homogene katalysatoren omdat de tijdsconstante voor smelten veel lager is (100-300 minuten) vergeleken met de volledig verstregelde commerciële UHMWPE welke een zeer hoge smelt tijdsconstante heeft (600-1000 minuten). Zoals verwacht is zelfs het α -relaxatie proces veel sneller voor polymeren gesynthetiseerd met de homogene

katalysatoren, vooral bij temperaturen beneden het smeltpunt van de nascent polymeren. Uit deze experimenten werd geconcludeerd dat het smelten eerst start door het smelten van de nascent kristallen, gevolgd door langzaam oplossen in de omhullende visceuse vloeistof, een proces dat veel complexer en tijdrovender is voor verstengeld UHMWPE.

Ten slotte werd een krachtige techniek zoals rheologie gebruikt om het aantal verstengelingen per keten te kwantificeren. In tegenstelling tot een volledig verstengeld UHMWPE welke een storage plateau modulus heeft van ongeveer 2×10^6 Pa, laten de polymeren verkregen met de twee homogene katalysatoren veel lagere waarden zien ($G' = 0.6 \times 10^6$ Pa). Omdat de waarde van de plateau modulus omgekeerd evenredig gerelateerd is aan het molgewicht tussen omstrengelingen (M_e), werd geconcludeerd dat de polymeren die werden verkregen met de homogene katalysatoren zoals beschreven in Hoofdstukken 2 en 3 sterk onverstengeld zijn. Bovendien laat een onverstengeld UHMWPE een opbouw van de modulus zien van de initiële lage waarden (0.6×10^6 Pa) oplopend naar een waarde van 2×10^6 Pa voor volledig verstengeld UHMWPE, wanneer het polymeermonster een aantal uren bij 160°C in de melt wordt gehouden. Zoals verwacht zien we voor de commerciële UHMWPE monster geen opbouw van de modulus. Het is echter wel aangetoond dat rheologie alleen gebruikt kan worden als een kwalitatieve methode door de matige reproduceerbaarheid van de metingen. Elk van de hierboven beschreven technieken heeft een waardevolle kwantitatieve bijdrage geleverd aan de schatting van het aantal omstrengelingen per keten in het nascent materiaal en we achten de niet-omstrengelde keten morfologie voor de UHMWPE's verkregen met de homogene katalysatoren bewezen.

Er zijn ook nog *in-situ* SAXS experimenten uitgevoerd om de invloed van de polymerisatie condities (heterogeen versus homogene katalysator; type homogene katalysator, type cocatalyst) op de nascent morfologie te bestuderen. Polymeren gesynthetiseerd met de homogene samarocoon katalysator lieten in het nascent materiaal de aanwezigheid zien van een halo bij kamertemperatuur. De toename van de intensiteit met verwarming is indicatief voor "long range order" in de dikte van de lamellen. Voor polymeren gesynthetiseerd met de bis(fenoxyimine)titanium, werd bij kamertemperatuur geen halo waargenomen. De afwezigheid van de halo in het commerciële materiaal en bij de UHMWPE gesynthetiseerd met de bis(fenoxyimine)titanium katalysator bij kamertemperatuur is een indicatie voor een brede lameldikte verdeling, welke smaller wordt bij verwarmen van het monster naar het smeltpunt. Een scherp contrast tussen de commerciële kwaliteit UHMWPE en het polymeer verkregen met de bis(fenoxyimine)titanium katalysator was dat de halo behouden bleef na

koelen van de commerciële monster, terwijl deze niet aanwezig is voor het bis(phenoxyimine)titanium katalysator materiaal. WAXS experimenten laten de aanwezigheid van een monoclinische fase zien naast de orthorhombische fase voor de polymeren gesynthetiseerd bij lage temperaturen tot 0°C. De monoclinische fase is afwezig voor de polymeren verkregen bij hogere temperaturen.

In conclusie, het oorspronkelijke doel van het project zoals beschreven in dit proefschrift is met succes voltooid. UHMWPE met een smalle molgewichtverdeling is gesynthetiseerd met verschillende homogene katalysatoren en met verschillende technieken is aangetoond dat het materiaal onverstrengeld is. Het resulterende polymeer laat een excellente verwerkbaarheid zien en na curing kan een volledig verstrengeld en volledig "fused" materiaal worden verkregen.

Om een commercieel attractieve route te ontwikkelen is een goedkope, actieve, niet-levende katalysator nodig.

Curriculum Vitae

Kirti Garkhail Sharma was born on the 5th of May 1973 in New Delhi, INDIA. She obtained her Bachelors degree in Chemistry from the Delhi University in 1993. Thereafter she pursued Masters Program in Chemistry from the Indian Institute of Technology, New Delhi and was awarded Master of Science degree in 1995. The title of the dissertation was “Studies on the reaction of N-Arylsulphonylaziridines with thiocyanates, as a route to 2-Imidazolidinethiones” and was carried out under the able supervision of Prof Dr N K Nadir. In the same year she joined Sripati Singhania R & D Centre (J. K. Pharmaceuticals) as Research Scientist and worked there till August 1997. Marriage brought her to the The Netherlands and after a break she initiated her Ph.D research on synthesis of easily processable UHMWPE under the able supervision of Dr. Robbert Duchateau in the Polymer Chemistry group at the Eindhoven University of Technology, The Netherlands. During the last four years the author has obtained NIOK Certificate on Catalytic Olefin Polymerization and completed one module of the RPK course (Registered Polymer Technologist). Soon she will be joining GE Advanced Materials as Product Developer at Bergen op Zoom, The Netherlands.

Acknowledgements

I profoundly thank Dr. Robbert Duchateau for his guidance, understanding, and valuable discussions throughout the course of this work. Many thanks also for your continuous encouragement, patience, and support, which made the completion of this work possible. I have thoroughly enjoyed working with you.

My sincere gratitude to Prof. Dr. Gert-Jan Gruter for giving me the opportunity to carry out my Ph.D work in his group. I am also grateful to him for the fruitful discussions and valuable input during the last 4 years and finding time to read and correct the manuscript in spite of his tight schedule. Thank you also for translating my summary overnight into Dutch.

I sincerely thank Dr. Sanjay Rastogi for his guidance, discussions, and support during the last 4 years. I am grateful for getting the opportunity to learn various techniques that were new to me.

I would like to express my sincere thanks to Prof. Dr. Günther Höhne for his dedication, patience, and enthusiasm in helping me with the TMDSC experiments and for reading through the manuscript. I enjoyed working with you.

My sincere thanks to Prof. Dr. Cor Koning for his interest in my work and for providing moral support and encouragement.

I am grateful to Prof. Dr. Piet Lemstra for agreeing to be my 2nd promoter and reading through my thesis.

I am very grateful to Dutch Polymer Institute (DPI) for the financial support to perform my research work.

An important part of the work would not have been possible without the efforts and enthusiasm of many people. I like to thank Dr. Robbert Duchateau and Dr. John Severn for helping me learn air and moisture sensitive techniques. Should I tell how much I enjoyed being alert and 'paranoid' during the whole day and having 'nightmares' during the night? Dr. Andries Jekel, thank you for your interest in my work and performing SEC analysis and your cooperation for doing urgent measurements. Thanks also to Dr. Valérie Grumel for repeating some SEC measurements. Dirk Lippits, thank you for helping me with initial rheology experiments. To Dr. Juanfran Vega, thank you for the useful discussions and suggestions regarding rheology measurements. I appreciate the efforts from Dr. Mariele Wouters (TNO) for her interest and efforts in repeating some rheology measurements. Thanks to Wouter Gerritsen, for performing TGA measurements and for ensuring proper running of the DSC instruments. I also thank Dr. Gerard van Doremaele and Dr. Tim Kid for the useful discussions during the DPI meetings and company visits to DSM.

Coming to our SPC group, I feel lucky to have been a part of it. First, I would like to thank everyone for making my stay very pleasant here. I am proud to say that our group is an excellent example of national integration both scientifically as well as socially. In the lab, it was fun working with Rachel, Joep, Stéphanie, Wouter, Soazig, Madri, Nilesh, Raf and John. Our lab was always so busy and lively with lot of talents apart from chemistry! Wish you all the success with your work. Thanks to Wouter van Meerendonk for his help in solving all the computers related problems. The whole SPC group has

benefited from your and Maarten Staal's efforts. To all my past and present roommates (Rachel, Gijsbert, Stéphanie, Maarten and Jan) thanks a lot for sharing good times. Rachel, it is amazing how much we have shared in the past 4 years. I hope to be in touch with you. Coming to other SPC members: Jens, Delphine, Jalena, Bas Staal, Bas Pierik, Robin, Madri and Rajan- it was always nice to have you all around. Best wishes for your future and let's remain in touch. During the last four years, I had the opportunity to work with other students Christina and Lars. I enjoyed working with you and I wish you good luck for your future. Thanks to my former SKA colleagues for welcoming me in their group.

I feel extremely lucky to get the love and support of friends (so far away from home) when I needed the most. Mohan, Nell, Sangeeta, Lavanya, Chethana/Vishwa, Koushik and Rob - your moral support and help enabled me get through the difficult times here and I will be ever grateful to all of you. Thanks for being there.

To my other friends: Sachin, Rajan, Ankur, Lopa, Sreepad, Ruchi, Reenu, Pooja, Sorinilla, Ionell, Marina, Mandira, Nikhil, Ritu, Keshav, Sreejit, Rajesh, Nilesh, Manoranjan, Vidhya, Suresh, Vishal, Jaya Mohan, Vadivu, Vandana/Srikanth - I could always count on you people and felt homely because of you all. To Ger, Indira/Ramesh/Adarsh- we did share good times and supported each other.

Like foundations determine the stability of a building, I am indebted to my family members (Thatha, Amba, Amma, Appa, Chitti's, Chittappa's, Neelu, Babu and Sitaram Mama) for their deep and steadfast belief in me and for their immense support and encouragement all through my life. I would not be where I am if it was not for your love and strength. I owe all my successes to you. Next, I am blessed with the most loving sisters and brothers (Aarti, Akku, Raju, Jeemu, Cidrul and Sam) who, stood with me like a rock and I know I can count on you anytime in my life. To Sanjeev and dearest Prakriti, your precious love and moral support have always been invaluable to me over the years. Thanks also to all other family members and friends who have been supportive and shared good times with me.